

**SORPTION OF As(V) FROM WATERS BY USE OF
NOVEL AMINE-CONTAINING SORBENTS
PRIOR TO
HGAAS AND ICP-MS DETERMINATION**

**A Thesis Submitted to
the Graduate School of Engineering and Sciences of
İzmir Institute of Technology
in Partial Fulfillment of the Requirements for the Degree of**

**MASTER OF SCIENCE
in Chemistry**

**by
Ezel BOYACI**

**July 2008
İZMİR**

ACKNOWLEDGEMENTS

I would like to acknowledge the help of many people during the course of my study. Firstly, I would like to thank my advisor Prof.Dr. Ahmet E. Erođlu for providing invaluable insights, timely encouragement as well as guidance, balanced by the freedom to express myself throughout this research work.

I am thankful to Prof.Dr. O.Yavuz Ataman, Prof.Dr. Emür Henden, Prof.Dr. Serdar Özçelik, Assist.Prof.Dr. Ali Çađır who readily agreed to be members of my thesis examining committee. I also thank to Prof.Dr Hürriyet Polat and Assoc.Prof.Dr Talal Shahwan for their constructive comments on the project.

I would like to extend my sincere thanks to Öznur Kaftan for her valuable suggestions on several sections of the thesis, to Dr. Hüseyin Özgener for providing help on elemental analysis, to the research scientists at the Center for Materials Research (IZTECH) for their help on facilities TGA, XRD and SEM, and also to the research scientists at the Environmental Research Centre for ICP-MS analyses.

My special thanks go to my friends Meral Karaca, Nazlı Efecan, Arzu Erdem, Aslı Erdem, Murat Erdoğan, İbrahim Karaman, Serkan Keleşođlu, Betül Öztürk, Ayşegül Şeker, Özge Tunusođlu, Semira Ünal, Müşerref Yersel and Sinan Yılmaz for many insightful conversations and helpful comments which made this thesis possible.

Finally, I dedicate this work to my parents and brother.

ABSTRACT

SORPTION OF As(V) FROM WATERS BY USE OF NOVEL AMINE-CONTAINING SORBENTS PRIOR TO HGAAS AND ICP-MS DETERMINATION

A novel sorption method utilizing several amine-containing sorbents was developed for arsenic determination in waters by hydride generation atomic absorption spectrometry (HGAAS) and inductively coupled plasma mass spectrometry (ICP-MS). Chitosan, chitosan-immobilized sodium silicate, chitosan-modified macroporous silicate, and aminopropyl triethoxysilane-treated macroporous silicate were among the sorbents investigated for As(V) sorption.

Sorption parameters were optimized for As(V) using chitosan and chitosan-immobilized sodium silicate and were then applied in all sorption studies. These parameters, namely, sorption pH, amount of sorbent, reaction temperature, and shaking time were 3.0, 50.0 mg, 25 °C, and 30 min, respectively. The sorption for chitosan under the optimized conditions was 89% (± 1) while that for As(III) was lower than 10% at all pHs. In addition, chitosan-modified and amine-modified macroporous silicate demonstrated 88% (± 3) and 68% (± 12) sorption, respectively. After the sorption, the release of arsenate from chitosan and chitosan-immobilized sodium silicate was realized using two eluents; namely, 2.0% (v/v) acetic acid which dissolved chitosan, and 1.0% (w/v) L-cysteine solution having a pH of 3.0 adjusted with HCl which eluted arsenate by reducing to arsenite. Their respective desorption percentages were 90% (± 1) and 100% (± 4) for chitosan, and 67% (± 2) and 100% (± 1) for chitosan-immobilized sodium silicate.

The preconcentration study performed using an absolute amount of 150.0 ng As(V) in bottled drinking water at the enrichment factors of 1, 2, and 10 has given 98% (± 3), 95% (± 2), and 78% (± 4) recoveries, respectively. The accuracy of the proposed methodology with chitosan was verified with spike recovery tests for various water types at a concentration of 10.0 $\mu\text{g/L}$ As(V). With matrix-matched calibration, the percentage spike recovery values were determined to be 114 (± 4), 112 (± 2), 43 (± 4), and 0 (± 1), for ultrapure, bottled, tap and sea water, respectively. These results have shown the strong suppression effect of the tap and the sea water matrixes.

ÖZET

SULARDAKİ As(V)'İN HGAAS VE ICP-MS İLE TAYİNİ ÖNCESİ AMİN İÇERİKLİ YENİ ADSORBANLARIN KULLANIMIYLA SORPSİYONU

Bu çalışmada, sulardaki As(V)'in hidrür oluşturmali atomik absorpsiyon spektrometri (HGAAS) ve indüktif eşleşmiş plazma kütle spektrometri (ICP-MS) ile tayini öncesi, çeşitli amin içerikli sorbentlerin kullanıldığı yeni bir sorpsiyon metodu geliştirilmiştir. Kitosan, kitosan-immobilize edilmiş sodyum silikat, kitosan ile modifiye edilmiş-makro gözenekli silikat ve aminopropil trietoksi silan ile muamele edilmiş-makro gözenekli silikat As(V) sorpsiyonu için incelenmiştir.

As(V) sorpsiyonu için optimum çalışma koşulları, kitosan ve sodyum silikata immobilize edilmiş kitosan kullanılarak belirlenmiş ve tüm sorpsiyon çalışmalarında bu parametreler kullanılmıştır. Sorpsiyon pH'sı, sorbent miktarı, reaksiyon sıcaklığı ve çalkalama süresi sırasıyla 3.0, 50.0 mg, 25 °C, ve 30 min olarak seçilmiştir. Optimize edilmiş koşullar altında kitosan sorpsiyonu As(V) için %89 (±1), As(III) için ise bütün pH'larda %10'un altında bulunmuştur. As(V)'in kitosan ile modifiye edilmiş silikat tarafından sorpsiyonu %88 (±3), amin ile modifiye edilmiş makro gözenekli silikat tarafından sorpsiyonu ise %68 (±12)'dir. Arsenatın kitosan ve sodyum silikata immobilize edilmiş kitosandan geri alınması için iki farklı eluent kullanılmıştır. Bu eluentlerden %2.0 (v/v)'lik asetik asit kitosani tamamen çözmekte, pH'sı HCl ile 3.0'e ayarlanmış %1.0 (w/v)'lik L-sistein ise As(V)'i As(III)'e indirgeyerek çözeltiyeye almaktadır. Bu iki çözelti ile elde edilen geri kazanım değerleri kitosan için %90 (±1) ve 100 (±4), sodyum silikata immobilize edilmiş kitosan için ise %67 (±2) ve %100 (±1)'dir.

Mutlak derişimi 150.0 ng olan As(V) ile 1, 2, ve 10 kez derişirme faktörleri kullanılarak yapılan önderişirme çalışmalarında sırasıyla, %98 (±3), %95 (±2), ve %78 (±4) geri kazanım elde edilmiştir. Önerilen kitosanlı metodun doğruluğu çeşitli sulara eklenen 10.0 µg/L As(V)'in geri kazanım testleri ile gösterilmiştir. Ultra saf, içme, çeşme ve deniz suyundaki yüzde katım/geri kazanım değerleri matriks benzeşimli kalibrasyon grafiği kullanılarak, sırası ile, 114 (±4), 112 (±2), 43 (±4), ve 0 (±1) olarak belirlenmiştir. Bu sonuçlar İYTE çeşme suyu ve deniz suyu matriksinin kuvvetli baskılama etkisine sahip olduğunu göstermiştir.

TABLE OF CONTENTS

LIST OF FIGURES.....	x
LIST OF TABLES	xiii
CHAPTER 1 INTRODUCTION	1
1.2. Arsenic Species in the Environment	1
1.3. Effect of Arsenic Species on the Environment and Health	2
1.4. Arsenic Determination Methods	3
1.5. Arsenic Removal Methods	4
1.5.1. Precipitative Processes.....	4
1.5.2. Adsorptive Processes	4
1.5.3. Ion Exchange.....	5
1.5.4. Membrane Processes	5
1.5.5. Alternative Methods	6
1.6. Chitosan for As Sorption	6
1.6.1. Synthesis	8
1.6.1.1. Method of Horowitz.....	8
1.6.1.2. Method of Rigby and Wolfrom	8
1.6.1.3. Method of Broussignac	8
1.6.1.4. Method of Fujita	9
1.6.2. Characterization Methods	9
1.6.2.1. Degree of Deacetylation.....	9
1.6.2.3. Solubility	10
1.6.2.4. Crystallinity	10
1.6.3. Immobilization Methods	11
1.7. Novel Amine-Containing Sorbents / Pore-Controlled Templates	12
1.7.1. Fundamentals of latex particles.....	12
1.7.1.1. Miniemulsion polymerization	12
1.7.1.2. Mechanism of Polymerization.....	13
1.7.1.2.1. Initiators and Monomers Used in Free Radicalic Polymerization.....	15

1.7.1.3. Particle Nucleation Mechanisms	17
1.7.1.4. Stability of Miniemulsion	17
1.7.1.5. Synthesis of Polystyrene Nanoparticles.....	17
1.7.2. Fundamentals of Template Supported Ordered Silica	
Network.....	18
1.7.2.1. Synthesis Methods.....	18
1.7.2.2. Silane Chemistry.....	19
1.7.2.2.1. Synthesis of Sol-Gel.....	19
1.7.2.2.2. Modification of Silica Surface.....	22
1.8. Aim of This Work	24
CHAPTER 2 EXPERIMENTAL.....	25
2.2. Reagents and Solutions.....	27
2.3. Synthesis and Characterization of Chitosan	33
2.3.1. Synthesis	33
2.3.2. Characterization.....	33
2.3.2.1. Infrared Spectroscopy	33
2.3.2.2. Degree of Deacetylation.....	34
2.3.2.2.1. Potentiometric Titration	34
2.3.2.2.2. Elemental Analysis	35
2.3.2.3. Molecular Weight Determination.....	35
2.4. Immobilization Methods.....	37
2.4.1. Immobilization of Chitosan on Sodium Silicate	37
2.4.2. New Amine-Containing Sorbents	37
2.4.2.1. Pore-Controlled Templates	37
2.4.2.1.1. Synthesis of Surfactant-Free Polystyrene	
Nanoparticles.....	37
2.4.2.1.2. Synthesis of Ordered Macroporous Silicate.....	39
2.4.2.1.3. Optimization of Synthesis Parameters of Macroporous	
Silicate Structures.....	40
2.4.2.1.4. Functionalization of Macroporous Silicate Structures.....	41
2.5. Sorption Studies	43
2.5.1. Effect of Solution pH.....	43
2.5.2. Effect of Shaking Time.....	44

2.5.3. Effect of Sorbent Amount (Solid/Liquid Ratio).....	44
2.5.4. Effect of Reaction Temperature	44
2.5.5. Effect of Ionic Strength.....	45
2.5.6. Repetitive Loading	45
2.6. Sorption Isotherm Models	45
2.7. Desorption Studies	47
2.8. Effect of the Acid Nature on As Signal.....	50
2.9. Interference Studies.....	50
2.10. Pre-Concentration.....	51
2.11. Speciation of Arsenic	51
2.12. Method Validation with Spiked Samples	54
2.13. Performance of the Study	54
2.14. Sorption Study of Modified Porous Silicate.....	55
CHAPTER 3 RESULTS AND DISCUSSION.....	56
3.1. Characterization	59
3.1.1. Degree of Deacetylation	59
3.1.2. Molecular Weight of Chitin and Chitosan.....	60
3.1.3. XRD Patterns of Chitin and Chitosan.....	61
3.2. Characterization of Polystyrene Nanoparticles.....	62
3.3. Synthesis of Ordered Macroporous Silicate	65
3.3.1. Characterization of Modified Macroporous Silicate Structures.....	68
3.4. Sorption Studies	68
3.4.1. Effect of Solution pH.....	68
3.4.2. Effect of Sorbent Amount.....	71
3.4.3. Effect of Shaking Time.....	71
3.4.4. Temperature Effect.....	72
3.4.5. Effect of Ionic Strength.....	73
3.4.6. Successive Loading	74
3.5. Sorption Isotherm Models	77
3.6. Desorption Studies	82
3.7. Effect of the Acid Nature on As Signal.....	84
3.8. Interference Studies.....	84

3.9. Pre-Concentration.....	86
3.10. Speciation of Arsenic	86
3.11. Method Validation with Spiked Samples	88
3.12. Performance of the Study	88
3.13. Sorption Study of Modified Porous Silicate.....	89
CHAPTER 4 CONCLUSION.....	90
REFERENCES.....	93

LIST OF FIGURES

<u>Figure</u>	<u>Page</u>
Figure 1.1. Distribution of arsenic species under aerobic and anaerobic conditions.....	2
Figure 1.2. Structure of chitin repeating unit.....	7
Figure 1.3. Structure of chitosan repeating unit.....	7
Figure 1.4. Effect of particle size on the stability for different types of emulsion	13
Figure 1.5. Initiation steps	13
Figure 1.6. Propagation step	14
Figure 1.7. Termination steps	14
Figure 1.8. Hydrolysis step of sol-gel process.....	20
Figure 1.9. Acid catalyzed proposed mechanism of hydrolysis	20
Figure 1.10. Base catalyzed proposed mechanism of hydrolysis	20
Figure 1.11. Condensation step of sol-gel process.....	21
Figure 1.12. Polycondensation of condensed silanol to produce silica network.....	22
Figure 1.13. Increasing strength of bond formation in modification step	23
Figure 1.14. Activation of silicate surface and post modification of silanol.....	23
Figure 1.15. Modification of silicate in situ	23
Figure 2.1. Segmented Flow Injection HGAAS system used in arsenic determinations.....	26
Figure 2.2. Five necked reaction flask used in the synthesis of polystyrene nanoparticles	38
Figure 2.3. Amine modification of mesoporous silicate surface	42
Figure 2.4. Experimental flowchart for arsenic speciation.....	53
Figure 3.1. SEM images of chitosan, silicate and chitosan-immobilized sodium silicate	57
Figure 3.2. TGA of chitosan, silicate and chitosan-immobilized sodium silicate	58
Figure 3.3. FTIR spectra of chitin and chitosan.....	59

Figure 3.4. Titration curve of chitosan, dissolved in HCl with standardized NaOH solution	60
Figure 3.5. Effect of concentration to reduced viscosity of chitosan.....	61
Figure 3.6. Effect of concentration to reduced viscosity of chitin	61
Figure 3.7. X-ray diffraction patterns for chitin.....	62
Figure 3.8. X-ray diffraction patterns for chitosan	62
Figure 3.9. SEM images of polystyrene nanoparticles at various magnifications.....	63
Figure 3.10. Particle size distribution of polystyrene nanoparticles.....	64
Figure 3.11. Particle size distribution of (a) batch 2 and (b) batch 3	65
Figure 3.12. SEM images of macroporous silicate structures	67
Figure 3.13. Effect of pH on the sorption of As(V).....	69
Figure 3.14. Effect of pH on the sorption of As(III)	69
Figure 3.15. Speciation diagram of As(V) at various pH values.....	70
Figure 3.16. Speciation diagram of As(III) at various pH values	70
Figure 3.17. Charge of chitosan flakes at various pH values	70
Figure 3.18. Effect of amount of sorbent on sorption	71
Figure 3.19. Effect of shaking time.....	72
Figure 3.20. Effect of temperature on sorption	73
Figure 3.21. The arsenic sorption capacity of chitosan at various concentrations of NaCl.....	74
Figure 3.23. Total amount increment of loaded arsenate after each successive loadings onto chitosan.....	76
Figure 3.24. Percent sorption of chitosan immobilized silicate for ten successive loadings	76
Figure 3.25. Total amount increment of loaded arsenate after each successive loadings onto chitosan-immobilized sodium silicate	77
Figure 3.26. Nonlinear fit of isotherm models for sorption of arsenate by chitosan.	78
Figure 3.27. Linear fit of Langmuir model for arsenate sorption by chitosan.....	78
Figure 3.28. Linear fit of Freundlich model for arsenate sorption by chitosan	79
Figure 3.29. Linear fit of Dubinin-Radushkevich model for arsenate sorption by chitosan.....	79

Figure 3.30. Nonlinear fit of isotherm models for sorption of arsenate by chitosan immobilized silicate.....	80
Figure 3.31. Linear fit of Dubinin-Radushkevich model for arsenate sorption by chitosan immobilized silicate.....	80
Figure 3.32. Linear fit of Freundlich model for arsenate sorption by chitosan immobilized silicate	81
Figure 3.33. Linear fit of Langmuir model for arsenate sorption by chitosan immobilized silicate	81
Figure 3.34. Effect of the acid matrix in arsenic signal generated	84

LIST OF TABLES

<u>Table</u>	<u>Page</u>
Table 1.1. Initiators usually used in microemulsion polymerization	15
Table 1.2. Some monomers used in microemulsion polymerization	16
Table 2.1. Operating parameters for the segmented flow injection (SFI-HGAAS) system	26
Table 2.2. Reagents used through the study	29
Table 2.3. IR band positions of some functional groups	34
Table 2.4. Effect of water/styrene ratio on particle size	39
Table 2.5. Summary of optimization parameter for ordered macroporous silicate	40
Table 2.6. Desorption conditions of arsenic from chitosan and chitosan-immobilized sodium silicate	49
Table 2.7. Preconcentration parameters	51
Table 3.1. Elemental analysis results of chitosan and chitosan-immobilized sodium silicate	60
Table 3.2. Comparison of degree of deacetylation of chitosan by titrimetric and elemental analysis methods	60
Table 3.3. Elemental composition of modified macroporous silicate	68
Table 3.4. Thermodynamic parameter of chitosan and immobilized chitosan	73
Table 3.5. Summary of models coefficients	81
Table 3.6. Desorption conditions of arsenic from chitosan and chitosan immobilized sodium silicate	83
Table 3.7. Percent sorption of chosen species by chitosan at optimized conditions for As(V)	85
Table 3.8. Summary of interference study	86
Table 3.9. Percent recovery at various enrichment factor from chitosan for arsenate ion	86
Table 3.10. The comparative spike recovery of As(V) and As(III) ions from chitosan and chitosan-immobilized sodium silicate	87
Table 3.11. The comparative spike recovery of As(V) and As(III) ions from Duolite GT-73	87

Table 3.12. Percent recovery of spiked arsenate ion.....	88
Table 3.13. Summary of method performance	89
Table 3.14. Sorption behaviour of modified macroporous silicate towards various ions.....	89

CHAPTER 1

INTRODUCTION

1.1. Environmental Considerations

Arsenic exposure to soil and ground waters, from its natural occurrence and industrial use in past decades as pesticides, preservative and using in mining processes caused to contaminate the useful sources of water around the world. Today, although avoiding or minimizing the usage of arsenic containing products is the one of the main task, arsenic in the environment has become an important danger of public health in many parts of the world. Everyone has daily bearing to arsenic because it is a natural distribution around the world. Normally arsenic is found in human habitat in a small amounts, e.g. in water, soil, indoor house dust, air, and food. The risk from arsenic intake for developing health problems can be increased when natural or human activities have caused greater than normal amounts of arsenic to accumulate in the environment, Finding new clean sources is not possible each time, which introduce the requirement of finding cheap, easily operable and non toxic removal technologies.

1.2. Arsenic Species in the Environment

Arsenic can be found in organic and inorganic forms in nature (EPA 1999) and exists in the -3, 0, +3 and +5 oxidation states (Mohan and Pittman 2007). The organic species are monomethyl arsenic acid (MMAA), dimethyl arsenic acid (DMAA), and arseno-sugars which are found mainly in foodstuffs (EPA 1999). Inorganic arsenic species occur as arsenite, As(III), with primary form of (H_3AsO_3) and arsenate, As(V), with primary forms of (H_2AsO_4^-) and (HAsO_4^{2-}) in natural waters (EPA 1999). The stability and dominance of specific anions in solution depends on the pH and redox potential (Eh) of solution. Figure 1.1 illustrates the distribution of arsenic species; arsenates are stable under aerobic (oxidizing) conditions whereas arsenites are predominant under anaerobic (reducing) conditions (Mandal and Suzuki 2002).

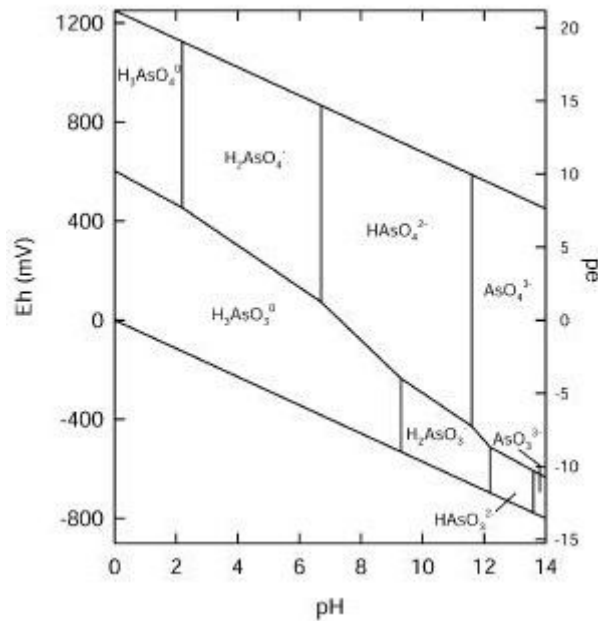


Figure 1.1. Distribution of arsenic species under aerobic and anaerobic conditions (Source:Smedley and Kinniburgh 2001)

1.3. Effect of Arsenic Species on the Environment and Health

Arsenic is a naturally occurring element in food, water and air (EPA 1999). Sources of the element in the environment can be natural and/or anthropogenic (Ebdon, et al. 2001). Before the contribution of human's activities to the nature, arsenic was distributed through earth crust, soil, water, air and living organisms (Mandal and Suzuki 2002). More than 200 mineral species contain arsenic, the most common of which is arsenopyrate (Vasireddy 2005). Volcanic action is the most important natural source of arsenic which is the main contributor of atmospheric flux of the element (Vasireddy 2005). The presence of arsenic in natural water is related to the dissolution of minerals and ores from arsenic containing rocks and sediments (Choong, et al. 2007). Waste discharges from industrial and mining activities, agricultural use of arsenical pesticides and use of chromated copper arsenate (CCA) wood preservative contribute to anthropogenic arsenic contamination of air, water and soil (Dambies, et al. 2002). Consumption of arsenic through a significant period of time in drinking water causes of the skin, lungs, kidney, liver and other sort of cancers. Vascular system effects have also been observed, including peripheral vascular disease which results in gangrene or Blackfoot Disease (EPA 1999). Short term exposure to As results in vomiting,

esophageal and abdominal pain, “rice water” diarrhea (Mohan and Pittman 2007). Toxicity of arsenic depends on factors such as physical state (gas, solution or powder particle), size, the rate of absorption into cells. The most important parameters are the chemical forms and oxidation state of the species (Mandal and Suzuki 2002). The decreasing order of toxicity of arsenicals is arsines > As(III) > arsenoxides > (As) V > arsonium compounds > As (Mandal and Suzuki 2002). Hence, drinking water containing As is a potential threat to the health of humans. The World Health Organization (WHO) revised the guideline for arsenic from 0.05 to 0.01 mg/L and has classified arsenic as the most toxic chemical with carcinogenic effects (Choong, et al. 2007). The Environmental Protection Agency (EPA) has also set the permissible value of arsenic in drinking water to 0.01 mg/L which is also used in the European Union (Choong, et al. 2007).

1.4. Arsenic Determination Methods

There are many methods for arsenic determination in various matrixes. Hydride generation atomic absorption spectrometry (HGAAS) is a useful technique applied either directly or after a suitable pre-treatment step (Menegario and Gine 2000, Bundaleska, et al. 2005, Yersel, et al. 2005). Hydride generation has the advantage of determining the different forms of arsenic (different oxidation states and forms bound to organic matter) on the basis of different kinetics of hydride generation by each species (Niedzielski, et al. 2002). Another advantage of hydride formation is the reduction of spectral interferences by separation of analyte from the matrix. However, gas phase and liquid phase interferences can be seen during or after the hydride generation step (Dedina and Tsalev 1995). Inductively coupled plasma-mass spectrometry (ICP-MS) is one of the most sensitive techniques for As determination. However, it has a major disadvantage that, in the chloride-containing matrixes, it is affected from spectral interference of $^{40}\text{Ar}^{35}\text{Cl}$ on the monoisotopic ^{75}As signal. This interference effect can be eliminated by matrix separation provided by hydride generation (Menegario and Gine 2000, Sabarudin, et al. 2005), or can be corrected with the use of interference-correction equations. Inductively coupled plasma-atomic emission spectrometry (ICP-AES) and HG-ICP-AES are other instrumental techniques used for arsenic determination (Dambies, et al. 2002, Faria, et al. 2002).

1.5. Arsenic Removal Methods

Arsenic removal from drinking water includes precipitation, adsorption, ion exchange, membrane filtration and other alternative processes. All processes are limited with lower efficiency for arsenite removal because of the uncharged state of the species under pH 9.

1.5.1. Precipitative Processes

Coagulation/filtration is the one of the precipitative methods which use alum, ferric chloride or ferric sulphate as coagulant. The removal of suspended or dissolved compounds by coagulation is a two stage process. The first step depends on destabilizing the compound in water by altering its physical/chemical properties. This results in coagulation which is removed by filtration as a second step. Removal is highly dependent upon initial arsenic concentration, dosage of coagulant, pH and the valence of the arsenic species (EPA 1999). Coagulation of As(V) with alumina-based material was studied and it was shown that removal of As(III) needs prechlorination to change the state of As(III) to As(V) (Gregor 2001). This study also show that prechlorination can have an adverse effect on other water quality parameters. Iron/manganese oxidation has been shown to lead to the formation of hydroxides that remove soluble arsenic from waters (EPA 1999). Other precipitative methods are lime softening (EPA 1999), coagulation assisted microfiltration (EPA 1999) and enhanced coagulation (EPA 1999).

1.5.2. Adsorptive Processes

Arsenic ions in water can be sorbed to the surface of oxidized activated alumina (EPA 1999). Activated alumina is considered as an adsorption substrate although the chemical reactions involve the exchange of As ions with the surface hydroxides on the alumina. Iron oxide coated sand was also used for arsenic removal where arsenic ions are exchanged with the surface hydroxides (EPA 1999).

1.5.3. Ion Exchange

Ion exchange is a process by which an ion on the solid phase is exchanged for an ion in the water. This solid phase is typically a synthetic resin which has been chosen for its specific adsorption property belonging only to contaminant of concern (EPA 1999). In a study by Oehmen and co-workers it has been shown that the ion exchange membrane bioreactor is effective in arsenate removal by eliminating the potential contaminant mainly resulted from by-products and microbial cells (Oehmen, et al. 2006). An alternative study for arsenic removal by ion exchangers had been reported by Dominguez and co-workers which synthesized fiber like ion exchange resin from vinylbenzyl chloride (Dominguez, et al. 2003). The fiber ion exchange resin had been shown preferable kinetic performance than commercial resins.

1.5.4. Membrane Processes

Membrane is a selective barrier permitting the passing of some constituents in solution and blocking the passage of others (EPA 1999). Membrane processes require a driving force and often are sorted according to the force applied. The generally pressure, concentration, electrical potential and temperature are used in movement of constituents through the membrane. Among all these methods, pressure-driven membrane processes are often used for arsenate removal. Pressure driven membrane processes are further classified by pore size into four categories: microfiltration (MF), ultrafiltration (UF), nanofiltration (NF), and reverse osmosis (RO) (EPA 1999). The pore size of the membrane is strongly dependent on the applied pressure. Nanofiltration and reverse osmosis, which have relatively small pore sizes and high pressure application remove constituents primarily through chemical diffusion. Contrary, relatively lower pressure is applied in microfiltration and ultrafiltration and removal is achieved through physical sieving. Membrane filtration methods such as nanofiltration and reverse osmosis were studied by Whyapa and co-workers and it has been shown that both As(V) and As(III) can be effectively removed from synthetic fresh water over a wide range of operational conditions (Whyapa, et al. 1997). The main drawback of membrane filtration is reported to be the high cost among the other methods also (Choong, et al. 2007).

1.5.5. Alternative Methods

All methods mentioned above for arsenic removal has limitation of cost or health hazard effects which direct scientist to search for environmentally safe alternative methods. Application of different biomasses in sorption studies for arsenic removal has important role with their advantages of low cost and environmentally friendly in nature. Chitin and its N-deacetylated derivative chitosan are among the most abundant biopolymers which have the advantages of low cost, nontoxicity, biodegradability, biocompatibility and the presence of large specific binding sites for sorption (Kumar 2000). Kartal and co-workers studied arsenic removal from chromated copper arsenate (CCA)-treated wood via biosorption by chitin and chitosan in 1, 5 and 10 days periods but an effective removal was not obtained (Kartal, et al. 2005). Molybdate-modified chitosan were used to improve the sorption capacity of chitosan, increased sorption capacity was obtained by the ability of molybdate ions to complex As(V) (Dambies, et al. 2002). Chitosan is also used as a resin for arsenic sorption in column studies with improved resistance to shrinkage which was obtained by 3,4-diamino benzoic acid functionalized cross linked chitosan (Sabarudin, et al. 2005). Boddu and co-workers used chitosan dip coated ceramic alumina for As(III) and As(V) removal in column with improved sorption capacity for As(III) (Boddu, et al. 2008). Guibal and co-workers had used chitosan for molybdate ion sorption and high capacity for Mo(VI) was reported (Guibal, et al. 1998, Dambies, et al. 2001). In the further study by the same group, the affinity of chitosan to molybdate ion was used as advantage of using molybdate loaded chitosan for removal of arsenic. The enhanced sorption capacities was reported for arsenic removal by prepared molybdate impregnated chitosan gel beads and molybdate coagulated chitosan beads (Chassary, et al. 2004). The reaction proceeds through the complexation of As(V) with molybdate ions.

1.6. Chitosan for As Sorption

Among numerous polysaccharides, cellulose and chitin are the most abundant organic compounds in the earth, with the largest amounts of production per year (Kurita 2006). Chitin (Figure 1.2), a polymer distributed widely in nature, consists of 2-acetamido-2-deoxy- β -D-glucose through a β (1 \rightarrow 4) linkage (Kumar 2000). Fungi,

Algae, Protozoa, Cnidaria, Aschelminthes, Endoprocta, Bryozoa, Phoronida, Brachiopoda, Echiurida, Annelida, Mollusca, Onychophora, Arthropoda, Chaetognatha, Pogonophora, and Tunicata contain chitin but exoskeletons are the most easily accessible sources of chitin. The shells of marine crustaceans such as crabs and shrimps are available as waste from the seafood processing industry and used for commercial production of chitin. The shells contain chitin, proteins, CaCO_3 , lipids and pigments (Kurita 2006). Extraction of chitin from shells requires demineralization with HCl and further treatment with NaOH for deproteinization (Planas 2002). Chitosan (Figure 1.3) is the N-deacetylated form of chitin which is produced by thermochemical alkaline treatment of chitin. It has a high nitrogen content (7%) which makes it as a useful chelating agent (Kurita 2006, Tolaimate, et al. 2000). Chitin and chitosan are attractive materials with unique properties of non-toxicity, film and fiber forming properties, adsorption of metal ions, coagulation of suspensions or solutes, and distinctive biological activities (Kurita 2006).

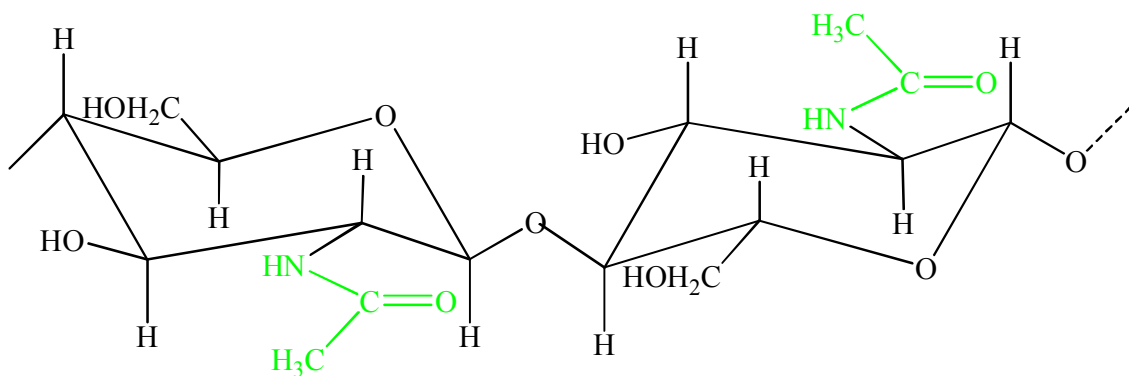


Figure 1.2. Structure of chitin repeating unit

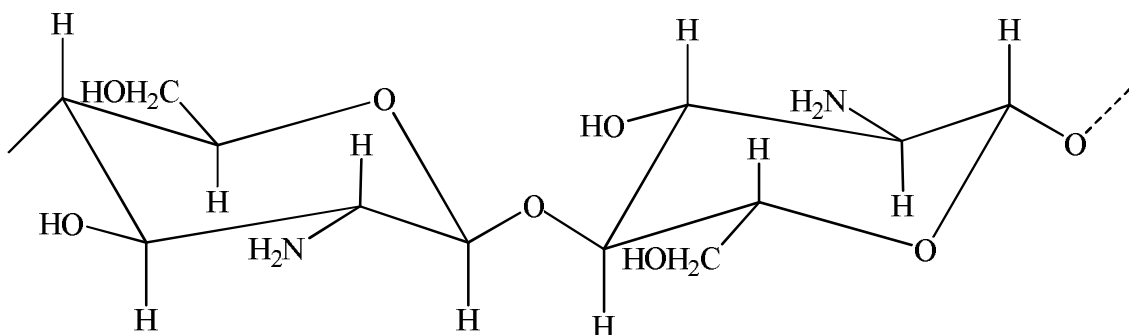


Figure 1.3. Structure of chitosan repeating unit

1.6.1. Synthesis

First chitosan were obtained in 1894 by Hoppe-Seyler by fused KOH at 180 °C with chitin and obtained a product with diminished acetyl content (Muzzarelli 1973). Although various methods for chitosan synthesis were given in literature, all of them are based on the alkaline treatment of chitin under high temperature. Different degree of deacetylation can be obtained depending on the treatment conditions. Some important synthesis methods are summarized below.

1.6.1.1. Method of Horowitz

Under stirring of 30 g of chitin in a nickel crucible with 150 g solid KOH, fusion is realized at 180 °C for 30 min. The melt is poured into ethanol and washed with water to neutrality. Product is dissolved in 5% formic acid and precipitated with NaOH for purification. This method produces a 95% removal of acetyl groups (Muzzarelli 1973 and references therein).

1.6.1.2. Method of Rigby and Wolfrom

Fifty grams of chitin are treated with 2400 mL of 40% (w/w) NaOH solution at 115 °C for 6 h under inert atmosphere. After washing with water until neutralization, 85% of removal of acetyl groups are obtained (Muzzarelli 1973 and references therein).

1.6.1.3. Method of Broussignac

Twenty seven grams of chitin are refluxed at 120 °C for 16 h in 360 g of nearly unhydrous mixture of 50% KOH, 25% ethanol and 25% monoethyleneglycol by weight. About 83% of deacetylation is obtained (Muzzarelli 1973 and references therein).

1.6.1.4. Method of Fujita

Ten parts of chitin are mixed with ten parts of 50% NaOH and 100 parts of paraffin at 120 °C for 2 h and the mixture is poured into 80 parts of cold water and washed. The product obtained by this method has a degree of deacetylation of 92% (Muzzarelli 1973 and references therein).

1.6.2. Characterization Methods

Sorption and solubility characteristics of chitosan deviate from one synthesis method to another since the treatment temperature, alkaline concentration and the duration of treatment differ. Each method produces different molecular weights and deacetylation degrees which call attention to the physicochemical characterisation requirements for chitosan.

1.6.2.1. Degree of Deacetylation

Chitosan is characterised by the degree of acetylation (DA) which is the ratio of 2-acetamido-2-deoxy-D-glucopyranose to 2-amino-2-deoxy-D-glucopyranose structural units or by the degree of deacetylation (DD) defined as $DD=1-DA$ (Kumar 2000). The DA has an influence on all the physicochemical properties such as molecular weight, viscosity and solubility; therefore, the determination of DA or DD is of crucial importance (Planas 2002). The major techniques for this purpose are IR spectroscopy (Pedroni, et al. 2003, Khan, et al. 2002), ¹H NMR (Tolaimate, et al. 2000, Hwang, et al. 2002, Pedroni, et al. 2003), UV spectroscopy (Pedroni, et al. 2003, Khan, et al. 2002), elemental analysis (Kasaai, et al. 2000, Jiang, et al. 2003) and titrimetric methods (Pedroni, et al. 2003, Khan, et al. 2002, Jiang, et al. 2003).

1.6.2.2. Molecular Weight

Molecular weight of chitosan is influenced primarily from the source of chitin and the treatment conditions applied in the synthesis (Weska, et al. 2007). The difficulty of determination of molecular weight of natural polymers due to wide range of

molecular weight distribution, thermodynamic deviations from ideal conditions, structural diversity, and strong intermolecular interactions is reported in literature (Tsaih and Chen 1999, and references therein). The primary methods for the determination of molecular weight are light scattering, membrane osmometry, size exclusion chromatography and viscosimetric (Hwang, et al. 2002, Kasaai, et al. 2000). Static light scattering is the most accurate one with the advantage of requiring no standart sample. However, dust contamination and aggregation tendency of polymer may cause interferences (Tsaih and Chen 1999, and references therein). Viscosimetry provides a simple method for molecular weight determination in which the viscosity average molecular weight of chitosan can be determined using the Mark-Houwink-Sakurada's empirical equation which relates the intrinsic viscosity to the molecular weight (Weska, et al. 2007). Another method is high-performance size exclusion chromatography which necessitates the use of calibration standards (Tsaih and Chen 1999).

1.6.2.3. Solubility

Chitosan is insoluble in organic solvents, bases, concentrated acids (except H₂SO₄) and water in the form of free amine (Kumar 2000, Planas 2002). On the other hand, it is soluble in dilute mineral acids such as HCl, HBr, HI, HNO₃, HClO₄ and some organic acids such as formic, acetic, lactic, pyruvic, and oxalic acids (Kurita 2006).

1.6.2.4. Crystallinity

It is difficult to find reproducible information on sorption performance since the characteristics of commercial chitosan materials are variable and this may explain the discrepancies observed between the different studies (Jaworska, et al. 2003). X-ray powder diffraction pattern of chitosan show a strong reflection at an angle (2θ) of 10.4° for hydrated crystal and less intense peaks at 20° and 22°, anhydrous crystal exhibited a strong peak at (2θ) of 15° and a peak supplementer at 20°. Amorphous chitosan does not show any reflective, but it exhibits a broad halo at 20° (Planas 2002). Jaworska and co-workers. showed that the crystallinity of chitosan sample depends on its source, fraction of acetylation and dissolving / drying procedures strongly influence the XRD patterns. The chain packing, crystallinity and deacetylation control the number of available free

amine groups and accessibility of water and metal ion to the sorption sites that may affect the sorption equilibrium (Jaworska, et al. 2003, Jaworska, et al. 2003).

1.6.3. Immobilization Methods

Immobilization of chitosan onto supporting surfaces plays a very important role in its use as a column material and increasing surface area of sorbent. Dip coating is one of the most known methods for immobilization of chitosan onto supporting surfaces. For example, Boddu and co-workers used ceramic alumina for chitosan coating and obtained composite materials which were used in the removal of As(III)/As(V), Cr(VI) from water and adsorption of heavy metals from wastewaters (Boddu, et al. 2008, Boddu and Smith, Boddu, et al. 2003). Liu and co-workers, immobilized chitosan onto nonporous glass beads through 1,3-thiazolidine linker in content of 0.73% (w/w) (Liu, et al. 2003). Another chitosan modification method of glass beads was realized by crosslinking chitosan with gluteraldehyde onto glass beads functionalized with aminopropyltriethoxysilane (Liu, et al. 2002). Chitosan content on the beads was measured as 0.3% (w/w).

Chitosan immobilization methods be sol-gel process are commonly known. These methods are used to increase the mechanical strength during preparation of biosensors as enzyme immobilization support (Miao and Tan 2001, Chen, et al. 2003, Wang, et al. 2003, Krajewska 2004, Yang, et al. 2004, Tan, et al. 2005, Xu, et al. 2006). The same immobilization method can be adapted for sorption studies keeping in mind that these methods are time consuming.

Sodium silicate was used as an immobilization matrix for plant coriander which is known as effective sorbent for removal of mercury form aqueous media. Easy formation and controllable immobilization onto sodium silicate makes it an interesting material in sorption studies (Karunasagar, et al. 2005). Sodium silicate shows sorption properties towards various heavy metals; however, it is difficult to interpret the sorption characteristic of the sorbent when it is immobilized. In case of arsenic, sodium silicate does not have any affinity for sorption, thus may provide an advantage of using sodium-silicate as an immobilization matrix. Different methods can be used for immobilization onto silica. Sol-gel method is time consuming while sodium silicate formation has an

ability of immobilizing wide range of sorbents with a short synthesis time and ease application.

1.7. Novel Amine-Containing Sorbents / Pore-Controlled Templates

Immobilization of chitosan onto silicate surfaces has advantages for preparation of amine containing novel resins for column study of arsenic and other species that are sorbed by chitosan. Previously used immobilization methods for chitosan on silicate surfaces resulted in a low amount of biosorbent (Liu, et al. 2002, Liu, et al. 2003) and enhanced introduction of chitosan to silicate surfaces can be achieved by increasing the specific surface area of supporting silicate surfaces. Macroporous silicate particles have large specific surface area for binding chitosan and other amine-containing functional groups. Synthesis of macroporous structures can be done by templating with latex particles. The size of latex particles controls the final pore volume of silicate. The term latex is used for any polymeric emulsion or polymer colloid. Polymer colloids are obtained by heterophase polymerization such as emulsion, micro-/mini-emulsion or suspension polymerization. Synthesis of uniform and monodisperse latexes which are stable in varying particle size is the advantage of miniemulsion method among the other polymerization methods (Munoz-Espi 2006).

1.7.1. Fundamentals of latex particles

1.7.1.1. Miniemulsion polymerization

Emulsion is a system of dispersed liquid droplets in another immiscible liquid. Generally, dispersed phase is organic and continuous phase is water and this type is known as “oil-in-water” emulsion. The reverse case is also possible and known as “water-in-oil” emulsion (O dian 2004, Munoz-Espi 2006).

Emulsion polymerization is classified in three types. Macroemulsion produces particles in a range of 1-100 μm with short stability time. Miniemulsion is a critically stabilized system with particle size range of 50-500 nm and microemulsion is the most stable system with particle size in a range of 10-100 nm (Landfester 2001). Figure 1.4 shows the relative stability of different droplet size as a function of time.

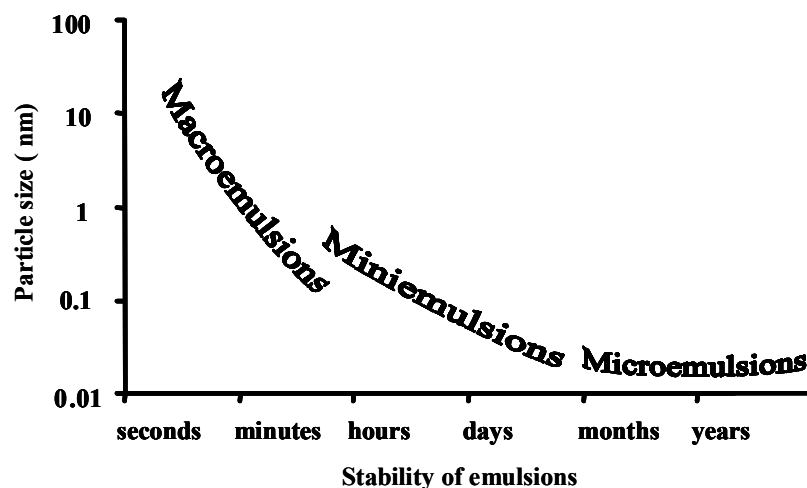


Figure 1.4. Effect of particle size on the stability for different types of emulsion
(Source: Munoz- Espi 2006)

1.7.1.2. Mechanism of Polymerization

Free radical polymerization can be conveniently carried out in heterogeneous media. Reaction mechanism consists of initiation, propagation and termination steps (Solomons and Fryhle 2000). Radicals are created in the chain initiation step (Figure 1.5). In the propagation step, one benzylic radical generates the other by the addition of initially formed radicals to the less substituted end of the double bond (Figure 1.6). Termination steps involve disproportionation or combination between two radicals (Figure 1.7) (Solomons and Fryhle 2000, Munoz-Espi 2006).

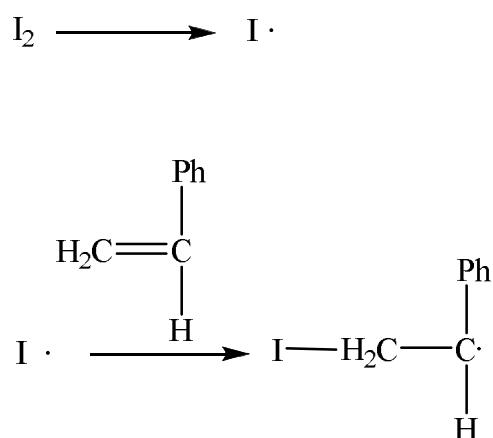


Figure 1.5. Initiation steps

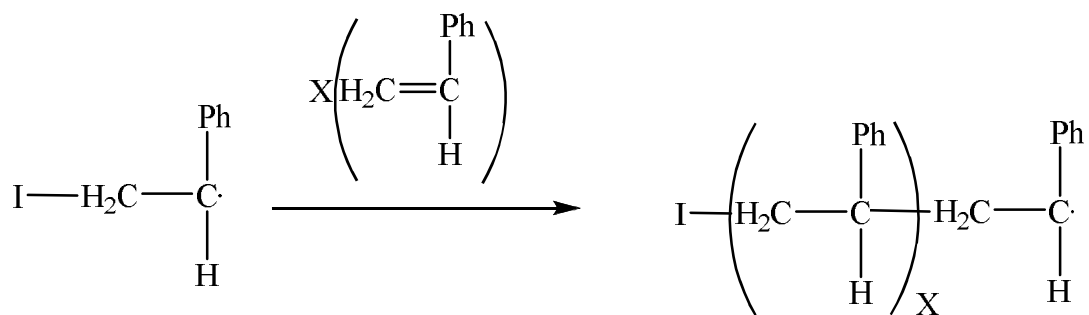


Figure 1.6. Propagation step

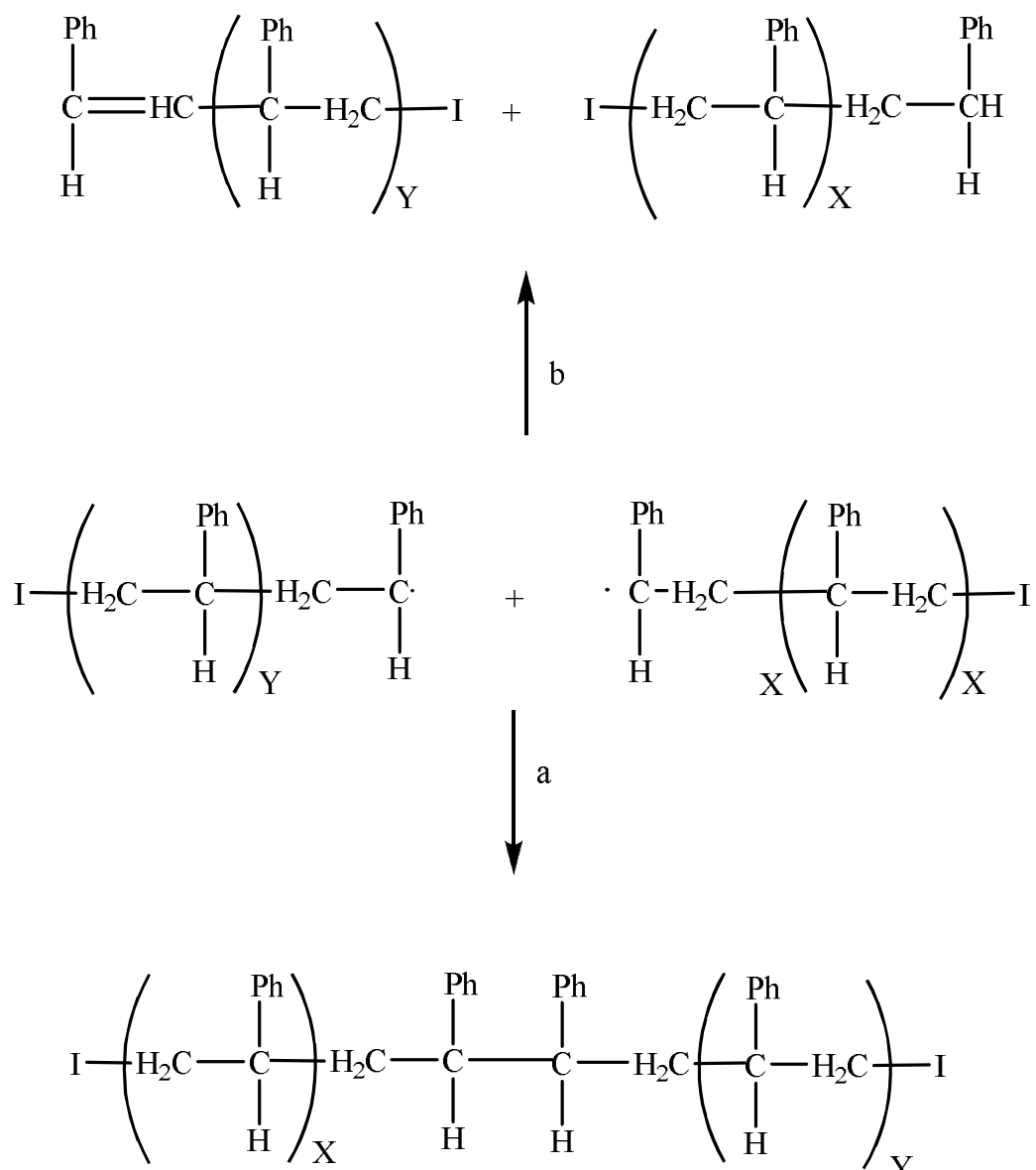


Figure 1.7. Termination steps

1.7.1.2.1. Initiators and Monomers Used in Free Radicalic Polymerization

Generally two types of initiators are used in free radical polymerization, azocompounds and peroxides. Initiators are sorted also as water soluble or oil soluble (Landfester 2001). Commonly used initiators and monomers used in polymerization are given in Table 1.1 and 1.2.

Table 1.1. Initiators usually used in microemulsion polymerization
(Source: Munoz-Espi 2006)

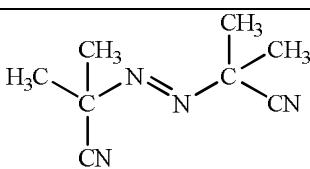
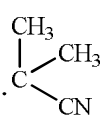
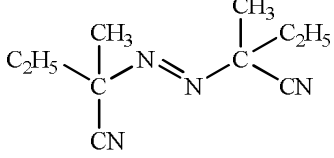
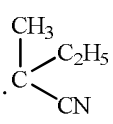
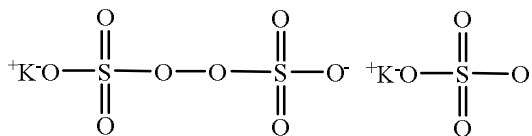
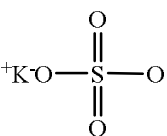
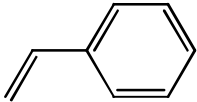
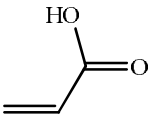
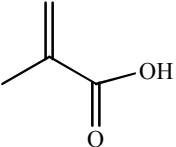
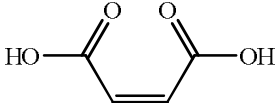
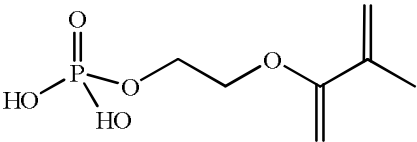
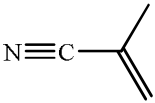
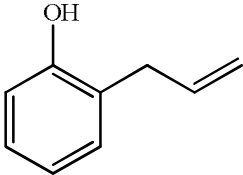
	Chemical structure	Radicals generated	Solubility in water (g/L) at 20 °C
AIBN 2,2-azobis(isobutyronitrile)			insoluble
AMBN 2,2-azobis(2- methylbutyronitrile)			insoluble
K ₂ S ₂ O ₈			52

Table 1.2. Some monomers used in microemulsion polymerization
(Source: Munoz- Espi 2006)

Monomer	Chemical structure	Solubility in water (g / L) at 20°C
Styrene		0.2
Acrylic acid		1000
Methacrylic acid		soluble
Maleic acid		788
Ethylene glycol methacrylate phosphate		-
Methacrylonitrile		25.7
2-allylphenol		7

1.7.1.3. Particle Nucleation Mechanisms

Micellar, homogeneous and droplet nucleation are the proposed mechanisms for particle formation (Munoz-Espi 2006). In micellar nucleation, radicals generated in water phase react with monomer by entering into monomer-swollen surfactant micelles. In homogeneous nucleation radicals are produced in water phase and react with monomer to produce water soluble oligomers. Oligomers act as nucleation sites and it is important in surfactant-free emulsion. In the droplet nucleation radicals enters the monomer and react as a nanoreactor (Antonietti and Landfester 2002, Munoz-Espi 2006).

1.7.1.4. Stability of Miniemulsion

Mainly two processes lead to destabilization of emulsion indicated by the formation of larger particles than initially formed; coalescence and Ostwald ripening. Coalescence occurs as a result of collisions between two droplets and produce larger droplets due to van der Waals attraction forces (Munoz-Espi 2006). Suppression is achieved by addition of surfactant to emulsion mixture. Ostwald ripening is a process of mass diffusion of oil phase if the small droplets are not stabilized against diffusional degradation. Suppression of Ostwald ripening can be achieved by the addition of small amounts of a third component called co-surfactant, which must be highly monomer soluble and water insoluble (Landfester 2001).

1.7.1.5. Synthesis of Polystyrene Nanoparticles

Tissot and co-workers. synthesised polystyrene by emulsion polymerization of styrene by using KPS ($K_2S_2O_8$) as initiator and Ralufon as surfactant at 70 °C and obtained 80% conversion (Tissot, et al. 2002). The requirement of surfactant removal steps is the main drawback of this method. Surfactant-free miniemulsion method is commonly used for synthesis of uniform polystyrene nanoparticles. For stabilization of surfactant-free emulsion styrene monomers were polymerized in the presence of sodium p-styrene sulphonate which acts as emulsifier and stabilizer during reaction (Nakamura, et al. 2005). In another study monodisperse polystyrene nanoparticles are synthesized

by using potassium persulphate as water soluble initiator and potassium bicarbonate as buffer. Varying the amount of co-monomer and by keeping all other parameters fixed, polystyrene nanoparticles with different sizes are produced. Increasing the co-monomer amount decreases the size of particles (Yi, et al. 2001). As an alternative method for synthesis of polystyrene nanoparticles was tried by Zhang and co-workers which was carried out polymerization in a microwave oven. The use of microwave was produced polystyrene nanoparticles with narrow size distribution without necessitating surfactant and emulsifier (Zhang, et al. 1997). Holland and co-workers, studied the effect of stirring speed to particle size while all other conditions are kept constant in surfactant free method and reported that increasing the stirring speed during polymerization decreases the size of particles (Holland, et al. 1999).

1.7.2. Fundamentals of Template Supported Ordered Silica Network

Synthesis of macroporous materials was thought to have a crucial importance on the basis of their large surface area for functionalization of silicate surface.

1.7.2.1. Synthesis Methods

Generally, sol-gel silicate formation route is applied in silicate template synthesis which is followed by functionalization. Gundiah used polymethylmethacrylate bead as template for synthesis of silica-alumina composite with mesoporous walls. Silica-alumina gel was synthesized in presence of cationic surfactant N-cetyl-N,N,N-trimethylammonium bromide under base-catalyzed sol-gel reaction. Composites were obtained by removing template with calcination at 400 °C for 2 h (Gundiah 2001). Wu and co-workers synthesized magnetic hollow silica particles by using polystyrene beads as template for obtaining hollow particles instead of calcination. Polystyrene beads were removed by extractive dissolution in toluene (Wu, et al. 2006). Holland and co-workers used tetraethoxysilane (TEOS) and tetramethoxysilane (TMOS) as precursor for silicate network synthesis under hydrolysis condition. Final silicate with larger inorganic content were obtained for nearly equiweighted mixture of TEOS / alcohol and 100% TEOS (Holland, et al. 1999).

1.7.2.2. Silane Chemistry

Silica is the main constituent of most rocks and most common substance on earth (El-Nahhal and El-Ashgar 2007). General form of silica contain four oxygen atoms connected in tetrahedral form.

1.7.2.2.1. Synthesis of Sol-Gel

Sol-gel is a method for synthesis of ceramic material known for 150 years. It involves the synthesis of inorganic compounds through the formation of colloidal suspension named sol and gelation of sol to form interconnected solid matrix known as gel (Brinker and Scherer 1990, Lev, et al. 1995). Alkoxysilanes $\text{Si}(\text{OR})_4$ are used as a precursor for silica synthesis which avoids the formation of salts as side products that are major limitation of silica gel synthesis from sodium silicate (El-Nahhal and El-Ashgar 2007).

Silica sols are formed by tetraalkoxysilanes with water. Condensation forms stable colloidal particles and as condensation proceeds three dimensional siloxane networks are formed which increase the viscosity of solution (Donatti, et al. 2006). The resulting gel is named as hydrogel and is constituted by a coherent solid silica network impregnated by a liquid phase (contain solvent and the reaction by-product). Conditions like temperature, pH of the medium, nature of the solvent, water content, type of the starting alkoxide and drying conditions are effective on hydrogel structure (Barreau and Miller 1996, Brinker and Scherer 1990). Xerogel is the next step of the process which is obtained by aging or drying hydrogel (pore filling solvents are removed). Porosity and surface area are affected from the aging and drying conditions such as temperature, pH and concentration of the hydrogel particles. If hydrogel is dried under supercritical conditions, aerogel is formed with large surface area and low density (Brinker and Scherer 1990).

First step in sol-gel process is the hydrolysis reaction which occurs while alkoxide precursor is mixed with water in the presence of alcohol to achieve sufficient homogenization. Hydrolysis leads to the formation of silanol groups (Figure 1.8). Intermediates produced in the alcohol-water medium include silanols, ethoxy silanols

and oligomers of low molecular weight which were formed at the first stages of the process.

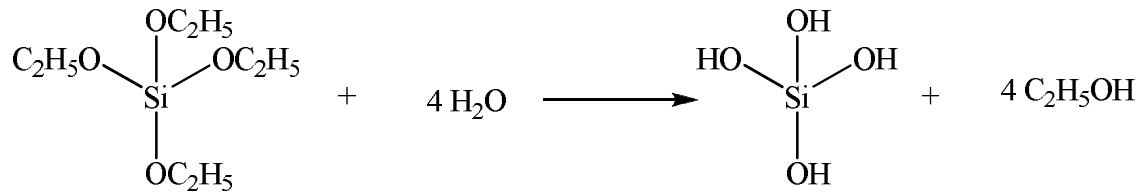


Figure 1.8. Hydrolysis step of sol-gel process

Hydrolysis reactions can be done either by acid or base catalysis. Figure 1.9 and 1.10 show acid- and base-catalyzed mechanism of hydrolysis. Two hydrolysis processes give different structures and morphology; acid catalysis form linear weakly cross-linked polymer, whereas base catalysis form more highly branched clusters as a result of rapid hydrolysis step (Brinker, et al. 1990).

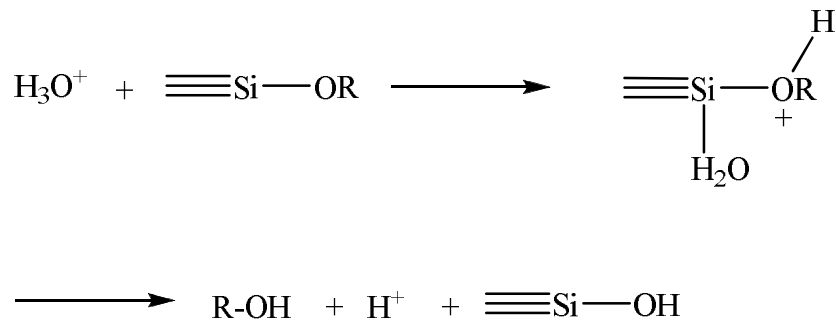


Figure 1.9. Acid catalyzed proposed mechanism of hydrolysis

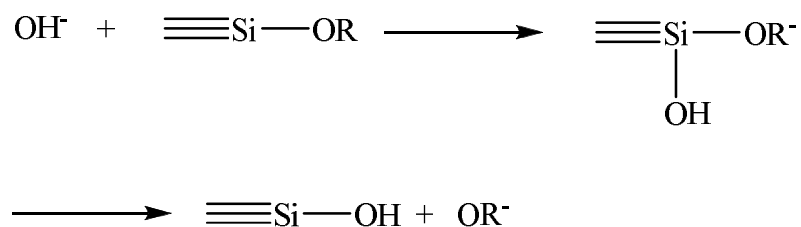


Figure 1.10. Base catalyzed proposed mechanism of hydrolysis

Second step of sol-gel synthesis is the polycondensation between the two silanol groups and condensation reaction between silanol and alkoxyde groups by releasing a water or alcohol unit, respectively (Figure 1.11). Further condensation results in SiO₂ network (Figure 1.12) (Hench and Vasconcelos 1990, Pajonk 2003, El-Nahhal and El-Ashgar 2007).

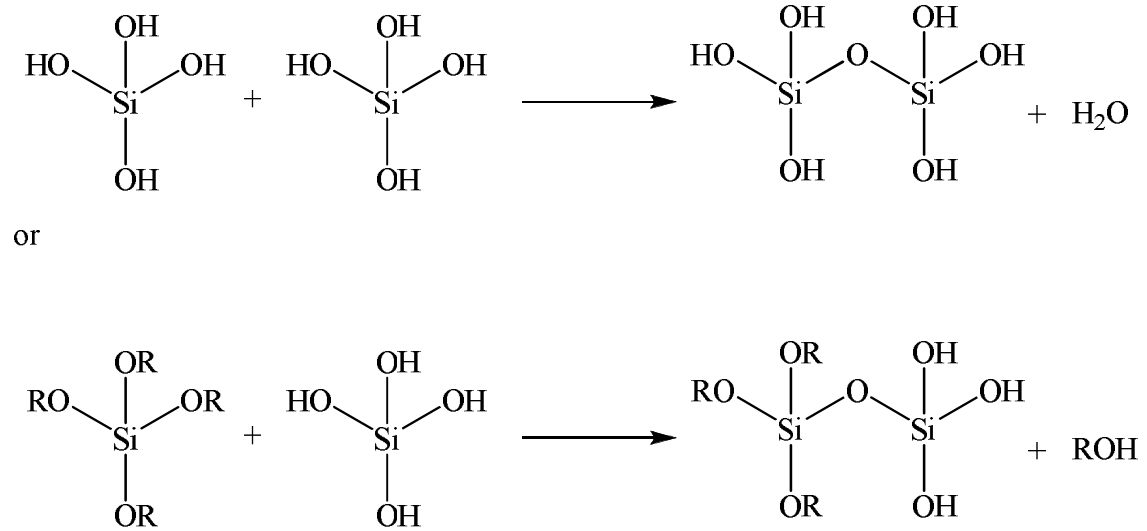


Figure 1.11. Condensation step of sol-gel process

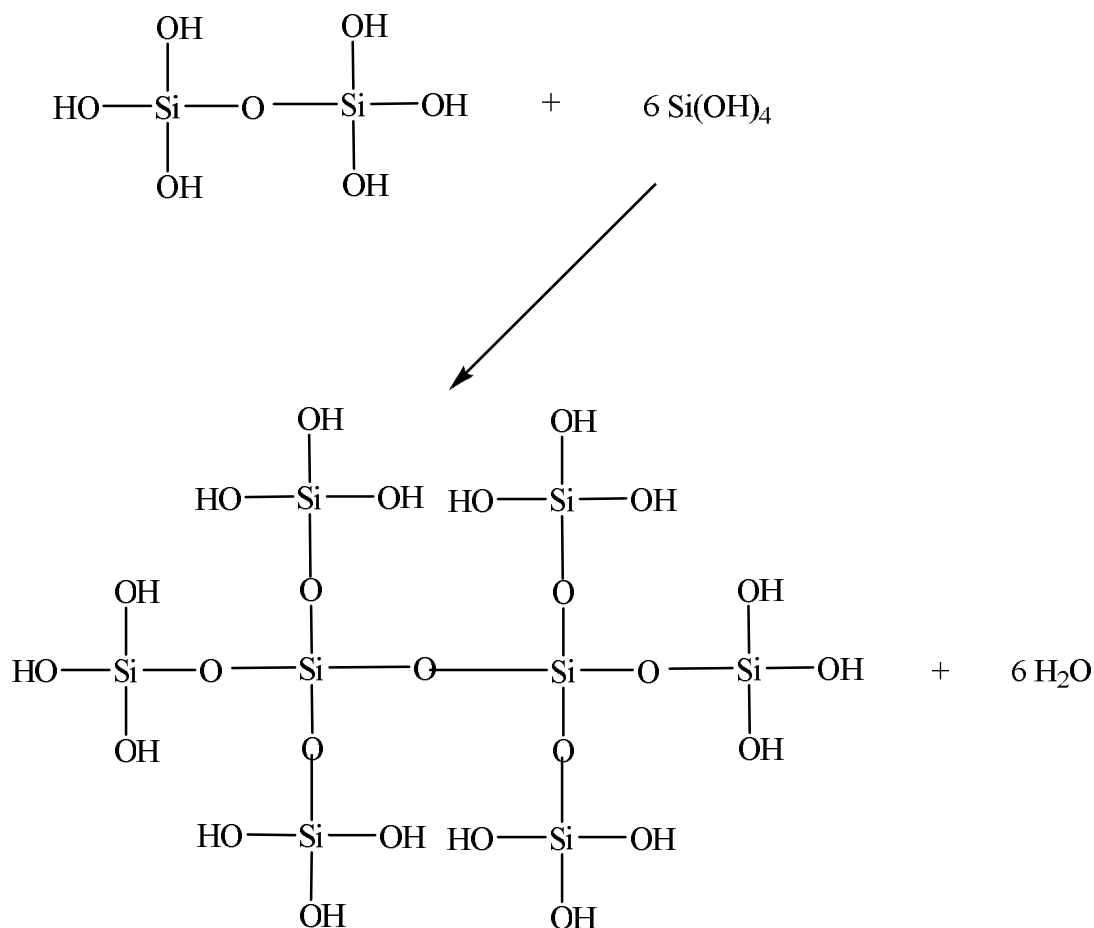


Figure 1.12. Polycondensation of condensed silanol to produce silica network

1.7.2.2.2. Modification of Silica Surface

Silicate surface contains silanol (Si-OH) or siloxane (Si-O-Si) groups which are capable to couple with organo-silanes. Silane coupling agents combine with surface silanol groups to form organic-inorganic network. However, bond formation is not completed until heat is applied to achieve complete bond formation between surface silanol groups and alkoxyde groups of coupling reagents (Figure 1.13). Two strategies are used for the modification of silica network; first route is the post treatment of polysiloxane with coupling reagent (Figure 1.14), and the second route is mixing tetraalkoxy silane with coupling reagent in alcoholic solution in presence of catalyst (Figure 1.15) (El-Nahhal and El-Ashgar 2007).

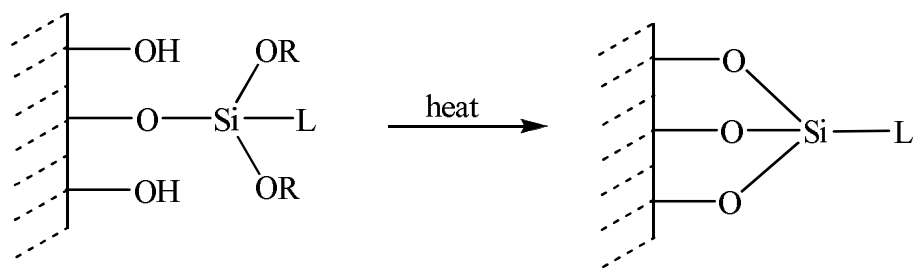


Figure 1.13. Increasing strength of bond formation in modification step

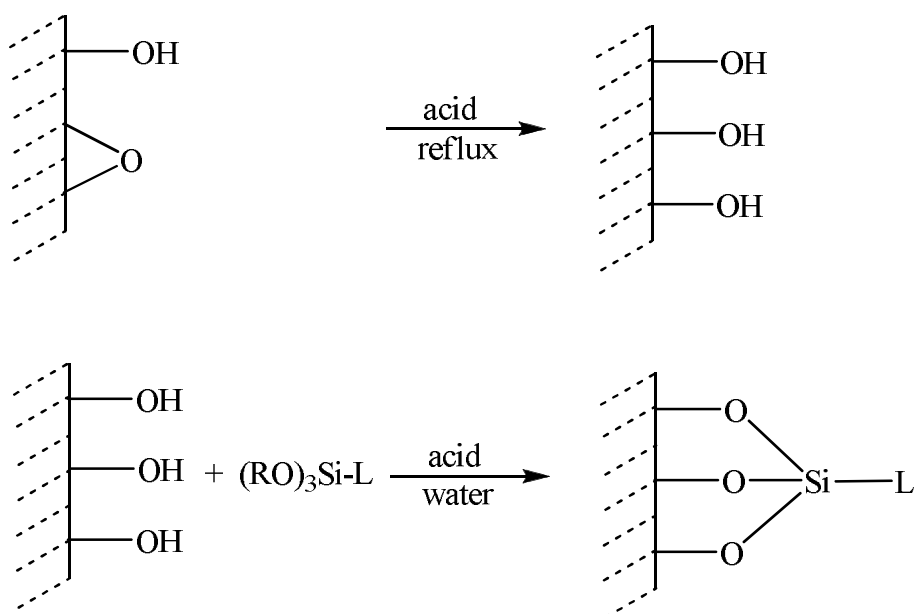


Figure 1.14. Activation of silicate surface and post modification of silanol

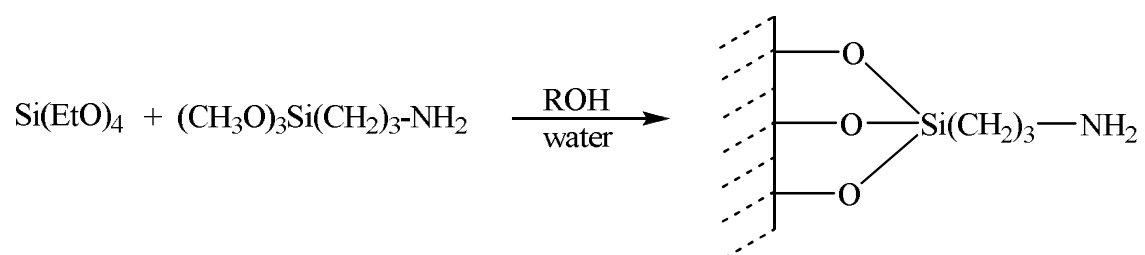


Figure 1.15. Modification of silicate in situ

1.8. Aim of This Work

The objective of this study is to develop new amine-containing sorbents for sorption of arsenate ion from waters. For this purpose initiating studies were started with chitosan, a amine functional group bearing natural polymer. The optimization of working parameters for arsenate sorption by chitosan was performed as: working pH, sorption temperature, sorption capacity, shaking time, amount of sorbent, successive loading of arsenate. The effect of ionic strength and potential interference ions on the sorption of arsenate were also studied. Speciation of arsenic species and validation of method were carried out. After sorption characteristics of chitosan was investigated the new-amine containing sorbents were prepared by two different routes. The first way was to immobilize chitosan sorbent onto polysilicate matrix. The second way that was used for development of new amine-containing sorbents was functionalization of macroporous silicate obtained by colloidal templating of polystyrene nanoparticles via sol-gel process. After characterization of novel sorbents their sorption properties were investigated at conditions optimized for arsenate removal by chitosan.

CHAPTER 2

EXPERIMENTAL

2.1. Apparatus

A Thermo Elemental Solaar M6 Series atomic absorption spectrometer (Cambridge, UK) with an air-acetylene burner was used in arsenic determinations utilizing the Segmented Flow Injection Hydride Generation (SFI-HGAAS) unit (Figure 2.1). An arsenic hollow cathode lamp at the wavelength of 193.7 and a deuterium lamp were employed as the source line and for background correction, respectively. In HGAAS, the quartz tube atomizer was 10 cm long, 8 mm in internal diameter and 10 mm in external diameter with a 4 mm a bore inlet tube fused at the middle for sample introduction. Air-acetylene flame was used for heating the quartz tube externally and nitrogen was used as the carrier gas. Operating parameters for the HGAAS system are given in Table 2.1.

In batch sorption studies, GFL 1083 water bath shaker (Burgwedel, Germany) equipped with microprocessor thermostate was used to provide efficient mixing. The elemental composition of chitosan was determined by LECO-CHNS-932 elemental analyzer (Mönchengladbach, Germany). Molecular weight determinations were performed in Petrotest capillary viscosimeter (Dahlewitz, Germany). Crystallographic properties were obtained with Philips X'Pert Pro X-Ray Diffractometer (Eindhoven, The Netherland). Interference studies were performed with Agilent 7500ce Series (Tokyo, Japan) inductively coupled plasma mass spectrometer (ICP-MS). IR measurements were performed with Perkin Elmer Spectrum 100 FTIR Spectrometer (Shelton, USA) with pike Miracle Single Reflection Horizontal ATR Accessory. The Diamond/KRS-5 Lens Single Reflection ATR plate was used as a sample holder. Spectra of samples were recorded in the range of 4000-450 cm^{-1} with a resolution of 4 cm^{-1} and scan number of 4. pH adjustments were performed with Ino Lab Level 1 pH meter (Weilheim, Germany). Images of sorbents and polystyrene were taken with Philips XL-30S FEG scanning electron microscope (Eindhoven, The Netherlands). Thermal properties of sorbents were analysed with Perkin Elmer Pyris Diamond

TG/DTA (Boston, MA, USA). Mastersizer 2000, Hydro 2000S (Malvern Worcs, U.K.) was used for determination of size distribution of polystyrene nanoparticles. Point of zero charge of chitosan flakes was determined with Zeta-Meter System 3.0+ (Staunton, USA).

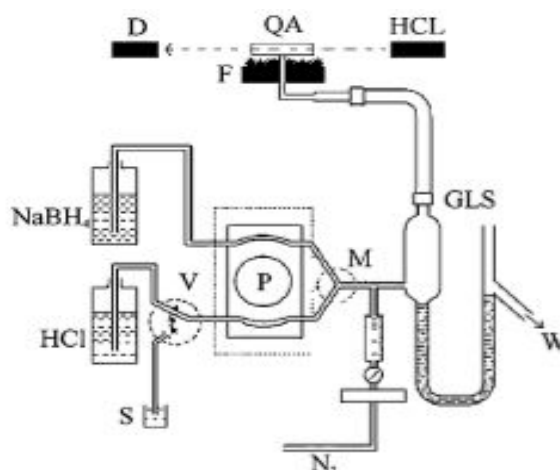


Figure 2.1. Segmented Flow Injection HGAAS system used in arsenic determinations. D: deuterium lamp, QA: quartz atomizer, HCL: hollow cathode lamp, F: flame, GLS: gas-liquid separator, W: waste, P: peristaltic pump, V: three way valve and S: sample
(Source:Yersel, et al. 2005)

Table 2.1. Operating parameters for the segmented flow injection (SFI-HGAAS) system

Operating parameters	
Carrier gas (N ₂) flow rate	200 mLmin ⁻¹
HCl flow rate	6.1 mLmin ⁻¹
HCl concentration	2.0 % (v/v)
NaBH ₄ concentration	1.0 % (w/v) stabilized with 0.10 % (w/v) NaOH
NaBH ₄ flow rate	3.0 mLmin ⁻¹
Sample flow rate	7-8 mLmin ⁻¹

2.2. Reagents and Solutions

All the chemicals were of analytical reagent grade. Ultra-pure water (18.2 M Ω) was used throughout the study. Glassware and plastic containers were cleaned by soaking in 10% (v/v) nitric acid for 24 h and rinsed with distilled water prior to use. Table 2.2 shows the reagents and their concentrations used through the study.

Standard Te(VI) stock solution (1000.0 mg/L): prepared by dissolving 0.536 g of Na₂TeO₄·2H₂O in ultrapure water and diluted to 250.0 mL with ultrapure water.

Standard Te(IV) stock solution (500.0 mg/L): prepared by pre-reduction of Te(VI) by boiling with 6.0 M HCl.

Standard As(V) stock solution (2000.0 mg/L): prepared by dissolving 0.766 g of As₂O₅ in 1.0% (v/v) HCl and diluted to 250.0 mL with ultrapure water.

Standard As(III) stock solution (2000.0 mg/L): prepared by dissolving 0.659 g of As₂O₃ in 5.0 mL NaOH and 2.5 mL H₂SO₄ and diluted to 250.0 mL with ultrapure water.

Standard Se(VI) stock solution (1000.0 mg/L): prepared by dissolving 0.598 g of Na₂SeO₄ in ultrapure water and diluted to 250.0 mL with ultrapure water.

Standard Se(IV) stock solution (1000.0 mg/L): prepared by dissolving 0.833 g of Na₂SeO₃·5H₂O in 1.0% (v/v) HNO₃ and diluted to 250.0 mL with ultrapure water.

Standard Sb(III) stock solution (1000.0 mg/L): prepared by dissolving 0.685 g of C₈H₄K₂O₁₂Sb₂·3H₂O in ultrapure water and diluted to 250.0 mL with ultrapure water.

Standard Sb(V) stock solution (1000.0 mg/L): prepared by dissolving 0.540 g of KSb(OH)₆ in ultrapure water and diluted to 250.0 mL with ultrapure water.

Chitosan flakes were prepared by refluxing a mixture of 15.0 g practical grade chitin containing 720.0 mL of 40% (w/w) NaOH solution for 6 h at 115 °C.

Polystyrene nanoparticles were synthesized from styrene and K₂S₂O₈. Silica coating of polystyrene nano particles were performed with tetraethyl orthosilicate via sol-gel process by supporting coating with triblock co-polymer surfactant Pluronic F-127 and co-surfactant N-pentane.

Sodium borohydrate solution of 1.0% (w/v) was prepared for a daily usage from fine granular product and stabilized by 0.10% (w/v) NaOH in water. L-cysteine at a

concentration of 0.50% (w/v) was added to all standards and samples to reduce As(V) to As(III) before HGAAS determinations.

N,N-Dimethylacetamide containing 5.0% (w/v) LiCl and 0.200 M NaCl containing 0.100 M acetic acid were used in molecular weight determination of chitin and chitosan, respectively.

Toluene was dried in a soxhlet extractor with a piece of sodium metal wire in the presence of benzophenone. Benzophenone functioned as an indicator of the completeness of the drying process in a way that when toluene is dried completely benzophenone forms radicals which impart a violet-blue colour to the solvent. After three recycles, drying step was completed and toluene was separated from benzophenone and Na metal and collected in the reservoir of the soxhlet extractor. All glassware utilized in the drying step was dried at 100 °C for 24 h before use.

Table 2.2. Reagents used through the study

Reagent	Concentration used	Company	Product Code	CAS no.	Purpose of use
Chitin (practical grade, from crab shell)		Sigma	C-923	[1398-61-4]	Chitosan synthesis and using as a sorbent
NaBH ₄ (granular)	1.0 % (m/v)	Merck	8.06373	[16940-66-2]	AsH ₃ generation in HGAAS
NaBH ₄ (granular)		Merck	8.06373	[16940-66-2]	Reducing of imine bond during chitosan modification of macroporous silicate
NaOH (pellets)	0.10 % (m/v)	Merck	1.06498	[1310-73-2]	Stabilization of NaBH ₄ solution
L-cysteine	0.50 % (w/v)	Merck	1.02838	[52-90-4]	Reduction of As(V) to As(III)
BaCl ₂ .2H ₂ O	0.200 M	Riedel-deHaen	11411	[10326-27-9]	Sulphate ion detection during chitosan immobilization onto polysilicate matrix
N,N-Dimethylacetamide (min. 99%)		Sigma	D 5511	[127-19-5]	Molecular weight determination of chitin
LiCl (99% + A.C.S. reagent grade)	5.0 % (m/v)	Aldrich	310468	[7447-41-8]	Molecular weight determination of chitin
NaCl	0.200 M	Riedel-de Haen	13423	[7647-14-5]	Molecular weight determination of chitosan
NaCl	0.100 M	Riedel-de Haen	13423	[7647-14-5]	Determination of effect of ionic strength on sorption of As(V) by chitosan
NaCl	0.010 M	Riedel-de Haen	13423	[7647-14-5]	Determination of effect of ionic strength on sorption of As(V) by chitosan
NaCl	0.001 M	Riedel-de Haen	13423	[7647-14-5]	Determination of effect of ionic strength on sorption of As(V) by chitosan

(cont. on next page)

Table 2.2. (Cont.) Reagents used through the study

Reagent	Concentration used	Company	Product Code	CAS no.	Purpose of use
Styrene		Merck	8.07679	[100-42-5]	Monomer in synthesis of polystyrene nanoparticles
K ₂ S ₂ O ₈		Merck	1.05091	[7727-21-1]	Initiator in synthesis of polystyrene nanoparticles
Tetraethyl orthosilicate (TEOS)		Fluka	86580	[78-10-4]	Sol-gel synthesis for coating polystyrene nanoparticles
Pluronic F-127		Sigma	P-2443	[9003-11-6]	Surfactant for coating polystyrene nanoparticles
N-pentane (95%)		Merck	1.07176	[109-66-0]	Co-surfactant for coating polystyrene nanoparticles
3-(Triethoxysilyl) propylamine (APTES)		Merck	8.26619	[14814-09-6]	Functionalization of silicate surface
(3-Mercaptopropyl) trimethoxysilane		Fluka	63800	[4420-74-0]	Functionalization of silicate surface
Methanol		Fluka	65541	[67-56-1]	Washing of unreacted reagents after glutaraldehyde step in macroporous silicate
Toluene		Riedel-de-Haen	24529	[108-88-3]	Washing of unreacted reagents after amine modification step in macroporous silicate
Acetone		Merck	1.00014	[67-64-1]	Washing of unreacted reagents after amine modification step in macroporous silicate
HCl		Merck	1.00314	[7647-01-0]	Hydrolysis of TEOS during coating of polystyrene nanoparticles
HCl	0.300 M	Merck	1.00314	[7647-01-0]	Determination of DD of chitosan

(cont. on next page)

Table 2.2 (Cont.) Reagents used through the study

Reagent	Concentration used	Company	Product Code	CAS no.	Purpose of use
HNO ₃ (65%)		Merck	1.00456	[7697-37-2]	Oxidation of As(III) to As(V)
NaOH	40.0 % (w/w)	Merck	1.06498	[1310-73-2]	Chitosan synthesis
NaOH	0.100 M	Merck	1.06498	[1310-73-2]	Extraction of inhibitor from styrene and titration of chitosan solution (determination of D.D.)
Acetic acid	2.0 % (v/v)	Riedel-de Haen	27225	[64-19-7]	Preparation of chitosan solution and various desorption solutions
Acetic acid	0.01M	Riedel-de Haen	27225	[64-19-7]	Activation of macroporous silicate
Dichloromethane		Riedel-de Haen	24233	[75-09-2]	Washing of unreacted reagents after amine modification step in macroporous silicate
Unhydrous CaCl ₂		Smyras	1620100	[10043-52-4]	Providing dry conditions for amine modification of macroporous silicate
Glutaraldehyde (25% aq.)		Alfa Aesar		[111-30-8]	Cross-linking agent for chitosan modification of macroporous silicate
SRM (Trace elements in natural water)		NIST	1640		Investigation of performance of the study
H ₂ SO ₄ (95-97%)	5.0 % (v/v)	Riedel-de Haen	07208	[7664-93-9]	Synthesis of polysilicate matrix for chitosan immobilization
As ₂ O ₅		Merck	1.09939	[1303-28-2]	Preparation of As(V) stock solution for sorption study
As ₂ O ₃		Fischer		[1327-53-3]	Preparation of As(III) stock solution for sorption study

(cont. on next page)

Table 2.2 (Cont.) Reagents used through the study

Reagent	Concentration used	Company	Product Code	CAS no.	Purpose of use
$\text{Na}_2\text{TeO}_4 \cdot 2\text{H}_2\text{O}$		Aldrich	41058-6	[26006-71-3]	Preparation of Te(VI) stock solution for Interference and sorption study
V(V) 1000 $\mu\text{g}/\text{mL}$		High-Purity Standards	100065-1		Interference and sorption study
Mo(VI) 1000 mg/L		Merck	1.70227		Interference and sorption study
Potassium antimonyl tartrate trihydrate		Sigma-Aldrich	P-6949	28300-74-5	Preparation of Sb(III) stock solution for interference and sorption study
Potassium antimonate		Riedel-de Haen	31149	[12208-13-8]	Preparation of Sb(V) stock solution for interference and sorption study
Duolite GT-73		Supelco	1-0354	[113834-91-6]	Sorption of As(III) in speciation study
Acetic acid (Glacial)	0.100 M	Riedel-de Haen	27225	[64-19-7]	Molecular weight determination of chitosan
Sodium silicate solution (27 %)	6 %	Sigma-Aldrich	338443	[1344-09-8]	Immobilization of chitosan onto polysilicate matrix
HCl	2.0 M	Merck	1.00314	[7647-01-0]	Desorption of As(III) from Duolite GT-73
HNO_3 (65%)		Merck	1.00456	[7697-37-2]	Acidification
$\text{Na}_2\text{SeO}_3 \cdot 5\text{H}_2\text{O}$		Merck	1.06607	[26970-82-1]	Preparation of Se(IV) stock solution for interference and sorption study
Na_2SeO_4		Fluka	71948	[13410-01-0]	Preparation of Se(VI) stock solution for interference and sorption study

2.3. Synthesis and Characterization of Chitosan

2.3.1. Synthesis

Chitosan flakes were synthesized from chitin under inert atmosphere by the method of Rigby and Wolfrom given in the monograph by Muzzarelli (1973). Briefly, 15.0 g of chitin were treated with 720 mL of 40.0% (w/w) aqueous NaOH solution in a one liter three-necked round bottomed flask with reflux condenser connected to its middle neck. A thermometer was connected to control the temperature during reaction and N₂ gas was bubbled through the solution from the side arm to provide inert atmosphere in the reaction medium. Constant reflux was obtained at 115 °C and continued for 6 hours. After cooling the alkaline mixture to room temperature, chitosan flakes were washed with distilled water until a neutral filtrate was obtained. Resulting chitosan flakes were dried at 60 °C for 2 h before use.

2.3.2. Characterization

A variety of methods was applied for the characterization of synthesized chitosan flakes. Infrared spectroscopy was used for qualitative observation of acetyl groups whether they are removed from chitin or not during the synthesis. Elemental analysis and potentiometric titrimetry were used for determination of degree of deacetylation which controls the solubility and sorption performance of flakes (Rhazi 2002). Molecular weights of chitin and chitosan were determined by capillary viscosimetry. Images of chitosan, sodium silicate and chitosan-immobilized sodium silicate were taken with scanning electron microscopy (SEM). XRD crystallographic properties and thermal gravimetric degradation were also investigated.

2.3.2.1. Infrared Spectroscopy

Infrared spectra of the dried chitosan and chitin (80 °C for 24 h) were recorded by an FTIR instrument using attenuated total reflectance unit. Characteristic peak positions for each compound are given in Table 2.3.

Table 2.3. IR band positions of some functional groups.
(Source:Solomons and Fryhle 2000)

Functional Group	Frequency range (cm ⁻¹)
O-H	3200-3600 (broad)
C-H	2850-2970 (strong)
N-H	3300-3500 (medium)
Carbonyl (amide)	1630-1690
C-O	1050-1300 (strong)
C-N	1180-1360 (strong)
N-H	1100-800
C-H	1340-1470 (strong)

2.3.2.2. Degree of Deacetylation

For the determination of deacetylation degree of chitosan, two methods, namely potentiometric titration and elemental analysis were performed for comparison.

2.3.2.2.1. Potentiometric Titration

Potentiometric method depends on the the titration of chitosan with standardized NaOH solution which is used to deprotonate positively charged amine groups in chitosan. For this purpose, 250.0 mg portion of chitosan were dissolved in 10.0 mL of 0.30 M HCl and after being diluted to 50.0 mL with ultrapure water, it was titrated with 0.100 M NaOH. The consumed volume of NaOH which corresponds to the amount of amine groups in chitosan is obtained from the difference between two inflection points of acid-base titration (Tolaimate 2000). Equation 2.1 describes the formulation used in the calculation of degree of acetylation (DA). In this equation, 161 is the molecular weight of glucosamine unit of chitosan, 42 is the difference in the molecular weights of chitin and chitosan repeating units, m is the mass of the chitosan sample taken, ΔV is the volume and M is the molarity of NaOH solution. Degree of deacetylation (DD) was calculated from Equation 2.2.

$$AD = \frac{\left(1 - 161 \times \frac{\Delta V \times M}{m}\right)}{\left(\frac{\Delta V \times M}{m} \times 42 + 1\right)} \quad (2.1)$$

$$DD = 1 - AD \quad (2.2)$$

2.3.2.2.2. Elemental Analysis

As it is known, elemental analysis provides the percent concentrations of C, N, H and S in a compound. Deacetylation process removes two carbon atoms and one oxygen atom from chitin structure. Chitosan and chitin structures differ in their C and O contents while N remains constant in both structures. Therefore, C/N ratios are used in the determination of degree of deacetylation by using Equation 2.3 (Kasaai, et al. 2000). Here, 5.145 is the ratio of C/N in completely N-deacetylated chitosan repeating unit and 6.816 is that of N-acetylated chitin repeating unit.

$$D.D. = \left(1 - \frac{C/N - 5.145}{6.816 - 5.145}\right) \times 100 \quad (2.3)$$

2.3.2.3. Molecular Weight Determination

In the determination of molecular weights of chitin and chitosan, viscosimetric method which relates intrinsic viscosity of polymer to its molecular weight according to Mark-Houwink-Sakurada relation (Equation 2.4) was used (Tsaih and Chen 1999, Kasaai, et al. 2000, Taghizadeh and Davari 2006, Weska, et al. 2007).

$$[\eta] = KM_v^\alpha \quad (2.4)$$

In this equation, $[\eta]$ defines the intrinsic viscosity, M_v is the average molecular weight of polymer, K and α are constants which are specific for a given polymer and vary for used solvent system and temperature (Planas 2002). In the method, 0.200 M NaCl/0.100 M HAc solvent system with the above-mentioned constants, $K = 1.81 \times 10^{-3}$, and $\alpha = 0.93$ at 25°C (Taghizadeh and Davari 2006, Kasaai 2007) were used for chitosan. The

corresponding solvent system was 5.0% (w/v) LiCl/DMAC and the related constants were $K=2.4 \times 10^{-1}$, $\alpha=0.69$ for chitin. Viscosimeter constant C was $0.004720 \text{ mm}^2/\text{sec}^2$.

A stock solution of chitosan was prepared in a way that 0.1250 g chitosan flakes were dissolved in 100.0 mL of 0.200 M NaCl/0.100 M HAc solvent system and the lower concentrations (0.000, 0.005, 0.010, 0.025, 0.050, 0.062, 0.080, and 0.100% w/v) were prepared from this stock by serial dilution with the same solvent. The viscosity of the samples was measured in a Petrotest capillary viscosimeter at 25 °C. The capillary viscosimeter was filled with the sample and after being equilibrated in water bath at 25 °C for 10 min, the sample was passed through the capillary for several times and then the running time was measured. The sample or solvent viscosity was calculated from Equation 2.5 using time interval in seconds (t) for the solution to pass between two indicated lines. The sample and solvent viscosity values were used to calculate the specific viscosity by Equation 2.6.

$$\eta_{\text{sample or solvent}} = C(\text{mm}^2 / \text{sec}^2) t(\text{sec}) \quad (2.5)$$

$$\eta_{\text{specific}} = \frac{(\eta_{\text{sample}} - \eta_{\text{solvent}})}{\eta_{\text{solvent}}} \quad (2.6)$$

The reduced viscosity was calculated from Equation 2.7 where c is the concentration of chitosan solution used in viscosity measurement.

$$\eta_{\text{reduced}} = \frac{\eta_{\text{specific}}}{c} \quad (2.7)$$

Huggins equation (Equation 2.8) is used for calculation of intrinsic viscosity (mL/g) which is the intercept of the equation derived from plot of reduced viscosity (mL/g) versus concentrations of chitosan solution (g/mL) (Tsaih and Chen 1999).

$$\eta_{\text{reduced}} = [\eta] + k[\eta]^2 c \quad (2.8)$$

The viscosity average molecular weight of chitosan was calculated according to Mark-Houwink-Sakurada relation (Equation 4) as explained before. The same methodology was applied in the case of chitin using the relevant solvent system and specific constants.

2.4. Immobilization Methods

2.4.1. Immobilization of Chitosan on Sodium Silicate

Polysilicate was used as immobilization matrix as reported in literature (Ülkü, et al. 1993, Karunasagar, et al. 2005). The procedure was as follows; 6.0% (w/w) sodium silicate was added dropwise into 15.0 mL of 5.0% (v/v) H_2SO_4 until pH is risen to 2. The solution pH was checked with pH paper instead of pHmeter in order not to cause any damage to the electrode system due to use of silicate solution. Then, 50.0 mL of 2.0% (w/v) chitosan dissolved in 2.0% (v/v) acetic acid was added dropwise to the silicate solution and the mixture was stirred for 15 minutes. The polymer gel was formed by rising the pH to 7 by dropwise addition of sodium silicate solution. Formed gel was washed with ultrapure water until the solution is free of sulphate ion. This was checked by the addition of 0.200 M BaCl_2 solution to the filtrate. Usually a cloudiness is observed as a result of precipitation reaction between barium and sulphate ions when sulphate is at an appreciable concentration. After the immobilization procedure had been completed, the chitosan-immobilized silicate was dried at 50°C overnight and ground by mortar and pestle before use.

2.4.2. New Amine-Containing Sorbents

2.4.2.1. Pore-Controlled Templates

2.4.2.1.1. Synthesis of Surfactant-Free Polystyrene Nanoparticles

Synthesis of polystyrene nanoparticles was performed by emulsifier-free miniemulsion polymerization method (Holland, et al. 1999). Inhibitor that is used to prevent self polymerization of styrene during storage was removed by extraction with NaOH solution as described in literature (Holland, et al. 1999, Sheng, et al. 2006). Briefly, a 70.0 mL of monomer was extracted with four successive portions of 67.0 mL of 0.100 M NaOH in a separatory funnel, which was followed by extraction with four portions of 67.0 mL of ultrapure water for removal of any traces of NaOH. After extraction the colour of styrene turned to pale yellow as the indication of inhibitor

removal. For synthesis of polystyrene nanoparticles a two liter five necked glass reactor which is shown in Figure 2.2 was used. Ultrapure water (567.0 mL) was placed in the reaction flask and heated to 70 °C. The purified 70.0 mL of styrene was added into the reaction flask and the mixture was equilibrated until the temperature reached to 70 °C. A thermometer was connected to one of the side arms of the reactor to control the reaction temperature. A glass pipe was connected to the other neck of the reactor for bubbling N₂ during the reaction to ensure an inert atmosphere in the reaction medium. The middle neck was used for overhead stirring at 360 rpm and the fourth arm was connected with a condenser to prevent evaporation losses. The last arm was used for introduction of the initiator and closed with glass stopper during the reaction. Water soluble initiator was prepared separately in a polyethylene beaker by dissolving 0.2210 g of potassium peroxodisulphate in 33.5 mL water. The initiator solution was also equilibrated to a temperature of 70 °C before introducing into the reaction flask. The mixture was then stirred at 360 rpm for 28 h under inert atmosphere. The resulting milky emulsion of polystyrene nanoparticles were filtered through glass wool to remove any agglomerates.



Figure 2.2. Five necked reaction flask used in the synthesis of polystyrene nanoparticles

The effects of water/styrene ratio, the reaction time and initiator amount to final particle size were also investigated under the same reaction conditions described above with the changed parameters that were summarized in Table 2.4.

Table 2.4. Effect of water/styrene ratio on particle size

Batch no	Styrene (mL)	Water (mL)	K ₂ S ₂ O ₈ (g)	Styrene/Water/K ₂ S ₂ O ₈ mole ratios	Reaction time (h)	Particle size (nm)
1	105.0	450.0	0.3315	1/27.4/0.0013	20	450
1	105.0	450.0	0.3315	1/27.4/0.0013	24	524
1	105.0	450.0	0.3315	1/27.4/0.0013	28	817
2	70.0	567.0	0.2210	1/51.7/0.0013	28	252
3	70.0	567.0	0.3315	1/51.7/0.0020	28	267

2.4.2.1.2. Synthesis of Ordered Macroporous Silicate

Synthesis of ordered silicate structures was carried out using the polystyrene nanoparticles as template in a sol-gel route with slight modifications of the method described by Sen, et al. (2004). For this purpose, the emulsion of polystyrene nanoparticles was centrifuged at 4000 rpm for 3 h with further drying at 60 °C for 2 hours. A sol-gel hydrolysis solution for synthesis of silicate was prepared by mixing 6.94 g of distilled water with 80.3 µL of concentrated HCl. Acid catalyzed hydrolysis was achieved by the addition of 12.40 g tetraethyl orthosilicate to the acidic solution described in the previous step with magnetic stirring at 500 rpm for 15 minutes. In another polyethylene beaker an amount of 2.4035 g of Pluronic F-127 surfactant were mixed with 3.0 mL of n-pentane as co-surfactant until a clear solution was obtained. The silicate and the surfactant solutions were mixed and stirred for 5 minutes. In order to coat the nanoparticles with silicate, 2.00 g of dried polystyrene was added to this mixture and stirring was continued for a further 15 minutes. The excess of hydrolysis solution was removed after centrifugation of the mixture for 15 min at 6000 rpm. The resulting silicate-coated polystyrene nanoparticles were first dried at 60 °C for 2 h and then were calcined at 550 °C for 10 h by gradual increasing of the temperature at a rate of 1 °C/min in order to obtain ordered macroporous silicate structures.

2.4.2.1.3. Optimization of Synthesis Parameters of Macroporous Silicate Structures

Effect of surfactant, co-surfactant, aging time and calcination conditions on final silicate structures were investigated as described in the following paragraphs and summarised in Table 2.5.

Firstly, a surfactant-free route was followed to see whether it was possible to obtain the ordered macroporous silicate or not. Secondly, significance of presence of surfactant (Pluronic F-127) and co-surfactant (n-pentane) was studied in two schemes. In the first case, both the surfactant and the co-surfactant were added whereas all other variables were kept constant in the method described in section 2.4.2.1.2. In the second case, the surfactant was added while the co-surfactant was not included in the mixture.

Effect of calcination conditions on the silicate structure was investigated by following a similar procedure except the final calcination step. The first approach (gradual increase of the temperature to the final calcination temperature) was explained in section 2.4.2.1.2 whereas the polystyrene removal step was carried out directly at a preset temperature of 550 °C in the second approach.

Effect of aging time on the final silicate structure was investigated by increasing the mixing periods by six times in the given procedure.

Table 2.5. Summary of optimization parameter for ordered macroporous silica

Batch	Polystyrene (g)	H ₂ O/TEOS/HCl (g)/(g)/(μL)	F-127 (g)	Pentane (mL)	Aging time	Calcination
1	2	6.94 / 12.42/ 80.3	2.4	3.0	x	gradual
2	3	6.94/ 12.42/ 80.3	2.4	3.0	x	gradual
3	2	6.94/ 12.42/ 80.3	2.4	3.0	6x	gradual
4	2	6.94/ 12.42/ 80.3	2.4	3.0	x	direct
5	2	6.94/ 12.42/ 80.3	-	-	x	gradual
6	2	6.94/ 12.42/ 80.3	2.4	-	x	gradual

2.4.2.1.4. Functionalization of Macroporous Silicate Structures

The outline of the functionalization of macroporous silicate structure is illustrated in Figure 2.3. The procedure was similar to the one given by Liu, et al. (2002) with slight modifications. The first step was the activation of the surface siloxane groups to silanol. For this purpose, 2.80 g of newly synthesized macroporous silicate (A) was first treated with 50.0 mL of 0.010 M acetic acid and then with ultrapure water until a neutral filtrate was obtained. This step was completed after drying the activated solid (B) at 120 °C for 24 h in a vacuum oven. The modification stage was carried out by mixing 2.50 g of activated silicate, 1.50 mL of APTES and a 10.0 mL portion of dry toluene in a two necked 25 mL flask. A condenser having an anhydrous CaCl₂ drying tube at the top was connected to the reaction flask. The reaction was proceeded under an inert atmosphere provided with N₂ bubbled through the side arm of the flask. The resulting mixture was stirred for 24 h at 100 rpm in an oil bath at a temperature of 80 °C. After the reaction was completed amine treated silicate was washed sequentially with 10.0 mL portions of toluene, dichloromethane and acetone and then air dried for 24 hours (C). Cross-linking agent (9.0 mL of stock 25% glutaraldehyde solution) were mixed with 2.30 g of amine treated silicate in a 50 mL beaker and magnetically stirred at 100 rpm and 25 °C for 1 hour. Afterwards, glutaraldehyde treated silicate was washed with 20 mL of methanol and was dried for 24 h at 80 °C (D). In the last step of the modification process, 2.10 g of glutaraldehyde modified macroporous silicate was treated with 50.0 mL of 2.0% (w/v) chitosan dissolved in 2.0% (v/v) acetic acid by stirring at 100 rpm. During cross-linking of chitosan onto silicate surface a 0.050 g total amount of NaBH₄ was added gradually into reaction medium in a period of 1 h by magnetic stirring at 25 °C. The purpose of adding sodiumborohydride is to achieve a more successive bonding of chitosan onto the surface by reduction of the imine bond. This bond is formed from schiff base reaction between the amine groups of chitosan and the aldehyde groups of the cross-linker (Solomons and Fryhle 2000). Finally, the resulting particles were centrifuged at 6000 rpm for 15 min and were washed with ultrapure water until a neutral supernatant solution was obtained. The functionalization procedure was completed with a drying period of 24 h at 80 °C.

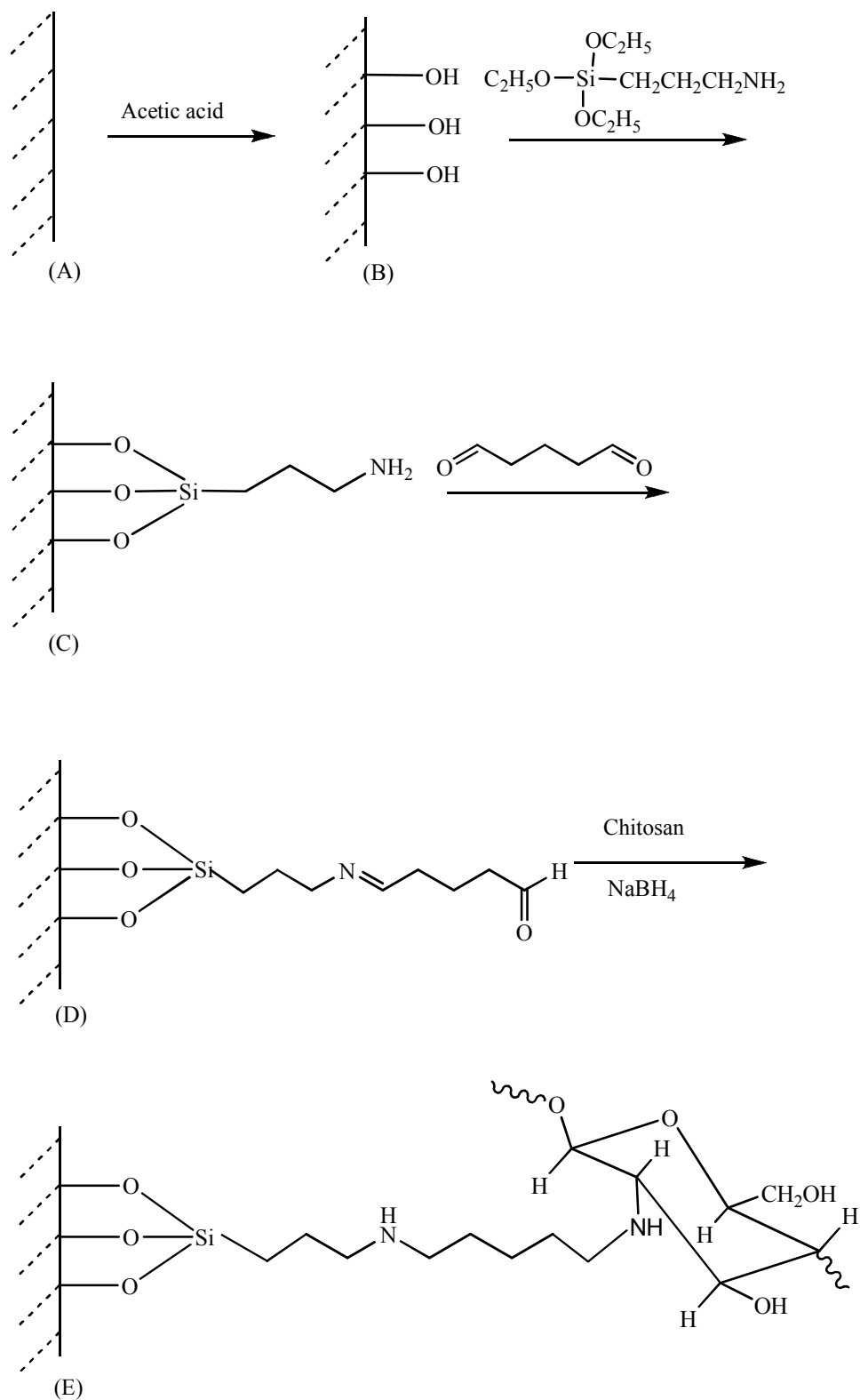


Figure 2.3. Amine modification of mesoporous silicate surface. Ordered mesoporous silicate (A), activated silicate (B), APTES-modified silicate (C), glutaraldehyde-treated silicate (D) and chitosan-modified silicate (E)

2.5. Sorption Studies

Sorption studies were performed for all the sorbents prepared; namely, chitin, chitosan, sodium-silicate and chitosan-immobilized sodium silicate through batch process. Effect of the sorbent amount, shaking time, solution pH, ionic strength, reaction temperature and successive loadings was investigated. In all these experiments, batch sorption was followed by the filtration of the mixture through blue-band filter paper and analysis of the filtrate for its arsenic content after acidification for HGAAS determination. Standard solutions in 2.0, 5.0, 10.0, 20.0 and 40.0 µg/L concentrations were prepared from appropriate dilution of 2000 µg/L of stock As(V) or As(III) solutions to the required volume. Before HGAAS determination all samples and standard solutions were acidified with the addition of appropriate amount of concentrated HCl to produce 1.0% (v/v) HCl in the final solution. For As(V) determination, L-cysteine was also added to all solutions so as to have 0.5% (w/v) concentration in the final solution. The purpose of this addition was to prereduce As(V) to As(III) before NaBH₄ reduction step since efficiency of the HGAAS method depends strongly on the oxidation state of As. The percentage of arsenic sorption was calculated using Equation 2.9, where C_i is the initial and C_f is the final concentration in the solution.

$$\text{Sorption \%} = \frac{C_i - C_f}{C_i} \times 100 \quad (2.9)$$

2.5.1. Effect of Solution pH

Solution pH is one of the most important parameters on the sorption of As species by the sorbents. For this reason, the initial experiments focused on the investigation of sorption pH with each sorbent; namely, chitin, chitosan, sodium silicate and chitosan-immobilized sodium silicate. Batch sorption studies were carried out at 25 °C with each sorbent separately after the initial pH of solutions was adjusted to 2.0, 3.0, 4.0, 5.0, 6.0, 8.0, and 10.0 with dilute HNO₃ or NH₃. After pH adjustment step, 50.0 mg sorbent was added into the 50 mL centrifuge tube containing 30.0 mL of 100.0 µg/L As(V) or 40.0 µg/L As(III) solution. The mixture was placed in a thermostated water

bath shaker and was shaken for 30 minutes which is followed by a filtration step. The filtrate was analyzed for its arsenic content by HGAAS as explained previously.

2.5.2. Effect of Shaking Time

Effect of shaking time on the sorption of arsenate ion by chitosan and chitosan-immobilized sodium silicate was investigated for time intervals of 1, 5, 15, 30, 60 and 120 min. Arsenate ion concentration, solution volume, sorbent amount, solution pH and reaction temperature were 100.0 µg/L, 30.0 mL, 50.0 mg, pH=3.0, and 25 °C, respectively.

2.5.3. Effect of Sorbent Amount (Solid/Liquid Ratio)

Effect of amount of chitosan and chitosan-immobilized sodium silicate on the sorption was investigated for 10.0, 20.0, 40.0, 50.0, 75.0 and 100.0 mg. Arsenate ion concentration, solution volume, shaking time, solution pH and reaction temperature were 100.0 µg/L, 30.0 mL, 30 min, pH=3.0, and 25 °C, respectively.

2.5.4. Effect of Reaction Temperature

Effect of reaction temperature on the sorption of arsenate ion by chitosan and chitosan-immobilized sodium silicate was investigated at 25, 50 and 70 °C sorption temperatures. Arsenate ion concentration, solution volume, shaking time, solution pH and sorbent amount were 100.0 µg/L, 30.0 mL, 30 min, pH=3.0, and 50.0 mg, respectively. These results were also used to investigate the thermodynamic parameters of sorption (ΔG , ΔS and ΔH) utilizing the well-known equations 2.10, 2.11 and 2.12 (Atkins and de Paula 2002, Yersel, et al. 2005):

$$\Delta G^{\circ} = -RT \ln R_d \quad (2.10)$$

$$\Delta H^{\circ} = R \ln \frac{R_d(T_2)}{R_d(T_1)} \left(\frac{1}{T_1} - \frac{1}{T_2} \right)^{-1} \quad (2.11)$$

$$\Delta S^o = \frac{\Delta H^o - \Delta G^o}{T} \quad (2.12)$$

R_d (mLg^{-1}) is the ratio of arsenate ion distributed between solid (sorbent) and liquid (aqueous solution of arsenate) phase at equilibrium and is defined by the Equation 2.13.

$$R_d = \frac{C_{solid}}{C_{liquid}} \quad (2.13)$$

where, C_{solid} is the concentration of arsenate in sorbent (mgg^{-1}) and C_{liquid} is the concentration of arsenate ion in solution after sorption (mgL^{-1}).

2.5.5. Effect of Ionic Strength

Effect of ionic strength on the sorption of arsenate ion by chitosan and chitosan-immobilized sodium silicate was investigated in 0.100, 0.010, 0.001 and 0.000 M NaCl solution. Arsenate ion concentration, solution volume, shaking time, solution pH, sorbent amount and reaction temperature were 100.0 $\mu\text{g/L}$, 30.0 mL, 30 min, pH=3.0, 50.0 mg, and 25 °C, respectively.

2.5.6. Repetitive Loading

Sequential (10 times) sorption of arsenate standard solutions by chitosan and chitosan-immobilized sodium silicate without any desorption between consecutive sorption steps was investigated at 100.0 and 1000.0 $\mu\text{g/L}$ concentrations. Solution volume, shaking time, solution pH, sorbent amount and reaction temperature were 30.0 mL, 30 min, pH=3.0, 50.0 mg, and 25 °C, respectively.

2.6. Sorption Isotherm Models

Isotherm is a curve describing the retention of a substance on a solid at various concentrations and is used to predict the mobility of the substance in the environment (Limousin, et al. 2007).

Adsorption isotherm defined by Langmuir assumes that the energy of adsorption is constant and adsorption occurs at fixed number of definite localized homogeneous

sites (finite number of binding sites) with monolayer coverage (Qi and Xu 2004, Gueu, et al. 2007, Limousin, et al. 2007).

Langmuir nonlinear form is given in Equation 2.14.

$$Q_e = Q_{\max} \frac{bC_e}{1 + bC_e} \quad (2.14)$$

where Q_{\max} (mmol/g) and b (L/mmol) are Langmuir constants, Q_{\max} is amount of arsenate ion adsorption corresponding to monolayer coverage, b is the affinity of arsenate for the sorbent, C_e (mmol/L) is the amount of arsenate in liquid phase at equilibrium and Q_e is the amount of arsenate adsorbed on the surface of sorbent (mmol/g) at equilibrium. The values of constants were evaluated from the linearized form of equation which is defined in Equation 2.15.

$$\frac{1}{Q_e} = \frac{1}{Q_{\max}} + \frac{1}{Q_{\max} b C_e} \quad (2.15)$$

The intercept and slope of plot of $1/Q_e$ vs. $1/C_e$ were used for evolution of Q_{\max} and b .

For heterogeneous surfaces isotherm was described by Freundlich which has limitation of low concentrations. The isotherm deviate as the saturation point is approached (Umplebay, et al. 2001).

Freundlich nonlinear isotherm is described by Equation 2.16.

$$Q_e = K_F C_e^{1/n} \quad (2.16)$$

where K_F and n are constants for a given sorbent-adsorbate system. These constants were evaluated from linearized form of equation in a following form (Equation 2.17)

$$\log Q_e = \log K_F + \frac{1}{n} \log C_e \quad (2.17)$$

The intercept and slope of plot of $\log Q_e$ versus $\log C_e$ equation, give K_F and $1/n$ respectively.

D-R isotherm model assumes that the ionic species preferentially bind to most energetically favorable sites of sorbent associated with multilayer adsorption of ions (Guibal, et al. 1998). D-R isotherm generally is described by the Equation 2.18 (Kavitha and Namasivayam 2007):

$$Q_e = q_s \exp(-B\varepsilon^2) \quad (2.18)$$

where

$$\varepsilon = RT \ln \left(1 + \frac{1}{C_e} \right) \quad (2.19)$$

D-R parameter, B, gives the information about the mean free energy of sorption per molecule of adsorbate which requires for transfer it to the surface of the solid from infinity in the solution, q_s corresponds to the sorption monolayer capacity (Şeker, et al. 2008). Mean free energy of sorption can be calculated from D-R parameter B by Equation 2.20.

$$E = (2B)^{-\frac{1}{2}} \quad (2.20)$$

The q_s and B constants are calculated from intercepts and slopes of plots of experimental plot of $\ln q$ versus ε^2 .

Isotherm models for the sorption of arsenate ion by chitosan and chitosan-immobilized sodium silicate was investigated for 50.0, 100.0, 200.0, 500.0, 1000.0, 2000.0, 5000.0, 10000.0 and 20000.0 $\mu\text{g/L}$ arsenate ion concentrations. Solution volume, shaking time, solution pH, sorbent amount and reaction temperature were 30.0 mL, 30 min, pH=3.0, 50.0 mg, and 25 °C, respectively.

2.7. Desorption Studies

Desorption of arsenate ion from chitosan and chitosan-immobilized sodium silicate was investigated for various eluents. The strategy to find a proper eluting solvent is as follows, mainly two types of desorbing matrices were considered. Firstly, desorption was carried out in a desorbing solution in which sorbent was dissolved. For this reason diluted acetic acid in which chitosan has solubility (Vasireddy 2005) was used as desorption matrix. The amount of varying parameter such concentration, time of desorption, volume of eluting solvent was given in Table 2.5 for both chitosan and immobilized chitosan. Secondly, desorption was carried out in desorbing solution in which sorbent was not dissolved. For this purpose basic and acidic solvents were tested. Since As(V) is selectively adsorbed onto sorbent the addition of L-cysteine reduces the arsenate to arsenite which was not adsorbed by chitosan and chitosan-immobilized

sodium silicate. So, reducing property of L-cysteine makes advantage of using it as desorption solution. The detailed properties of each eluting solution were given in Table 2.6. Standards for drawing calibration curve were prepared in the same matrix of each desorption solutions. Before HGAAS both samples and standarts were acidified with concentrated HCl to produce 1.0% (v/v) of HCl in the final solution. For reduction of As(V) to As(III) L-cysteine was added to produce 0.5% (w/v) in the solution (if desorption matrix had already contain reducing agent this step was ignored).

Table 2.6. Desorption conditions of arsenic from chitosan (C) and chitosan-immobilized sodium silicate (IC). Sorption parameters: sorption pH: 3.0, Sorption temperature: 25 °C, amount of sorbent: 50.0 mg

Sorbent	Volume of As(V) (mL)	Concentration of As(V) (µg/L)	Shaking time for desorption (min)	Eluent	Volume of eluent (mL)	L-cysteine (% w/v)
C	30.0	100.0	30	2.0 % HAc	30.0	-
IC	30.0	100.0	30	2.0 % HAc	30.0	-
IC	30.0	100.0	30	4.0 % HAc	30.0	-
IC	30.0	100.0	60	2.0 % HAc	30.0	-
IC	30.0	100.0	30	2.0 % HAc	50.0	-
IC	30.0	100.0	30	2.0 % HAc	30.0	0.5
C	15.0	10.0	30	pH 3.0 (adjusted with HCl)	15.0	0.01
C	15.0	10.0	30	pH 3.0 (adjusted with HCl)	15.0	0.05
C	15.0	10.0	30	pH 3.0 (adjusted with HCl)	15.0	0.1
C	15.0	10.0	30	pH 3.0 (adjusted with HCl)	15.0	0.5
C	15.0	10.0	30	pH 3.0 (adjusted with HCl)	15.0	1
C	30.0	40.0	30	Ultrapure water	30.0	0.5
C	30.0	40.0	30	1.0 % HCl	30.0	0.5
C	30.0	40.0	30	1.0 M HNO ₃	30.0	-
C	30.0	40.0	30	pH 10.0 (adjusted with NH ₃)	30.0	0.5
C	30.0	40.0	30	1.0 M NH ₃	30.0	-
C	30.0	40.0	30	pH 10.0 (adjusted with NH ₃)	30.0	-

2.8. Effect of the Acid Nature on As Signal

Effect of the nature of the acid on arsenic signal during hydride generation was investigated in various prepared acid matrices. Arsenate standard solutions in a concentration of 0.0, 5.0, 10.0 and 20.0 $\mu\text{g/L}$ were prepared in following matrices: 2.0% (v/v) acetic acid, 1.0% (v/v) HCl, 2.0% (v/v) acetic acid + 1.0% (v/v) HCl, pH 1.0 adjusted with HCl solution, pH 1.0 adjusted with HCl + 1.0% HCl (v/v) solution and pH 1.0 adjusted with HNO_3 + 1.0% HCl (v/v) solution. Prior to HGAAS all samples were reduced with added amount of L-cysteine to all standard solutions so as to have 0.5% (w/v) concentration in the final solutions. The ability of arsine generation from each solution was inspected from slope of the calibration curve for each matrix.

2.9. Interference Studies

Interference studies were performed for Mo(VI), V(V), Sb(III), Sb(V), Te(IV), Te(VI), Se(IV), Se(VI) ions. The sorption of Mo(VI), V(V), Se(IV) and Se(VI) by chitosan had been already known. The hydride formation ability of Sb(III), Sb(V), Se(IV), Se(VI), Te(IV), Te(VI) pay attention for their interference probability during arsenate ion sorption by chitosan (Dedina and Tsalev 1995). Firstly, the sorption of each ion by chitosan was investigated in 100.0 and 1000.0 $\mu\text{g/L}$ concentrations at conditions optimized for arsenate ion sorption (solution volume, shaking time, solution pH, sorbent amount and reaction temperature were 30.0 mL, 30 min, pH=3.0, 50.0 mg, and 25 $^\circ\text{C}$, respectively). The percent sorption of each ion was determined by ICP-MS after acidification with concentrated HNO_3 so as to have 1.0% (w/v) acid concentration in the final solutions.

In the second part of interference study 10.0 $\mu\text{g/L}$, 100.0 $\mu\text{g/L}$, 1000.0 $\mu\text{g/L}$ of each species were added separately into 10.0 $\mu\text{g/L}$ and 100.0 $\mu\text{g/L}$ As(V) solutions, respectively. The sorption experiments were performed under optimized conditions for arsenate ion sorption described in previous paragraph, which is followed by a filtration step. After proper acidification and reduction steps ICP-MS and HGAAS were used for interpretation of experimental data.

2.10. Pre-Concentration

Pre-concentration experiment was done for As(V) spiked bottled water at 25 °C with given parameter in Table 2.7. Sorption experiment was carried out with chitosan for concentration and volume of solutions given in Table 2.6. Shaking time, solution pH, sorbent amount and reaction temperature were 30 min, pH=3.0, 50.0 mg, and 25 °C, respectively. Before HGAAS determination all samples and standard solutions were acidified with the addition of appropriate amount of concentrated HCl to produce 1.0% (v/v) HCl in the final solution. For As(V) determination, L-cysteine was also added to all solutions so as to have 1.0% (w/v) concentration in the final solution. Desorption matrix was prepared as 1.0% (w/v) L-cysteine solution after adjustment of pH to 3.0 with HCl. Desorption was done in a water bath shaker for 30 min at 25 °C reaction temperature. Before arsenic determination all samples were acidified with HCl to final 1.0% (v/v) acid concentration. To prevent any deviation due to matrix differences between samples and standards, matrix matched standards were prepared under same sorption/desorption condition described above.

Table 2.7. Preconcentration parameters

Initial As(V) concentration (µg/L)	Volume of solution (mL)	
	Sorption	Desorption
10.0	15.0	15.0
5.0	30.0	15.0
1.0	150.0	15.0

2.11. Speciation of Arsenic

For speciation of As(V) and As(III), chitosan, chitosan-immobilized sodium silicate and a synthetic resin, Duolite GT-73, were used in a two-stage batch type process. Duolite GT-73 was employed for the sorption of As(III) since it has –SH functional groups which are selective towards the lower oxidation states of As, Sb, and the like (Erdem and Eroğlu 2005, Dominguez, et al. 2002). Three different solutions, namely, As(III) only, As(V) only and the mixture of As(III) and As(V) were prepared in

a way that the concentrations of the species were 100.0 µg/L in each case. Solution volume, shaking time, solution pH, sorbent amount and reaction temperature were 30.0 mL, 30 min, pH=3.0, 50.0 mg, and 25 °C, respectively. In a typical analysis (which flowchart is illustrated in Figure 2.4), e.g. for As(III), 30.0 mL of 100.0 µg/L As(III) were prepared, the pH was adjusted to 3.0, and the solution was equilibrated in the 25 °C water bath of the thermostated shaker. After the addition of 50.0 mg of chitosan or chitosan-immobilized sodium silicate, the mixture was shaken for 30 min and then was filtered through blue band filter paper. The solid and the liquid parts were separated and the filtrate was kept for As(III) sorption (next paragraph). Solid chitosan (or chitosan-immobilized sodium silicate) remained on the filter paper was taken into 30.0 mL of 1.0% (w/v) L-cysteine solution of which pH was adjusted to 3.0 and shaking was continued for a further 30 min for desorption. This eluate was analyzed by both HGAAS and ICP-MS for its As(V) concentration.

A 50.0 mg of Duolite GT-73 resin was added into the filtrate saved in the previous step. The mixture was shaken for 30 min at the same conditions described before which was followed by filtration through blue band filter paper. The solid resin remaining on the filter paper was shaken in 30.0 mL of 0.050 M KIO₃ prepared in 2.0 M HCl. After being filtered, the eluate was analyzed by both HGAAS and ICP-MS for its As(III) concentration by using matrix matched standards. Matrix matched standards were prepared under the same sorption/desorption condition described above in concentrations of 5.0, 10.0, 25.0, 50.0, 100.0 and 200.0 µg/L

Before HGAAS determination all samples and standards were acidified with concentrated HCl and reduced with L-cysteine in a concentration of 1.0% (v/v) and 1.0% (w/v) in the final solutions, respectively (reduction step was ignored in case of already L-cysteine containing solutions). The arsenic recovery by ICP-MS was determined after acidification (1.0% v/v HNO₃ in the final solution) of 1/10 fold diluted samples and standards prepared in the experiments mentioned above.

As(V) solution and mixture solution of As(III) and As(V) were also subjected to the same procedure described above for As(III) solution.

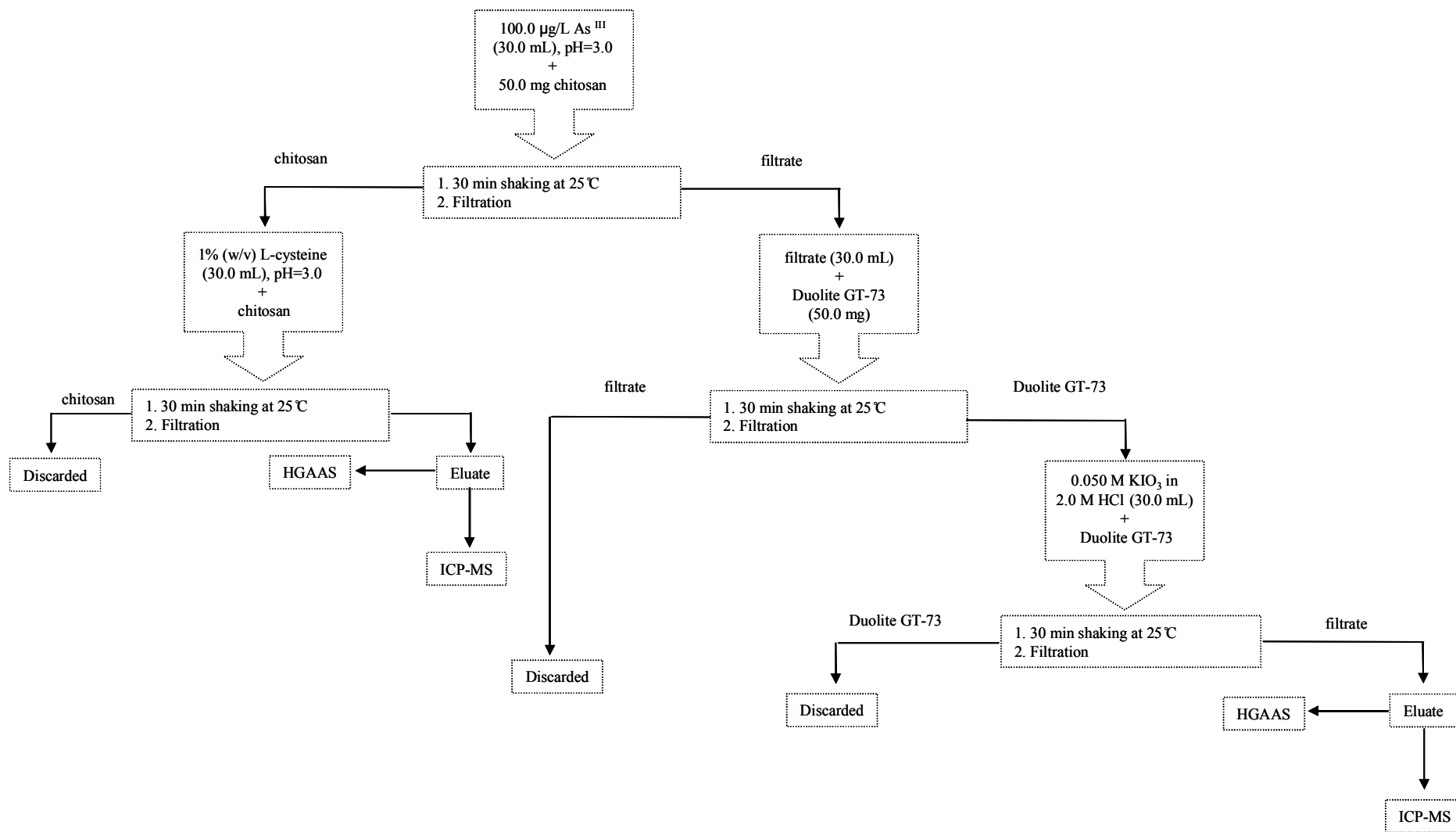


Figure 2.4. Experimental flowchart for arsenic speciation

2.12. Method Validation with Spiked Samples

Four types of water (tap, distilled, sea and bottled water) samples were spiked with arsenate standard solution. Sorption of arsenate ion by chitosan in various type of water samples was investigated. Arsenate ion concentration, solution volume, shaking time, solution pH, sorbent amount and reaction temperature were 10.0 $\mu\text{g/L}$, 15.0 mL, 30 min, pH=3.0, 50.0 mg, and 25 $^{\circ}\text{C}$, respectively. After filtration the sorbent was washed with little ultrapure water and used in desorption of arsenate ion from the sorbent. Desorption conditions were used as described in the section 2.10. Matrix matched standards were used for evaluation of data.

2.13. Performance of the Study

The accuracy of the method was investigated by analyzing the arsenic concentration of a standard reference material and standard solutions of As(III) and As(V). The arsenic content of standard reference material was given as 27.0 $\mu\text{g/L}$ As. The sorption characteristics of SRM was indicated that the arsenic is found in As(III) form with pre-oxidation step requirement. The oxidation was carried out by diluting 5.0 mL of SRM with 10.0 mL of ultrapure water in a teflon beaker. After addition of 3.0 mL conc. HNO_3 , heating was applied on hot plate until evaporation of solution was completed. The remaining residue was washed with ultrapure water and after pH was adjusted to 3.0. As(V) solution in a concentration of 9 $\mu\text{g/L}$ was obtained after dilution to 15.0 mL. This solution was named as batch 1. In the Batch 2 SRM was used directly without pre-oxidation step. 5.0 mL of SRM was diluted with ultrapure water and after pH was adjusted to 3.0 solution was diluted to 15.0 mL mark. Batch 3 and batch 4 were prepared by following the same applied procedure in batch 1 and batch 2, respectively with 27.0 $\mu\text{g/L}$ As(III) containing standard solution. Batch 5 was prepared from 27.0 $\mu\text{g/L}$ As(V) containing standard solution as described in procedure given for batch 2. Chitosan was used as sorbent for sorption of arsenic from each solution described above. Arsenate ion concentration, solution volume, shaking time, solution pH, sorbent amount and reaction temperature were 9.0 $\mu\text{g/L}$, 15.0 mL, 30 min, pH=3.0, 50.0 mg, and 25 $^{\circ}\text{C}$, respectively. After filtration of the sorption solution, the filtrate was retained for determination of sorption percentage of arsenic. The desorption of arsenic adsorbed

onto chitosan flakes was carried out in desorption matrix which was prepared as 0.5% (w/v) L-cysteine solution after adjustment of pH to 3.0 with HCl. Desorption was done in a water bath shaker for 30 min at 25 °C reaction temperature. Before arsenic determination in HGAAS all samples were acidified with HCl to final 1.0% (v/v) acid concentration.

2.14. Sorption Study of Modified Porous Silicate

Sorption studies were performed for sorbents after each functionalization step of chitosan modification (activated, amine modified, aldehyde modified, chitosan modified). Sorptions were carried out with ions that sorption characteristics with chitosan have already specified in the interference study of arsenic; namely Te(VI), Se(VI), V(V), Mo(VI), As(V) and As(III). In addition to chitosan modified macroporous silicate structures, newly synthesized mercapto modified and amine-mercapto modified macroporous silicate structures were used in sorption study with ions mentioned above. Sorption of each ion by each sorbent was investigated separately in a batch type of reaction. Ion concentration, solution volume, shaking time, solution pH, sorbent amount and reaction temperature were 100.0 µg/L, 20.0 mL, 30 min, pH=3.0, 50.0 mg, and 25 °C, respectively. In all these experiments, batch sorption was followed by the filtration of the mixture through blue-band filter paper and acidification of filtrate with the addition of appropriate amount of concentrated HNO₃ to produce 1.0% (v/v) acid in the final solution. Analysis of the filtrate for its ionic content was performed in ICP-MS.

CHAPTER 3

RESULTS AND DISCUSSION

3.1. Characterization of Chitosan

The images of chitosan flakes, silicate and chitosan-immobilized sodium silicate obtained by scanning electron microscopy were given in Figure 3.1. In contrary to chitosan itself the increasing surface porosity of chitosan-immobilized sodium silicate is appeared in similar magnification of images. Thermal gravimetric analysis of chitosan (Figure 3.2.) shows a weight loss in two stages. The first stage ranges between 25-266 °C and reveals about 9% loss in weight associated with second stage weight loss of 33% due to rapid thermal degradation of chitosan between 266 and 328 °C. The first stage weight loss between 25-98 °C and 98-266 °C corresponds to the water molecules adsorbed onto surface and bonded water molecules, respectively. The results are in agreement of thermal gravimetric analysis obtained for chitosan in different studies in literature (Huacai, et al. 2006, Tirkistani 1996). As in case of chitosan, sodium silicate matrix shows weight loss about 9% in a same temperature range due to water molecules in the structure. The chitosan-immobilized sodium silicate has characteristics between chitosan and immobilization matrix. Formation of chitosan via deacetylation of chitin was characterized by FTIR. Disappearance of carbonyl peak of amide at 1630-1660 cm^{-1} is indicative of the deacetylation process (Figure 3.3). The other identified peaks from chitin and chitosan are same due to the similarities between the structures. The peaks identified from both structures are O-H in arange of 3000-3600 cm^{-1} , C-H in a range of 1200-1600 cm^{-1} and around 2900 cm^{-1} , N-H at around 1050 cm^{-1} , C-O at around 1200 cm^{-1} and C-N in a range of 1200-1600 cm^{-1} .

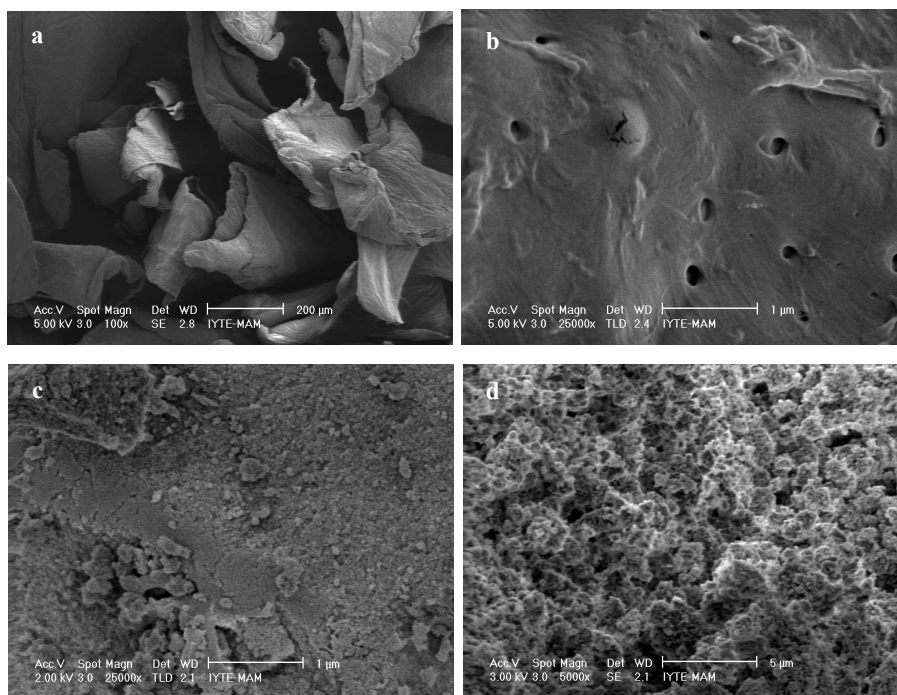


Figure 3.1. SEM images of (a and b)chitosan, (c) silicate and (d)chitosan-immobilized sodium silicate

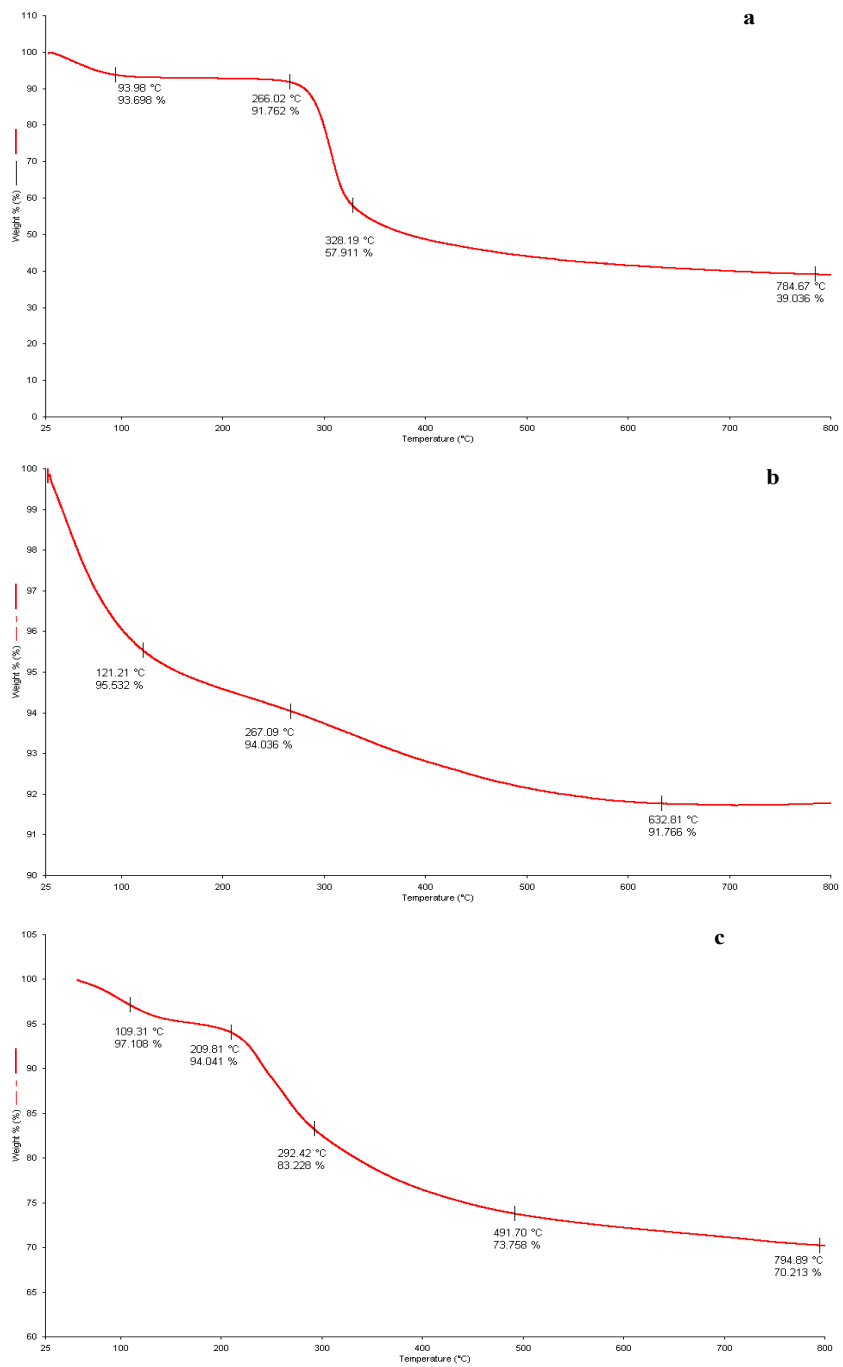


Figure 3.2. TGA of (a)chitosan, (b) silicate and (c)chitosan-immobilized sodium silicate

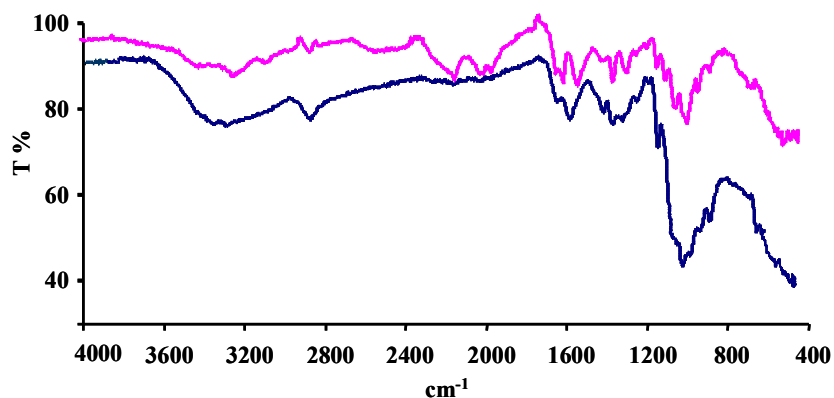


Figure 3.3. FTIR spectra of chitin (—) and chitosan (—)

3.1.1. Degree of Deacetylation

Elemental analysis results which are summarized in Table 3.1 show similar amine percentage for synthesized chitosan as indicated in literature (Tolaimate 2000). Also, the percentage of chitosan immobilized onto sodium silicate was calculated from the carbon ratios of chitosan-immobilized sodium silicate to pure chitosan sample. The amount of chitosan in sodium silicate matrix was calculated as 33.3% chitosan in the total mass. The potentiometric titration graph of chitosan was illustrated in Figure 3.4 where the difference between two inflection points corresponded to amount of protonated amine groups in chitosan. From the titrimetric method for determination of degree of deacetylation 85.4% removal of acetyl groups was calculated which was in agreement with result obtained from elemental analysis method. Calculated degree of deacetylation by mentioned methods are given in Table 3.2 for comparison between them. Potentiometric titration curve (Figure 3.4) can also be used for the determination of pKa value of chitosan. pKa was calculated from the half neutralization point of chitosan as 6.2 which is in agreement with the values given in the literature.

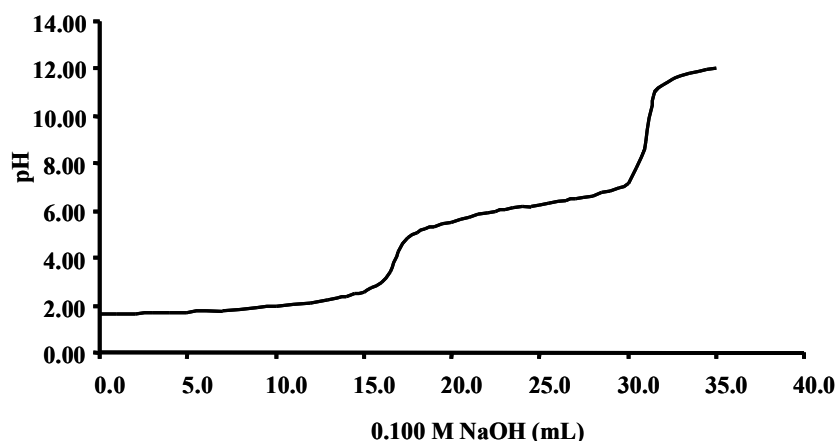


Figure 3.4. Titration curve of chitosan, dissolved in HCl with standardized NaOH solution

Table 3.1. Elemental analysis results of chitosan and chitosan-immobilized sodium silicate

Compound	Sorbent amount (mg)	C %	H %	N %	S %
Chitosan	1.9910	40.77	7.23	7.55	0.00
Chitosan-immobilized sodium silicate	1.9970	13.57	3.41	2.43	0.71

Table 3.2. Comparison of degree of deacetylation of chitosan by titrimetric and elemental analysis methods

Method	D.A %	D.D %
Potentiometric titrimetry	14.6	85.4
Elemental analysis	15.3	84.7

3.1.2. Molecular Weight of Chitin and Chitosan

Molecular weight of chitin and chitosan were calculated from relation between reduced viscosity of polymer and concentration as indicated in Figure 3.5 and Figure 3.6. According to Mark-Houwink-Sakurada equation the molecular weights of chitin and chitosan were calculated as 210 kDa and 3340 Da, respectively. The calculated molecular weights indicate that the chitin used in this study is low molecular weight and deacetylation process treatment not only remove acetyl groups also decrease the molecular weight of chitosan by cleavage of glycosidic bonds.

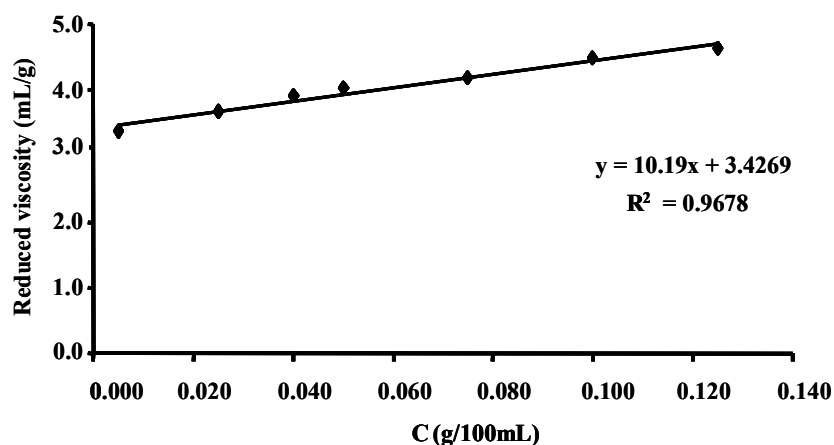


Figure 3.5. Effect of concentration to reduced viscosity of chitosan

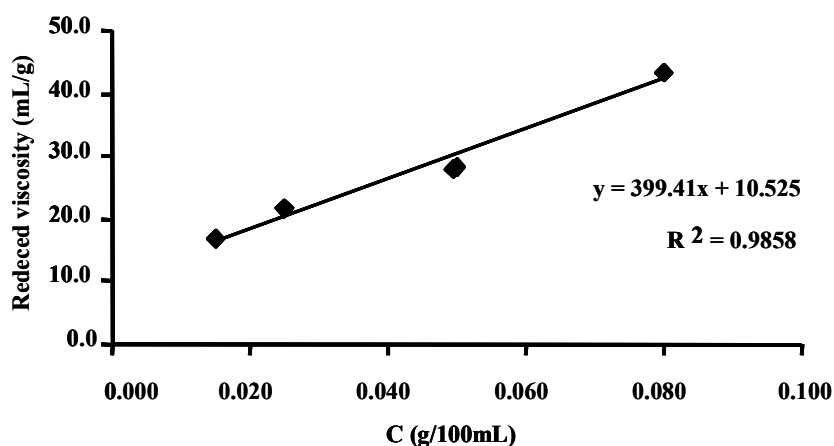


Figure 3.6. Effect of concentration to reduced viscosity of chitin

3.1.3. XRD Patterns of Chitin and Chitosan

The X-ray diffraction patterns for chitin and chitosan were given in Figure 3.7 and Figure 3.8, respectively. The most significant difference appeared between the two XRD figure is the decreasing the crystallinity of compound after deacetylation process. Deacetylation procedure involve the disappearance of small peaks, only peaks at $2\theta=9-10^\circ$ and $2\theta=19-20^\circ$ remained. Decreasing of the crystallinity from chitin to chitosan was also observed by different groups in literature and they showed that these retained peaks corresponded to hydrated crystals of chitosan (Jaworska, et al. 2003, Ogawa, et al. 1991).

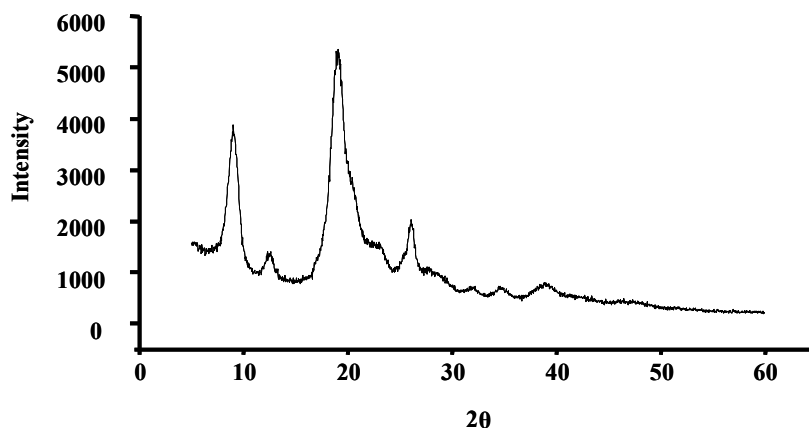


Figure 3.7. X-ray diffraction patterns for chitin

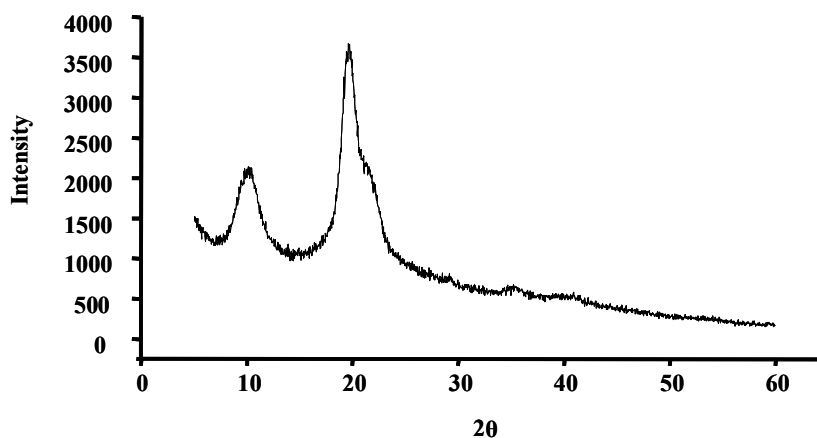


Figure 3.8. X-ray diffraction patterns for chitosan

3.2. Characterization of Polystyrene Nanoparticles

Images of polystyrene nanoparticles obtained by scanning electron microscopy were given in Figure 3.9. The images on different magnifications show monodispersed spherical polystyrene nanoparticles with mainly tetrahedral holes in their close packed form. Octahedral holes are also observed from images. The particle size distribution was used for determination of the mean particle size after sampling at various reaction time intervals. The synthesis conditions for polystyrene nanoparticles had been given in Table 2.3. The effect of reaction time on particle size was investigated in reaction named batch 1. The particle size of polystyrene nanoparticles after 20, 24 and 28 h sampling are illustrated in Figure 3.10. The determined particle size after each time interval shows that the reaction was not completed before indicated time and particles

were still growing upto last hour. Figure 3.11 (a) shows the effect of water to styrene ratio. Increasing the water to styrene ratio decrease the particles size of polystyrene from 817 nm to 252 nm. The effect of the amount of added initiator is illustrated in Figure 3.11 (b). Under fixed water/styrene ratio increasing the amount of the initiator by 50% was not effective in the mean particle size of resulting nanoparticles. However, the amount of the initiator had been influential in broadening of the size distribution of particles.

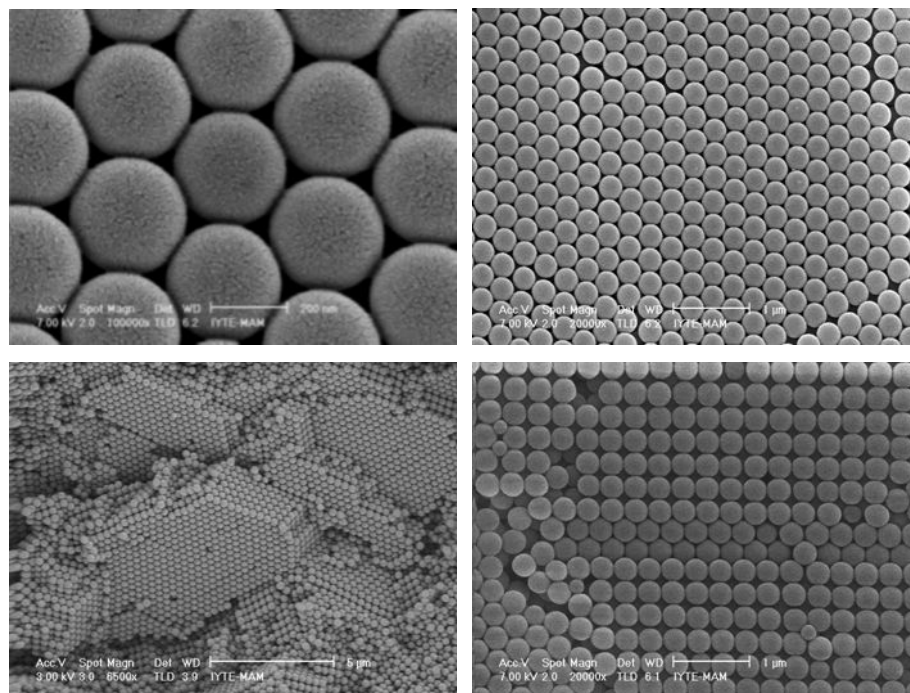
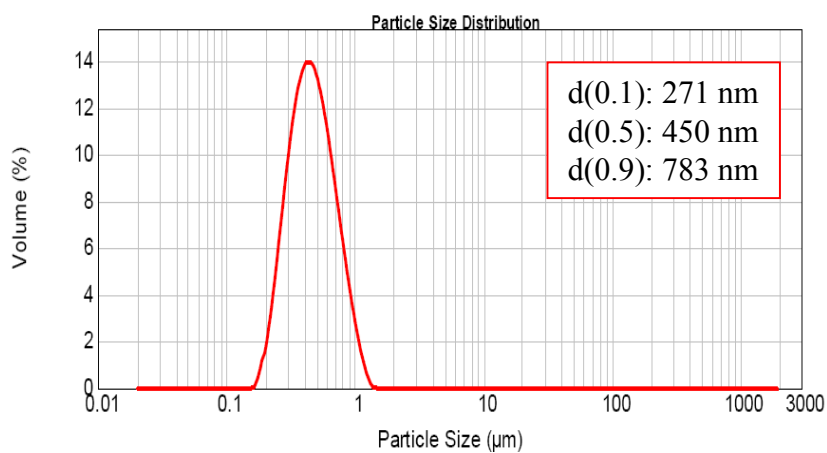
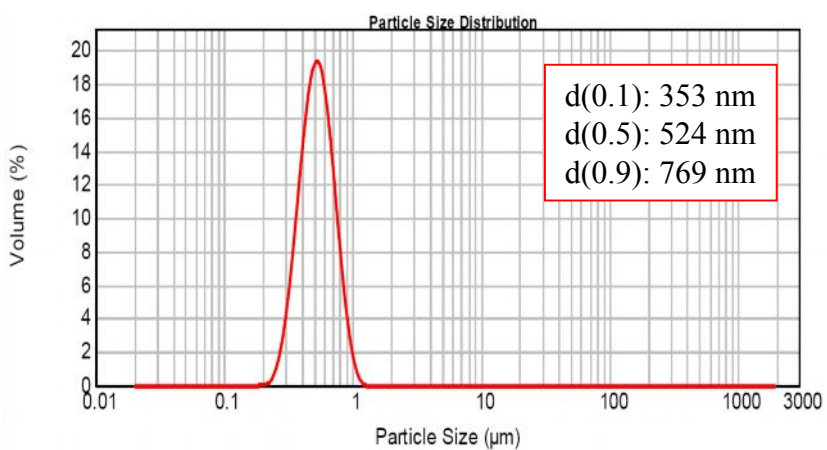


Figure 3.9. SEM images of polystyrene nanoparticles at various magnifications

a)



b)



c)

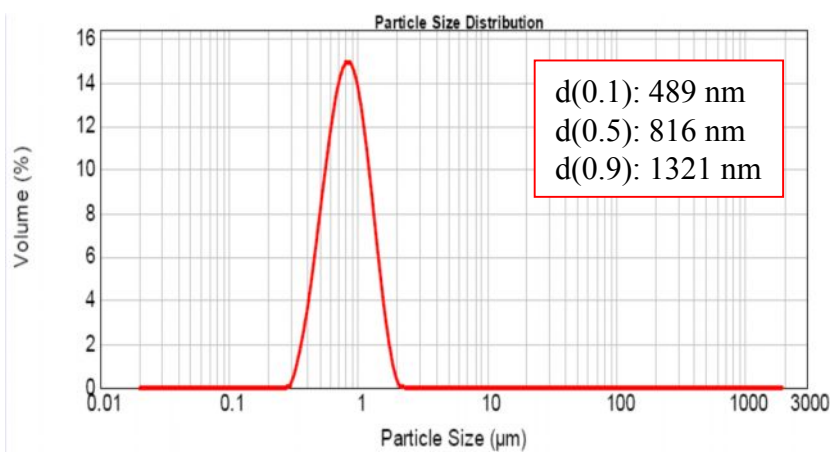
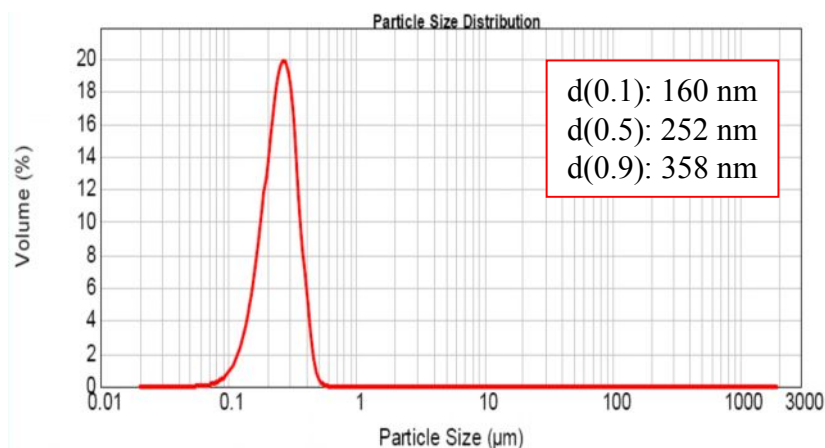


Figure 3.10. Particle size distribution of polystyrene nanoparticles in batch 1 after (a) 20 h, (b) 24 h, (c) 28 h reaction period

a)



b)

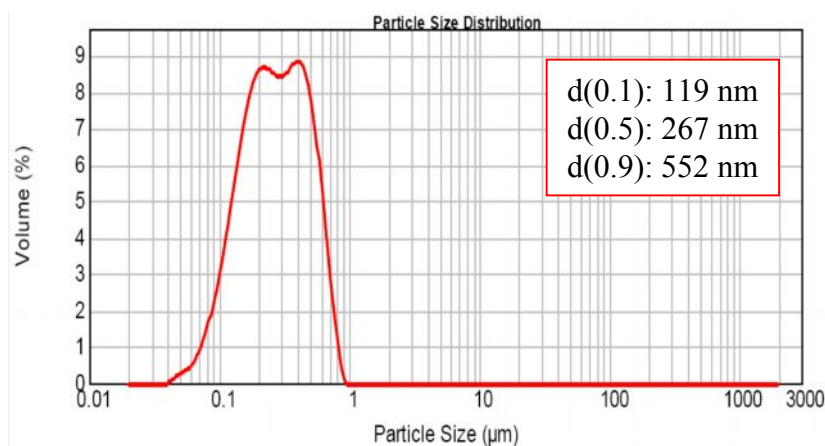


Figure 3.11. Particle size distribution of (a) batch 2 and (b) batch 3

3.3. Synthesis of Ordered Macroporous Silicate

Effect of some parameters to final structure of macroporous silicate were investigated for conditions summarized in Table 2.4. The results of this study are given Figure 3.12. The first batch process was used as ideal situation for synthesis of ordered macroporous silicate structure (Figure 3.12 (a) and (b)) Increasing the amount of polystyrene added to sol-gel mixture destroy the ordered structures in batch 2 (Figure 3.12 (c)). This observation can be related to the limited amount of surfactant that was used for effective coating of silicate around polystyrene nanoparticles. Batch 3 was performed by increasing the time of aging during hydrolysis of sol-gel and coating steps. Figure 3.12 (d) illustrates the effect of the aging time on silicate structure. The macroporous silicate with unbroken spherical structure could be demonstrative of

strengthen the final product. Effect of the calcination conditions was investigated at batch 4 by direct calcination of silicate coated particles at 550 °C. Figure 3.12 (d) shows that direct calcinations expel the decomposition gases unevenly from the structure. Effect of the surfactant on the final structure was inspected by removing both surfactant and co-surfactant in batch 5. SEM images given in the Figure 3.12 (f) and (g) show disordered distribution of pores with unevenly distributed wall thickness. These results showed that the surfactant is one of the most important parameter for synthesis of ordered macroporous structures by mediating a surface for efficient coating. Effect of co-polymer was investigated at batch 6 by removing only pentane from reaction solution. The effect of co-polymer is distinguished in the Figure 3.12 (h) and (i) as less important parameter than surfactant. But, its absence also decreases the order of silica structure.

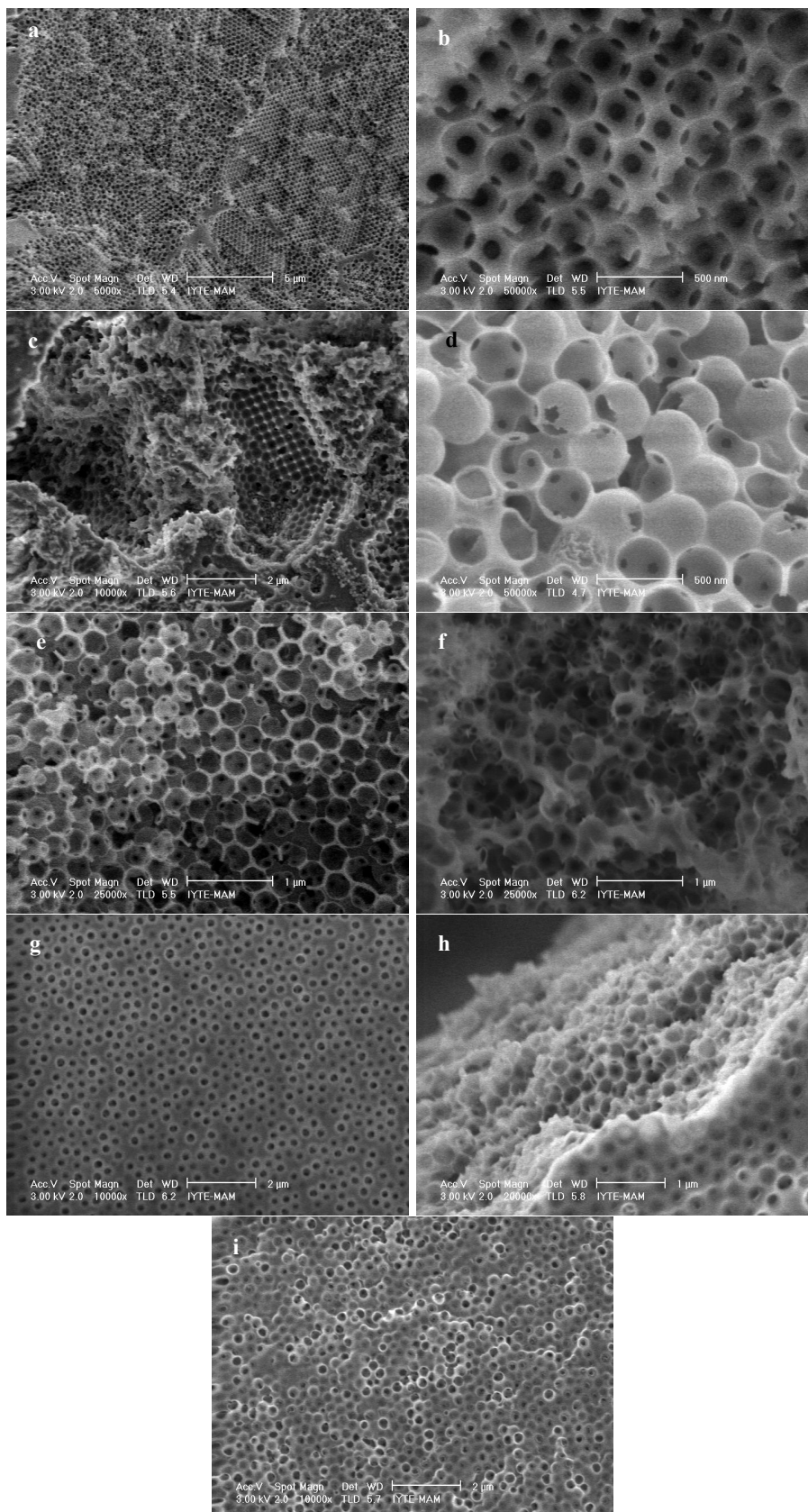


Figure 3.12. SEM images of macroporous silicate structures of (a, b) batch 1, (c) batch 2, (d) batch 3, (e) batch 4, (f, g) batch 5 and (h, i) batch 6

3.3.1. Characterization of Modified Macroporous Silicate Structures

The amount of amine and mercapto functional groups on surface of macroporous silicate structures were established by elemental analysis. Table 3.3 shows the determined percent elemental composition of modified silicate after each step.

Table 3.3. Elemental composition of modified macroporous silicate

Sorbent	C %	H %	N %	S %
Activated silicate	3.61	0.99	0.06	0.00
Amine modified silicate	2.66	0.88	0.65	0.03
Glutaraldehyde modified silicate	10.85	1.77	1.28	0.00
Chitosan modified silicate	8.79	1.59	1.02	0.02
Mercapto modified silicate	2.41	0.79	0.07	0.26
Amine-mercapto modified silicate	1.87	0.73	0.11	0.26

3.4. Sorption Studies

3.4.1. Effect of Solution pH

Sorption characteristic of As(V) and As(III) by chitin, chitosan, sodium silicate and chitosan-immobilized sodium silicate were given in Figure 3.13 and Figure 3.14, respectively. Chitosan and chitosan-immobilized sodium silicate had maximum sorption at pH 3.0 while sodium silicate and chitin did not show any affinity for As(V) as indicated in Figure 3.13. In case of As(III) (Figure 3.14), all sorbents showed the same trend of sorption and arsenite ions were not adsorbed by any given sorbent surface under working conditions. The nature of sorption behaviour of chitosan at pH 3.0 can be explained by electrostatic attractions between protonated amine groups of chitosan and H_2AsO_4^- ion, which is the main species in As(V) solution at pH 3.0 (Figure 3.15). Below pH 3 chitosan flakes easily were dissolved in solution that enables them of using as a biosorption material. Zeta potential of chitosan shows the increasing positive charge onto chitosan flakes as pH was lowered (Figure 3.17) which also support the electrostatic nature of sorption. There is no any other pH with the same electrostatic

behaviour that biosorbent and arsenic species have opposite charges from examination of speciation graph for both As(V) and As(III) (Figure 3.15 and Figure 3.16).

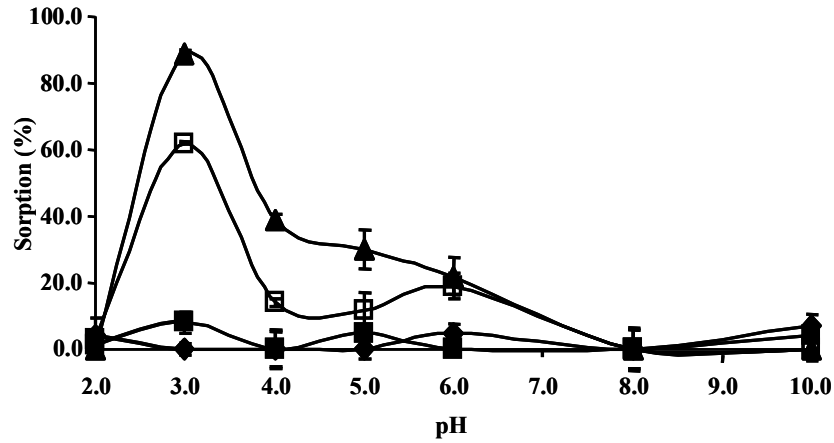


Figure 3.13. Effect of pH on the sorption of 100.0 µg/L 30.0 mL As(V) solution, 30 min shaking time, 50.0 mg sorbent. at 25 °C sorption temperature. (▲) chitosan, (■) sodium silicate, (◆) chitin, (□) chitosan-immobilized sodium silicate

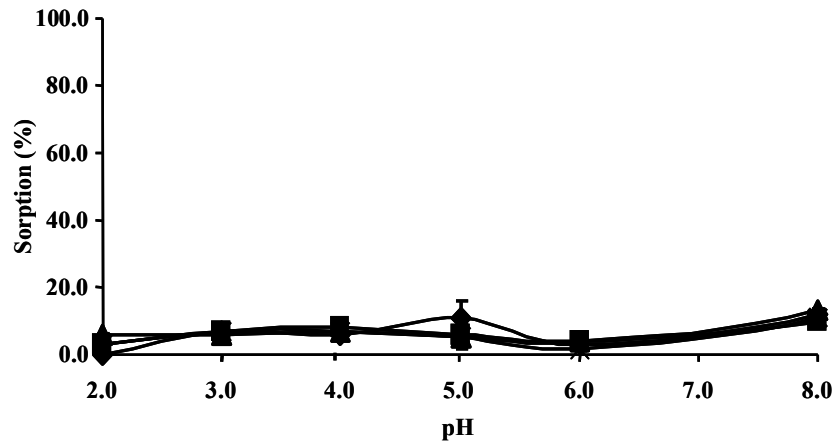


Figure 3.14. Effect of pH on the sorption of 40.0 µg/L 30.0 mL As(III) solution 30 min shaking time and 50.0 mg sorbent at 25 °C sorption temperature. (▲) chitosan, (■) sodium silicate, (◆) chitin, (□) chitosan-immobilized sodium silicate

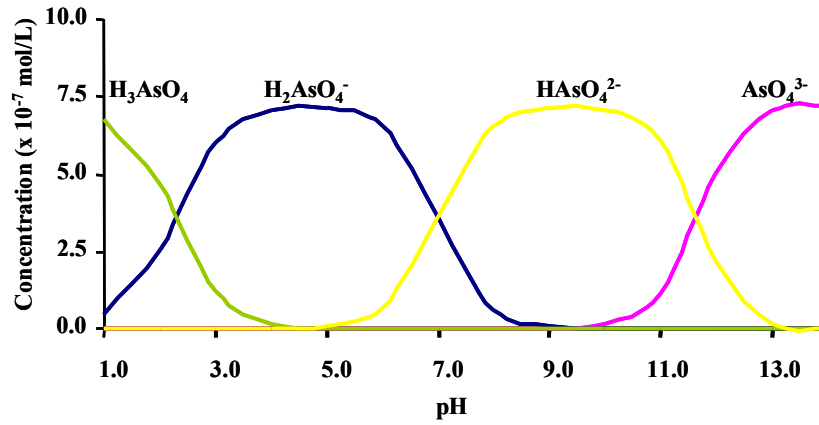


Figure 3.15. Speciation diagram of As(V) at various pH values. (—) H_3AsO_4 , (—) H_2AsO_4^- , (—) AsO_4^{3-} and (—) HAsO_4^{2-}

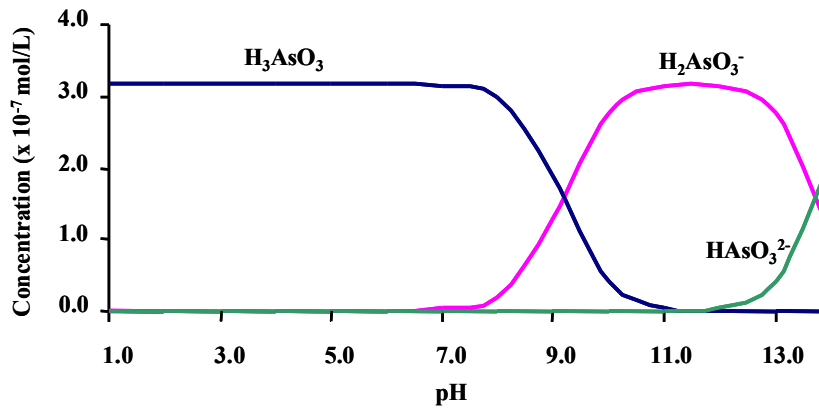


Figure 3.16. Speciation diagram of As(III) at various pH values. (—) H_3AsO_3 , (—) H_2AsO_3^- and (—) HAsO_3^{2-}

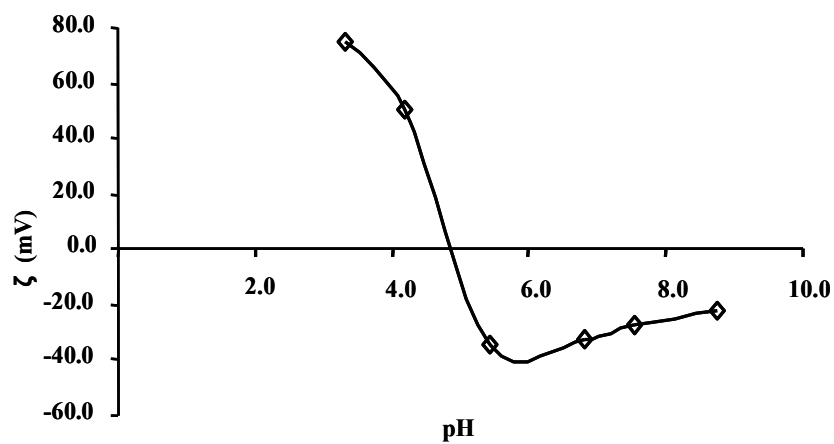


Figure 3.17. Charge of chitosan flakes at various pH values

3.4.2. Effect of Sorbent Amount

The arsenic sorption behaviour with discrete amount of chitosan and chitosan-immobilized sodium silicate is given in the Figure 3.18. Similar sorption results were obtained with both sorbents at each amount that was tested. Effect of sorbent amount for the given concentration of As(V) shows maximum at 50.0 mg both for chitosan and chitosan-immobilized sodium silicate which also support the advantage of immobilization. In immobilization matrix chitosan content was only 33% of original chitosan amount, so identical sorption behaviour can be explained by large surface porosity and more available sides for sorption. The larger surface area of immobilization can be seen from SEM images of chitosan and immobilized chitosan (Figure 3.1). This observation is also indicative of large capacity of chitosan for arsenate ion sorption.

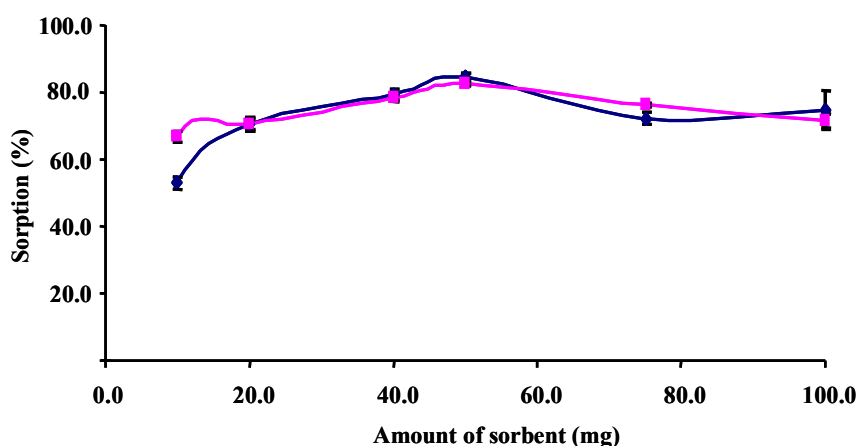


Figure 3.18. Effect of amount of sorbent on sorption at pH 3.0 in 100.0 $\mu\text{g/L}$ 30.0 mL As(V) solution at 25 $^{\circ}\text{C}$ sorption temperature. (\blacklozenge) chitosan, (\blacksquare) immobilized chitosan

3.4.3. Effect of Shaking Time

Batch sorption time were investigated for 1, 5, 15, 30, 60 and 120 minutes as illustrated in Figure 3.19. The sorption values obtained with chitosan immobilized silicate are higher than chitosan itself. This could be explained by increasing surface

area of immobilized material which is advantageous of providing more functional groups available for sorption. However, sorption equilibration time were same for both sorbents and equilibrium was reached in 15 min which is indicative of diffusion restricted sorption.

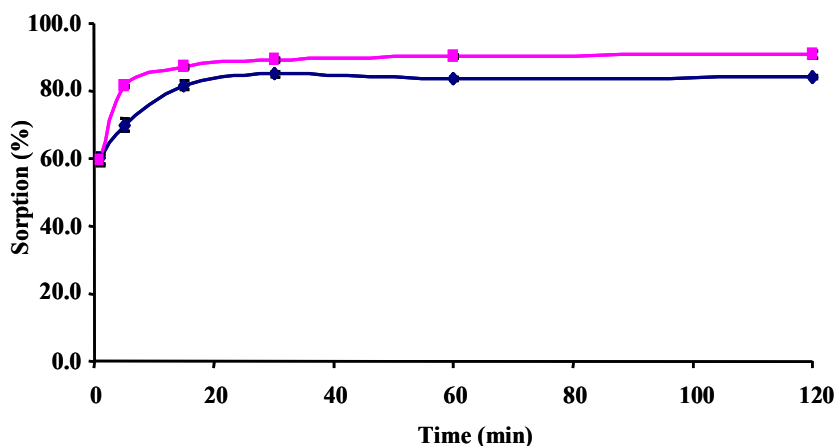


Figure 3.19. Effect of shaking time for 50.0 mg chitosan and immobilized chitosan at pH 3.0 in 30.0 mL, 100.0 $\mu\text{g/L}$ As(V) solution at 25 $^{\circ}\text{C}$ sorption temperature. (\blacklozenge) chitosan, (\blacksquare) immobilized chitosan

3.4.4. Temperature Effect

Temperature effect on the sorption of arsenic was studied at 25, 50 and 70 $^{\circ}\text{C}$. The sorption behaviours of chitosan and chitosan-immobilized sodium silicate as a function of temperature are given in the Figure 3.20. Decreasing trend of sorption for both sorbents as temperature increases was observed which indicate the sorption of arsenate shows exothermic behaviour associated with decrease in entropy indicating that the spontaneous sorption is enthalpy-driven. The summary of thermodynamic parameters is given in the Table 3.4.

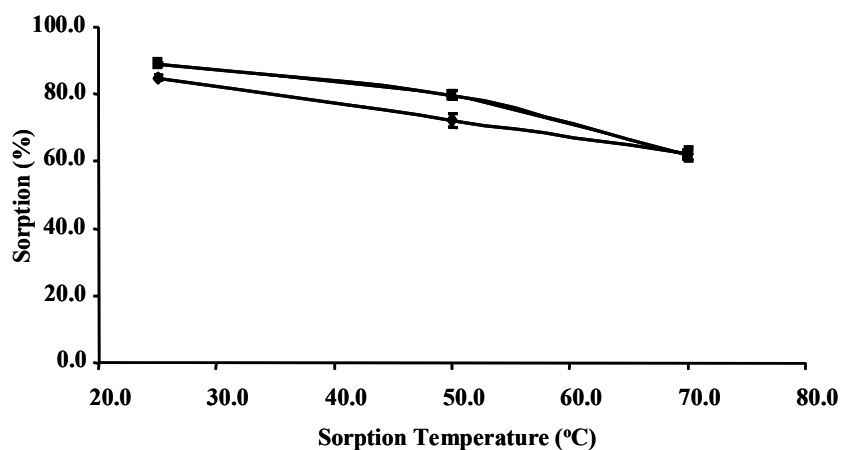


Figure 3.20. Effect of temperature on sorption for 50.0 mg chitosan and immobilized chitosan at pH 3.0 in 30.0 mL, 100.0 $\mu\text{g/L}$ As(V) solution. (\blacklozenge) chitosan, (\blacksquare) immobilized chitosan

Table 3.4. Thermodynamic parameter of chitosan and immobilized chitosan

	$\Delta G(\text{kJ/mol})$		$\Delta H(\text{kJ/mol})$	$\Delta S(\text{J/molK})$	
	298 K	323 K		298 K	323 K
Chitosan	-20.2	-19.8	-24.7	-15.1	-15.1
Immobilized chitosan	-21.1	-20.9	-23.8	-9.1	-9.1

3.4.5. Effect of Ionic Strength

Effect of ionic strength on the sorption performance of chitosan was investigated by addition of various concentration of NaCl into arsenic solution as illustrated in Figure 3.21. Even addition of 0.001 M NaCl was reduced the sorption capacity of chitosan for arsenic, while for 0.100 M NaCl concentration no sorption was observed. These results are in agreement with sorptions obtained in tap water and sea water spiked solution, where due to high ionic strength sorption was not observed for sea water samples.

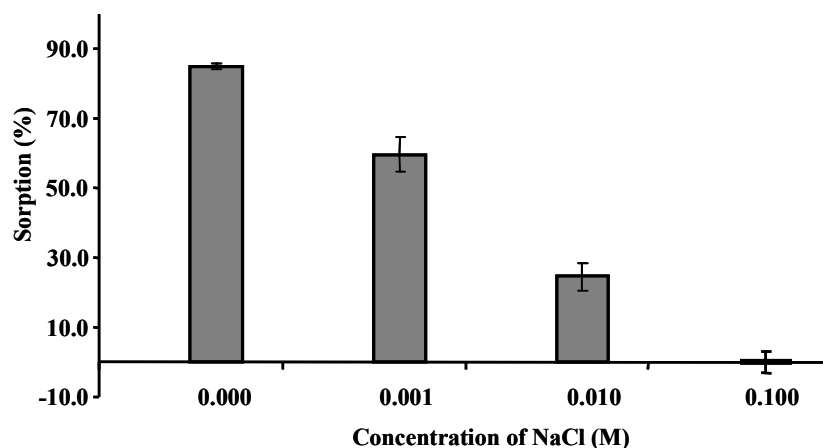


Figure 3.21. The arsenic sorption capacity of chitosan at various concentrations of NaCl. 50.0 mg chitosan at pH 3.0 in 30.0 mL, 100.0 $\mu\text{g/L}$ As(V) solution at 25 $^{\circ}\text{C}$ sorption temperature

3.4.6. Successive Loading

Sequential sorption of arsenate by chitosan and chitosan-immobilized sodium silicate for two different concentrations was investigated as explained in section 2.5.6. It can be seen from Figure 3.22 that the sorption percentage starts to decrease with the third loading and previously-sorbed arsenate even starts to be released from chitosan surface after the sixth loading. This observation can not be related to the sorption capacity of chitosan since a similar trend was observed for both 100.0 and 1000.0 $\mu\text{g/L}$ concentrations. In order to clarify this further, the cumulative amount of arsenate on the sorbent (mmol/g) was also plotted as a function of load number (Figure 3.23). As seen from the figure, the amount of arsenate at the sixth load is approximately 0.015 mmol/g which is still lower than the maximum sorption capacity of chitosan (as will be shown later in section 3.5 and Figure 3.26, the plateau which shows the maximum sorption capacity can be taken as at least 0.04 mmol/g). Several reasons can be suggested to explain the decrease in sorption capacity. Firstly, a gradual dissolution of flakes was observed after each loading which might have caused a decrease in the sorption capacity. More importantly, the dissolution of chitosan flakes must have been associated with the release of previously-adsorbed species from the surface which eventually increased the arsenate concentration in the solution. Secondly, although it needs a further justification, it can be speculated that the surface positive charge of chitosan after each loading could

have been reduced which might also have changed the thickness of double layer around the particles. This might have resulted in a decrease in the sorption percentage after each step.

In contrast to chitosan, chitosan-immobilized sodium silicate have shown a better chemical stability in a way that no negative sorption (release from chitosan surface) was observed although the sorption percentage started to decrease after the second load for both concentrations (Figure 3.24). As in the case of chitosan, the decrease in the sorption percentage of chitosan-immobilized sodium silicate can not be explained by the reduction in the sorption capacity of the immobilized sorbent either. Similarly, from the cumulative amount of arsenate on the immobilized sorbent (Figure 3.25) the amount of arsenate even at the tenth load is approximately 0.016 mmol/g which is about half of the maximum sorption capacity of chitosan-immobilized sodium silicate (as will be shown later in section 3.5 and Figure 3.30, the plateau which shows the maximum sorption capacity, can be taken as at least 0.035 mmol/g).

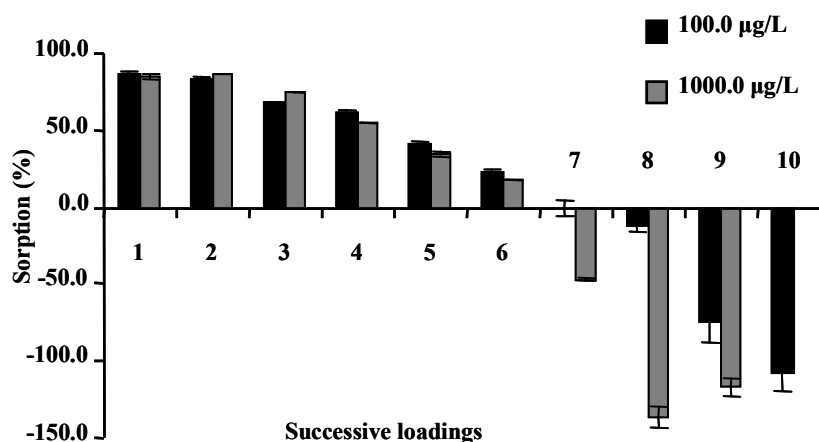


Figure 3.22. Percent sorption of chitosan for ten successive loadings in pH 3.0, 30.0 mL of 100.0 and 1000.0 µg/L As(V) concentrations, 50.0 mg sorbent, 30 min at 25°C, batch sorption

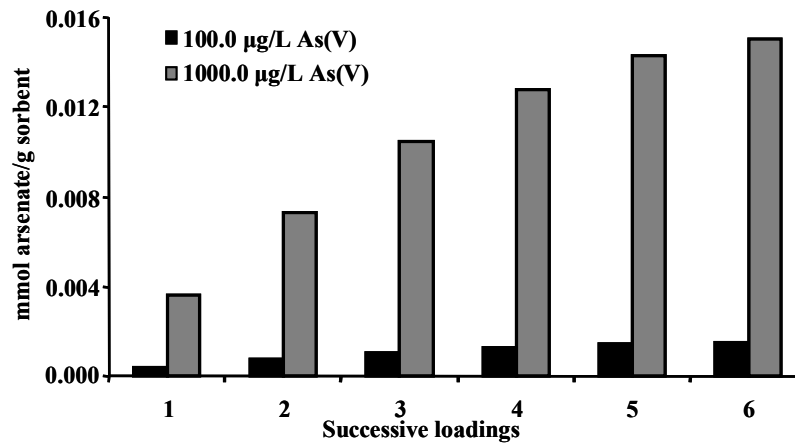


Figure 3.23. Total amount increment of loaded arsenate after each successive loadings onto chitosan

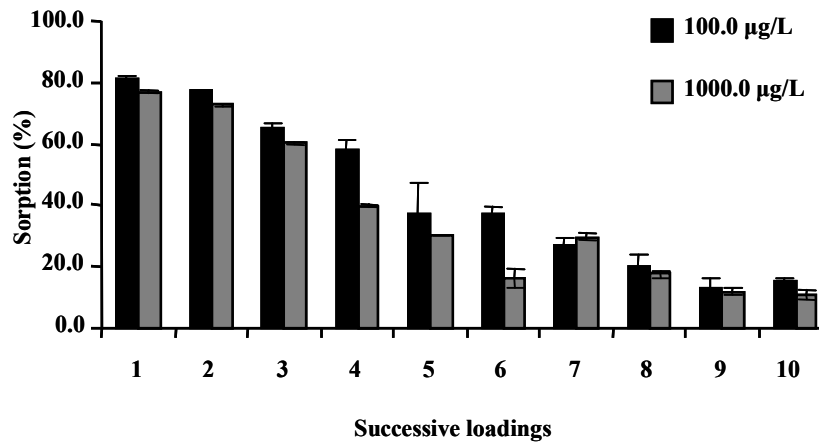


Figure 3.24. Percent sorption of chitosan immobilized silicate for ten successive loadings in pH 3.0, 30.0 mL of 100.0 and 1000.0 µg/L As(V) concentrations, 50.0 mg sorbent, 30 min at 25 °C batch sorption

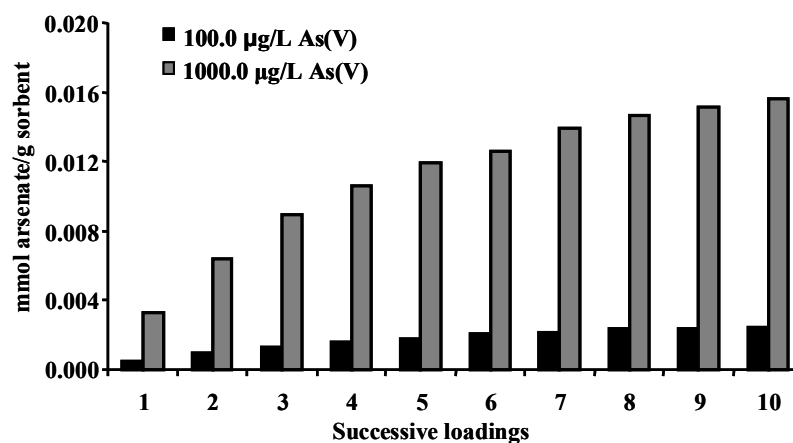


Figure 3.25. Total amount increment of loaded arsenate after each successive loadings onto chitosan-immobilized sodium silicate

3.5. Sorption Isotherm Models

Freundlich, Dubinin-Radushkevich and Langmuir isotherm models were tested for sorption of arsenate ion by chitosan and chitosan immobilized silicate. Both linear and non linear forms of isotherms illustrated between Figure 3.26 and Figure 3.33. Linearized form of models were used for calculations of coefficients which are summarized in Table 3.5. Both chitosan and chitosan immobilized silicate experimental results best fit with D-R model. Nonlinear form of Freundlich model shows nearly linear fit which was expected for low concentrations. Langmuir model had larger deviation from experimental results which indicate that the sorption sites were not monolayer covered. Since the isotherm model are more representative for higher concentrations these deviations can be reasonable for concentrations that were studied.

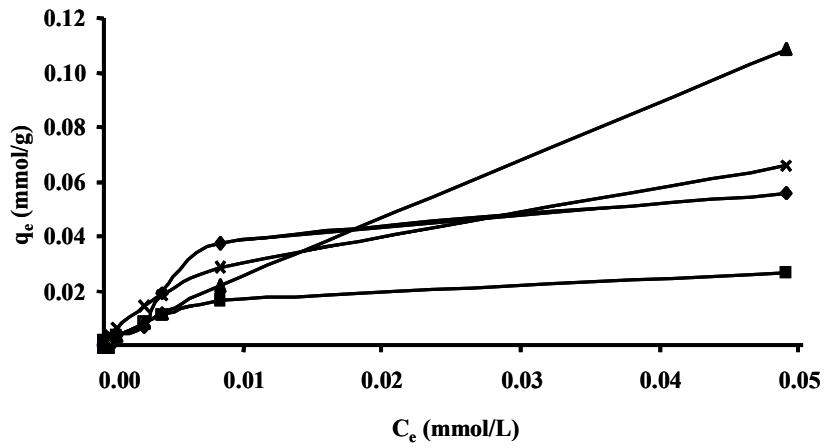


Figure 3.26. Nonlinear fit of isotherm models for sorption of arsenate by chitosan.
 (▲) Freundlich model, (×) Dubinin–Radushkevich model, (◆) experimental,
 (■) Langmuir model

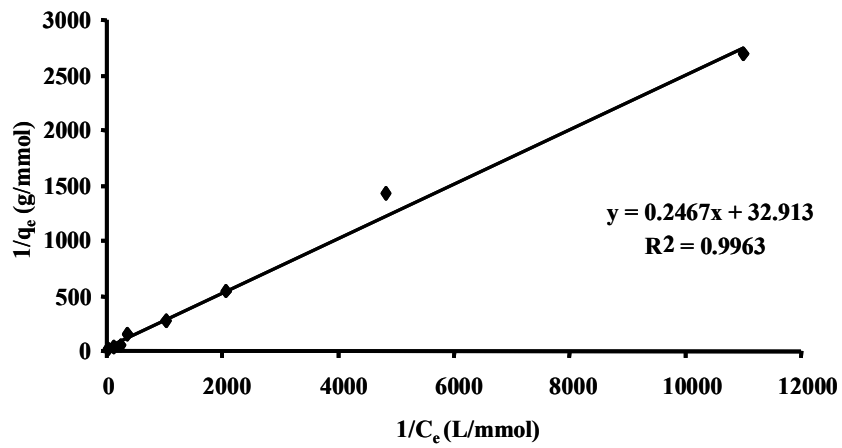


Figure 3.27. Linear fit of Langmuir model for arsenate sorption by chitosan

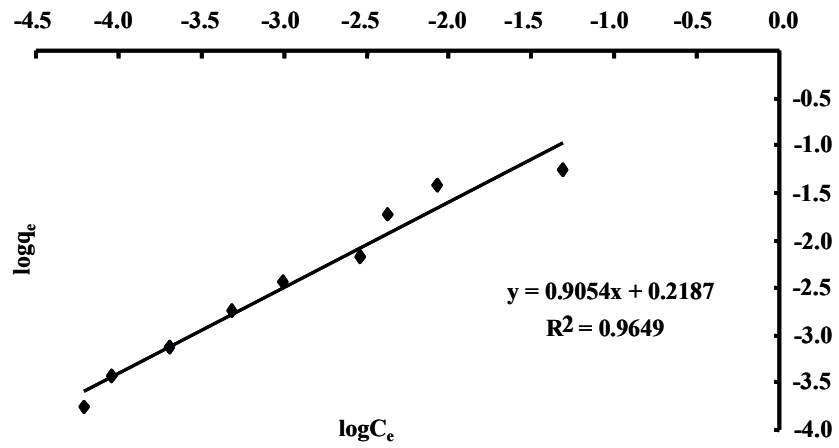


Figure 3.28. Linear fit of Freundlich model for arsenate sorption by chitosan

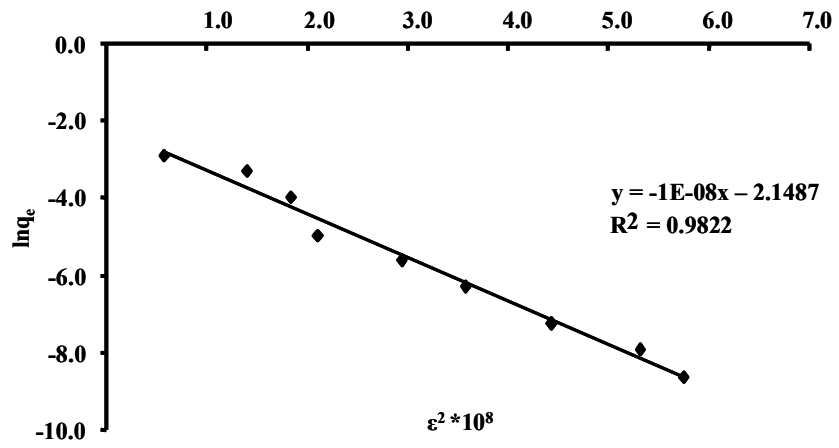


Figure 3.29. Linear fit of Dubinin-Radushkevich model for arsenate sorption by chitosan

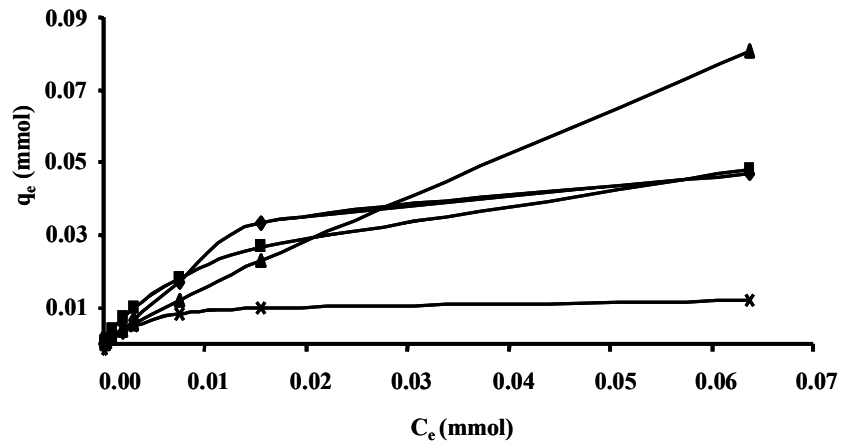


Figure 3.30. Nonlinear fit of isotherm models for sorption of arsenate by chitosan immobilized silicate. (\blacktriangle) Freundlich model, (\times) Langmuir model, (\blacklozenge) experimental, (\blacksquare)Dubinin–Radushkevich model

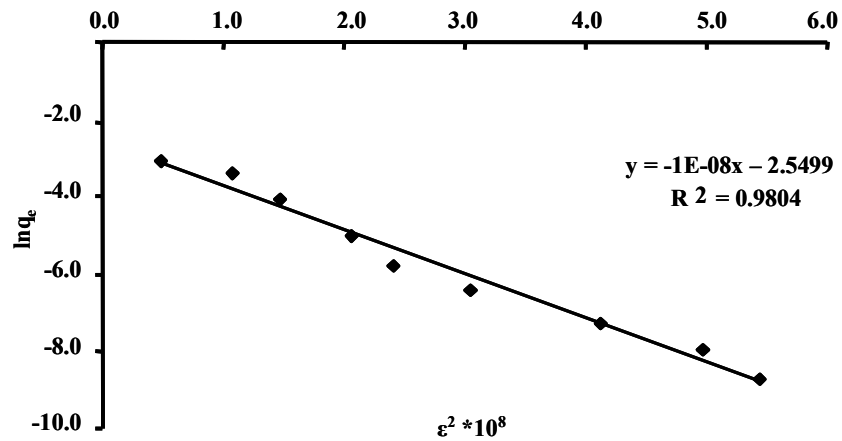


Figure 3.31. Linear fit of Dubinin-Radushkevich model for arsenate sorption by chitosan immobilized silicate

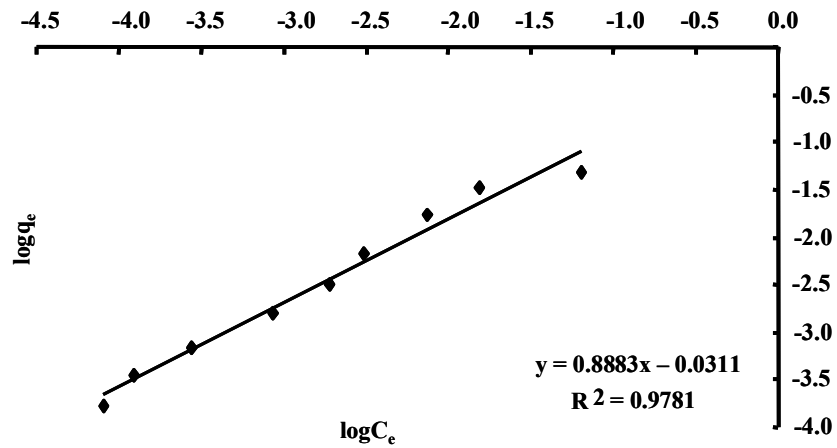


Figure 3.32. Linear fit of Freundlich model for arsenate sorption by chitosan immobilized silicate

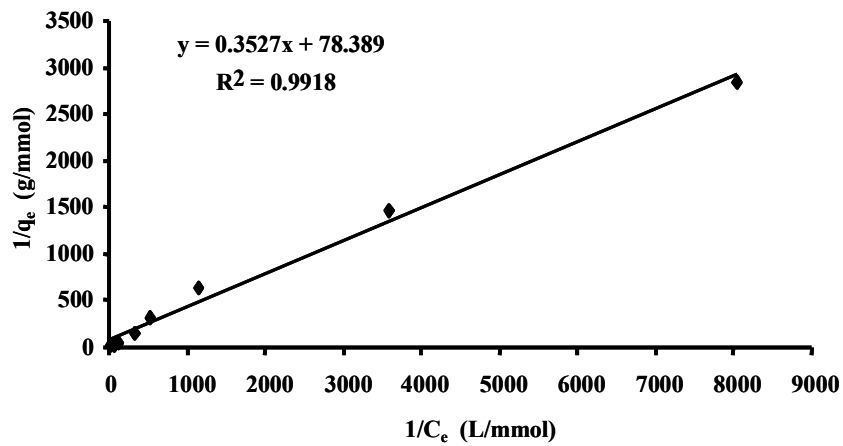


Figure 3.33. Linear fit of Langmuir model for arsenate sorption by chitosan immobilized silicate

Table 3.5. Summary of models coefficients

Adsorption model	Parameter	Chitosan	Chitosan Immobilized Sodium Silicate
Langmuir	R^2	0.9963	0.9918
	Q_{\max}	0.03038	0.01276
	b	133.43	222.25
Freundlich	R^2	0.9649	0.9781
	K_F	1.655	0.9309
	$1/n$	0.9054	0.8883
Dubinin-Radushkevich	R^2	0.9822	0.9804
	B	$1 \cdot 10^{-8}$	$1 \cdot 10^{-8}$
	q_s	0.1166	0.0781
	E	7.07 kJ/mol	7.07 kJ/mol

3.6. Desorption Studies

Desorption studies was performed as described in section 2.7 for chitosan and chitosan-immobilized sodium silicate. Table 3.6 summarizes the desorption percentage of various desorbing matrices. Chitosan flakes were completely dissolved in 2.0% (v/v) acetic acid solution. The dissolution of flakes have been associated with the 90% release of previously-adsorbed arsenate from the surface. So acetic acid solution is suitable desorbing solvent for chitosan. In case of chitosan-immobilized sodium silicate, acetic acid was not effective eventhough acid concentration, time of desorption and solution volume were doubled . Addition of reducing agent to acetic acid matrix was completely desorbed arsenate ions. This behaviour can be explained by reducing ability of L-cysteine. The thiol groups in L-cysteine converted As(V) to As(III) that was not adsorbed by chitosan (Le, et al. 1994). The stability of sorbent has importance in column study so finding a solution which desorbed arsenate from chitosan without dissolving flakes is a challenging task. The reduction ability of L-cysteine was tested in different acidic and basic conditons. The results show that under the acidic conditions desorption with reducing agent was effective but the acidity of solution is the most important parameter, since chitosan flakes was dissolved under acidic conditions. So pH=3.0 was chosen as a minimum pH at which flakes are not dissolved and the reduction occurs successively.

Table 3.6. Desorption conditions of arsenic. Chitosan (C) and chitosan immobilized silicate (IC). Sorption conditons: 50.0 mg sorbent, pH 3.0, 25 °C solution temperature and 30 min sorption time

Sorbent	Volume of As(V) (mL)	Concentration of As(V) ($\mu\text{g/L}$)	Shaking time for desorption (min)	Eluent	Volume of eluent (mL)	L-cysteine (% w/v)	Desorption %	
C	30.0	100.0	30	2.0 % HAc	30.0	-	89.9	(± 0.6)
IC	30.0	100.0	30	2.0 % HAc	30.0	-	67.3	(± 1.5)
IC	30.0	100.0	30	4.0 % HAc	30.0	-	61.8	(± 2.9)
IC	30.0	100.0	60	2.0 % HAc	30.0	-	64.9	(± 0.8)
IC	30.0	100.0	30	2.0 % HAc	50.0	-	82.3	(± 1.8)
IC	30.0	100.0	30	2.0 % HAc	30.0	0.5	99.8	(± 0.2)
C	15.0	10.0	30	pH 3.0 (adjusted with HCl)	15.0	0.01	48.1	(± 3.5)
C	15.0	10.0	30	pH 3.0 (adjusted with HCl)	15.0	0.05	44.3	(± 2.3)
C	15.0	10.0	30	pH 3.0 (adjusted with HCl)	15.0	0.1	43.9	(± 0.9)
C	15.0	10.0	30	pH 3.0 (adjusted with HCl)	15.0	0.5	67.2	(± 1.3)
C	15.0	10.0	30	pH 3.0 (adjusted with HCl)	15.0	1	100.0	(± 3.9)
C	30.0	40.0	30	Ultrapure water	30.0	0.5	39.4	(± 3.6)
C	30.0	40.0	30	1.0 % HCl	30.0	0.5	94.3	(± 1.0)
C	30.0	40.0	30	1.0 M HNO ₃	30.0	-	2.1	(± 0.2)
C	30.0	40.0	30	pH 10.0 (adjusted with NH ₃)	30.0	0.5	0.3	(± 0.5)
C	30.0	40.0	30	1.0 M NH ₃	30.0	-	0.3	(± 0.8)
C	30.0	40.0	30	pH 10.0 (adjusted with NH ₃)	30.0	-	0.4	(± 1.0)

3.7. Effect of the Acid Nature on As Signal

Effect of the acid nature is illustrated in Figure 3.34. Steeper calibration curve provide more efficient response for arsenic determination. Standard arsenic solutions prepared in 2.0% acetic acid solution resulted in a steeper calibration curve. Addition of 1.0% HCl to the acetic acid matrix decreased the absorbance. Increasing the HCl concentration was suppressed the arsenic signal more than twice, while nitric acid produced the lowest signal. Since arsine is easily generated from As(III), reducing conditions are important for hydride generation. The addition of nitric acid prior determination provides oxidizing environment which converts some of the already reduced As(III) to As(V) which is not effective in the arsine generation.

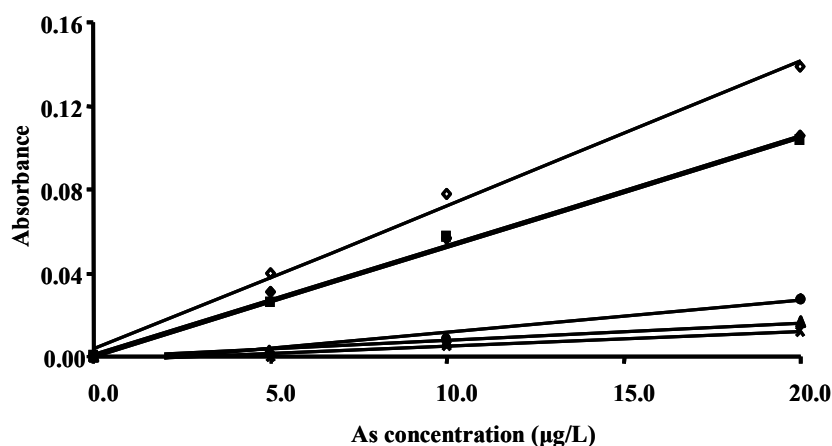


Figure 3.34. Effect of the acid matrix in arsenic signal generated in 2.0% acetic acid (◇), 1.0% HCl + 2.0% acetic acid (■), pH 1.0 adjusted with HCl + 1.0% HCl (▲), pH 1.0 adjusted with HCl (●), 1.0% HCl (◆), pH 1.0 adjusted with HNO₃ + 1.0% HCl (×)

3.8. Interference Studies

Interference studies were performed for Te(IV), Te(VI), Sb(III), Sb(V), Se(IV), Se(VI), Mo(VI) and V(V) as described previously in section 2.9. In the first part of the study sorption of chosen species by chitosan were investigated. Table 3.7 shows the result obtained for sorption characteristics of species by chitosan. Except of Te species

chitosan shows affinity to all species. Mo(VI), V(V) and Se(VI) almost completely were removed from solutions in both concentrations. These results were in agreement with several studies of Guibal and co-workers, they found that the sorption of Mo(VI) by cross-linked chitosan beads was maximum at pH 3 (Guibal, et al. 1998). Similarly Qian and co-workers. found that optimum pH value for maximum adsorption of V(V) ions was 3 (Qian, et al. 2004). Table 3.8 demonstrated the effect of each species on sorption or hydride generation of As(V). Interfering case is described as > 15% changes in sorption or changes in absorbance. As understand from the Table 3.8, Te(IV) shows interference effect by decreasing the percent sorption of arsenic when was added in 1000.0 µg/L while in lower concentration does not effect. Sb(V) and Sb(III) show interference characteristics as in case of Te(IV) but by decreasing the hydride signal while was added in large concentrations. So interference of the Sb species can be overcome by using ICP-MS instead of hydride techniques in As(V) sorption study. V(V) and Mo(VI) were showed interference while As(V) concentration is 100.0 µg/L and did not effect while arsenic concentration is low. This interference was seen in all concentrations of V(V) and 10.0 µg/L Mo(VI) concentrations by increasing the sorption capacity while in higher Mo(VI) concentrations interfere by decrease the sorption capacity.

Table 3.7. Percent sorption of chosen species by chitosan at optimized conditions for As(V)

Element	Sorption %	
	100.0 µg/L	1000.0 µg/L
Sb(V)	66.1 (± 0.9)	65.2 (± 2.3)
Sb(III)	31.3(± 0.8)	19.4 (± 2.3)
Se(VI)	99.9 (± 0.2)	90.4 (± 2.8)
Se(IV)	60.4 (± 0.6)	55.2 (± 1.4)
Mo(VI)	99.3 (± 0.4)	99.4 (± 0.1)
V(V)	99.8 (± 2.0)	99.1 (± 0.2)
Te(VI)	0.3 (± 0.5)	0.1 (± 1.0)
Te(IV)	14.1 (± 0.6)	0.1 (± 1.8)

Table 3.8. Summary of interference study; N: no interference, I: interference (a: decrease in sorption capacity; b: decrease in hydride signal; c: increase in sorption capacity)

Element	10.0 µg/L As(V)			100.0 µg/L As(V)		
	10.0 µg/L	100.0 µg/L	1000.0 µg/L	10.0 µg/L	100.0 µg/L	1000.0 µg/L
Te(IV)	N	N	I ^a	N	N	I ^a
Te(VI)	N	N	N	I ^a	N	N
Se(IV)	N	N	N	N	N	I ^a
Se(VI)	N	N	N	N	N	N
Sb(V)	N	N	I ^b	N	N	I ^b
Sb(III)	N	N	I ^b	N	N	I ^b
V(V)	N	N	N	I ^c	I ^c	I ^c
Mo(VI)	N	N	N	I ^c	I ^a	I ^a

3.9. Pre-Concentration

Pre-concentration experiment was done for As(V) spiked bottled water at 25 °C with given parameter in Table 3.9. Percent recovery of enrichment factor 1 and 2 were effective in preconcentration while factor of 10 was decreased the recovery percentage.

Table 3.9. Percent recovery at various enrichment factor from chitosan for arsenate ion

Enrichment factor	Initial		Final		Recovery %
	Volume (mL)	Concentration (µg/L)	Volume (mL)	Concentration (µg/L)	
1	15.0	10.0	15.0	9.8 (± 0.3)	98.1 (± 2.9)
2	30.0	5.0	15.0	9.5 (± 0.2)	95.4 (± 1.7)
10	150.0	1.0	15.0	7.8 (± 0.4)	78.2 (± 4.4)

3.10. Speciation of Arsenic

Speciation of arsenate and arsenite ions was performed with chitosan, chitosan-immobilized sodium silicate and commercial Duolite GT-73 resins described in section

2.11. Chitosan and chitosan-immobilized sodium silicate are effective in sorption of arsenate as found through the study. Duolite GT-73 is a SH functionalized resin knowing that is selective for lower oxidation states of species so it should be effective for arsenite removal. Table 3.10 illustrates the comparative spike recovery from chitosan and chitosan-immobilized sodium silicate from each species. Both chitosan and chitosan-immobilized sodium silicate have been found as effective in arsenate recovery from spiked solutions, whereas these sorbents are not efficient in arsenite recovery. These results are in concurrence with our previous results obtained through the study. The crosscheck of ICP-MS with HGAAS show that results are in agreement. This proves both the accuracy and the confidence of the method developed. In case of sorption performed with Duolite GT-73 (Table 3.11) arsenite recovery was achieved but the amount is lower. This observation is related to the Duolite GT-73 sorption and release performance. Since, used conditions for synthetic resin were not optimized and used as described in literature for Sb speciation (Erdem and Eroğlu 2005).

Table 3.10. The comparative spike recovery of As(V) and As(III) ions from chitosan and chitosan-immobilized sodium silicate

Concentration	Spike Recovery (%)			
	Chitosan		Chitosan-immobilized sodium silicate	
	ICP-MS	HGAAS	ICP-MS	HGAAS
100.0 µg/L As(V)	110.0 (± 3.7)	96.3 (± 2.5)	104.6 (± 3.5)	102.2 (± 5.8)
100.0 µg/L As(III)	10.6 (± 0.4)	10.0 (± 0.7)	13.1 (± 0.2)	13.6 (± 2.3)
100.0 µg/L As(V) + 100.0 µg/L As(III)	111.2 (± 2.4)	95.9 (± 3.3)	104.1 (± 1.0)	102.4 (± 2.7)

Table 3.11. The comparative spike recovery of As(V) and As(III) ions from Duolite GT-73

Concentration	Spike Recovery (%) for Duolite GT-73			
	Chitosan		Chitosan-immobilized sodium silicate	
	ICP-MS	HGAAS	ICP-MS	HGAAS
100.0 µg/L As(V)	1.7 (± 6.1)	0.0 (± 3.8)	16.6 (± 7.2)	13.8 (± 7.6)
100.0 µg/L As(III)	62.2 (± 13.9)	60.0 (± 5.3)	70.8 (± 13.3)	79.8 (± 3.5)
100.0 µg/L As(V) + 100.0 µg/L As(III)	70.1 (± 21.2)	90.0 (± 1.0)	110.7 (± 5.9)	114.0 (± 1.7)

3.11. Method Validation with Spiked Samples

Chitosan was used in recovery of arsenate from four different type of water spiked samples as described in section 2.12. Distilled and bottled water have nearly same and high recovery percentage while tap water percent recovery reduces to lower than 50%. Arsenate could not be recovered from sea water spiked sample which means no sorption was obtained from sea water (Table 3.12). This observation is in agreement with results obtained from effect of ionic strength of solution on sorption of arsenate by chitosan. Sea water ionic content from salts and other dissolved ions increase the ionic strength, while tap water of Urla region indicate the presence of water hardness which explain the low percent recovery due to competitive ions.

Table 3.12. Percent recovery of spiked arsenate ion from distilled, bottled, tap and sea water samples after desorption from chitosan

Water Type	Spiked As(V) concentration ($\mu\text{g/L}$)		Recovery %
	Initial	Final	
Distilled water	10.0	11.4 (± 0.5)	114.2 (± 4.5)
Bottled water	10.0	11.2 (± 0.2)	112.3 (± 1.6)
Tap water ^a	10.0	4.3 (± 0.4)	43.2 (± 4.2)
Sea water	10.0	0.0 (± 0.1)	0.0 (± 0.8)

3.12. Performance of the Study

The study was carried out to investigate the performance of the method which is summarized in Table 3.13. The details of the method were described in section 2.13. The sorption of As(V) samples was in agreement with sorption results obtained in various parts of sorption studies (sections 3.4 and 3.5). As(III) was adsorbed only if pre-reduction step was applied as expected from results obtained in section 3.4.1. Similar results were observed in case of SRM which indicates that the arsenic is presented in trivalent form. The sorption had been achieved with of As(V) was higher than the sorptions observed in case of pre-oxidized SRM and As(III) samples. This indicated that pre-oxidation step was not completed.

Table 3.13. Summary of method performance

Batch number	Arsenic spike source	Pre-oxidation	Sorption%	Desorption %
1	SRM	+	84.3	67.7
2	SRM	-	0.1	0.1
3	As(III)	+	83.8	58.3
4	As(III)	-	16.1	0.3
5	As(V)	-	96.3	53.4

3.13. Sorption Study of Modified Porous Silicate

Sorption study of modified porous silicate was investigated as explained in the section 2.14. Sorption behaviour of each sorbent toward the given ions is summarized in the Table 3.14. Under studied conditions the activated silicate is not effective in removal of species. Each modified sorbent has distinct sorption capacity for each separate ion. Amine modified silicate is suitable sorbent for As(V) sorption, while glutaraldehyde modified is suitable for Mo(VI) ion. Chitosan modified silicate has larger sorption percentage for V(V) and Se(VI) ions while no one of the prepared sorbent is effective in Te(VI) removal.

Table 3.14. Sorption behaviour of modified macroporous silicate towards various ions. Sorption parameters; sorbent amount: 50.0 mg, solution pH: 3.0, solution volume: 20.0 mL, concentration of species: 100.0 $\mu\text{g/L}$, sorption temperature: 25 $^{\circ}\text{C}$

Sorbent	Sorption %					
	As(V)	As(III)	Se(VI)	V(V)	Te(VI)	Mo(VI)
Activated silicate	28.3	36.9	0.5	0.1	0.4	35.8
Amine modified silicate	87.8	55.2	86.6	38.3	0.1	78.5
Glutaraldehyde modified silicate	78.3	41.4	89.1	57.7	0.3	95.5
Chitosan modified silicate	69.1	38.8	96.7	80.5	0.1	99.3
Mercapto modified silicate	42.4	49.3	81.3	99.9	0.5	69.8
Mercapto-amine modified silicate	39.9	49.4	77.8	78.3	0.1	89.3

CHAPTER 4

CONCLUSION

This study has demonstrated that both the chitosan itself and the chitosan-immobilized inorganic substrates can effectively be employed in the sorption of As(V) from ultrapure water. The high sorption efficiency of chitosan for arsenate has also led the search for new amine containing sorbents for the same purpose. Among the sorbents investigated, chitosan, chitosan-immobilized sodium silicate, chitosan-modified macroporous silicate, and aminopropyl triethoxysilane-modified macroporous silicate have given promising results for As(V) sorption. Therefore, only the results of the experiments carried out with these four sorbents were given in the thesis.

As can easily be expected, the first step after the synthesis has always been the characterization of the novel materials. Scanning electron microscopic investigation of chitosan and chitosan-immobilized sodium silicate has indicated that the surface porosity has been increased during the immobilization procedure in addition to the successful fixation. The results of TGA analysis of chitosan indicated a two-stage weight loss corresponding first to the loss of absorbed water (9%) between 25-266 °C, and second to the degradation of chitosan for a further loss of 34% summing up to 43% loss between 266-328 °C. Sodium silicate, on the other hand, shows approximately 6% weight loss in the same range due only to the removal of water. The chitosan-immobilized sodium silicate has shown an intermediate behaviour between these two extremes as expected. The deacetylation degree of chitosan was determined by two independent methods, namely, potentiometric titration and elemental analysis. The results obtained from these two methods were in agreement with each other; such as, 85.4% removal of acetyl groups was obtained with potentiometric titrimetry and 84.7% removal of acetyl groups with elemental analysis. The molecular weights of chitin and chitosan determined by capillary viscosimetry were 210 kDa and 3340 Da, respectively. The former value, 210 kDa, is indicative of low molecular weight chitin and deacetylation treatment causes a further decrease in the size of the polymer chain by almost 70 times by cleavage of glycosidic bonds.

The morphology of polystyrene nanoparticles used as template and macroporous silicate structures synthesized using these nanospheres were also investigated by SEM and the images have indicated a very regular association of the particles producing tetrahedral holes in their close-packed organization. Particle size distribution of polystyrene nanoparticles has also indicated the monodispersed distribution of particles.

The success of amine modification of macroporous structures was checked by their C, N, and H contents. The elemental analysis of modified macroporous silicate has shown that the percentage of amine groups introduced onto silicate surface was less than 1.5%. Although a higher value was expected due to a larger surface area, this was not observed experimentally.

Several strategies were followed for the synthesis of new amine containing sorbents. The first one was the immobilization of chitosan onto sodium silicate with a straightforward synthesis route. A second advantage of this strategy was that the surface of the novel material had more porosity compared to chitosan itself. The second strategy consisted of three stages; namely, the synthesis of size-controlled template through surfactant-free miniemulsion polymerization of styrene in the first step, then the subsequent synthesis of ordered macroporous silicate structures using the template prepared in the previous step, and finally the modification of the resulting structure with chitosan and aminopropyl triethoxysilane.

The initial studies have focused on the examination of sorption behaviour of chitosan. The sorption of arsenate and arsenite ions at various pHs was investigated for chitin, chitosan, sodium silicate and chitosan-immobilized sodium silicate. None of these materials showed sorption towards arsenite ion. On the other hand, both chitosan and chitosan-immobilized sodium silicate demonstrated a maximum sorption to arsenate ion at pH=3.0. The importance of this pH comes from the combination of two effects; first, the amino groups of chitosan are protonated, and second, arsenic is in H_2AsO_4^- form which support the electrostatic nature of sorption. Actually, the percent sorption for arsenate ion at pH=3.0 which is about 85% was in accordance with the percent fraction of the species at this pH (85% H_2AsO_4^- and 15% H_3AsO_4).

Effect of reaction temperature on the sorption of arsenate by chitosan and chitosan-immobilized sodium silicate was investigated at 25, 50 and 70 °C. The maximum sorption was achieved at the sorption temperature of 25 °C with both sorbents which is indicative of exothermic nature of the sorption. The kinetics of the sorption shows that the maximum removal of arsenate ion was attained in 15-30 min time interval for both

chitosan and chitosan-immobilized sodium silicate. Although the amount of chitosan immobilized in the silicate matrix is only one third of pure chitosan, they both have shown identical sorption characteristics. The similar sorption characteristics of these two sorbents were also observed in successive loading experiments which indicated that the new sorbent possibly had a greater number of available functional groups after immobilization. The chitosan flakes, after 6 loadings, starts to release previously adsorbed arsenate as a result of gradual dissolution of flakes, while chitosan-immobilized sodium silicate showed sorption at least up to 10 loadings without any release of arsenate. Another advantage of sodium silicate immobilization method is the ease of preparation and its inertness towards arsenic species.

Desorption study showed that 2.0% acetic acid dissolved chitosan completely and enabled the previously adsorbed arsenite to pass into the solution. This has given a 100% elution efficiency. A similar performance was also achieved with the use of 1% (w/v) L-cysteine solution of which pH was adjusted to 3.0. This eluent possibly reduced the adsorbed As(V) to As(III) which is not retained by chitosan.

Interference studies were carried out with two types of ions. The ions in the first group was expected to have similar chemical characteristics as arsenate ion at pH 3.0. Vanadium(V) and Mo(VI) were among these ions and both had interference effect in 100.0 µg/L As(V) concentrations. The ions in the second group of potential interferences were chosen from hydride forming elements. Te(IV), Sb(III) and Sb(V) had an interference effect when the interferant concentration is 1000.0 µg/L

Method validation realized with both spiked solutions and a standard reference material (SRM) shows that the method works well for As(V) species at a wide range of concentrations. A pre-oxidation step is required for the determination of As(III) species. Various types of water samples were spiked with As(V) and it was observed that the method is applicable for the determination of As(V) in ultra pure water and bottled drinking water. Seawater and İYTE's tap water were not effectively used due to high ionic strength resulted from various dissolved ions in their matrices. This observation is in agreement with the results obtained for effect of ionic strength on the sorption of arsenate by chitosan. The speciation study of arsenic species also supported the validity of the developed method.

REFERENCES

- Antonietti, M. and K. Landfester. 2002. Polyreactions in miniemulsions. *Progress in Polymer Science* 27:689-757.
- Atkins, Peter and Julio de Paula. 2002. *Atkins' Physical Chemistry*. New York:Oxford university press.
- Barreau, S. and J.N. Miller. 1996. Sol-gel systems for biosensors. *Analytical Communications* 33:5H-6H.
- Boddu, V., K.Abburi, J.L. Talbott, E. Smith. 2003. Removal of hexavalent chromium from wastewater using a new composite chitosan biosorbent. *Environmental Science & Technology* 37:4449-4456.
- Boddu, V.M. and E.D. Smith. A composite chitosan biosorbent for adsorption of heavy metals from wastewaters.
- Boddu, V.M., K. Abburi, J.L. Talbott, E.D. Smith, R. Haasch. 2007. Removal of arsenic (III) and arsenic (V) from aqueous medium using chitosan-coated biosorbent. *Water Research* 42(3):633-642.
- Brinker, Jeffrey C. and George W. Scherer 1990. *Sol-Gel Science*. San Diego:Academic Press.
- Bundaleska, J.M., T. Stafilov, S. Arpadjan. 2005. Direct analysis of natural waters for arsenic species by hydride generation atomic absorption spectrometry. *International Journal of Environmental and Analytical Chemistry* 85:199-207.
- Chassary, P., T. Vincent, E. Guibal. 2004. Metal anion sorption on chitosan and derivative materials:a strategy for polymer modification and optimum use. *Reactive & Functional Polymers* 60:137-149.
- Chavez, J.J.E., M.L. Cervantes, A. Naik, Y.N. Kalia, D.Q. Guerrero, A.G. Quintanar. 2006. Application of thermoreversible Pluronic F-127 Gels in Pharmaceutical Formulations. *J Pharm Pharmaceut Sci* 9:339-358.
- Chen, X., J. Jia, S. Dong. 2003. Organically modified sol-gel/chitosan composite based glucose biosensor. *Electroanalysis* 15:608-612.
- Choong, T.S.Y., T.G. Chuah, Y. Robiah, F.L. Gregory Koay, I. Azni. 2007. *Desalination* 217:139-166.
- Dambies, L., T. Vincent, E. Guibal. 2002. Treatment of arsenic- containing solutions using chitosan derivatives: uptake mechanism and sorption performances. *Water Research* 36:3699-3710.
- Dambies, L., T. Vincent, A. Domard, E. Guibal. 2001. Preparation of chitosan gel beads by ionotropic molybdate gelation. *Biomacromolecules* 2:1198-1205.

- Dedina, Jiri and Dimiter L. Tsalev. 1995. *Hydride Generation Atomic Absorption Spectrometry*. Chichester: John Willey & Sons.
- Dominguez, L., J. Economy, K. Benak, C.L. Mangun. 2003. Anion exchange fibers for arsenate removal derived from a vinylbenzyl chloride precursor. *Polymer for Advanced Technologies* 14:632-637.
- Dominguez, L., Z. Yue, J. Economy, C.L. Mangun. 2002. Design of polyvinyl alcohol mercaptal fibers for arsenite chelation. *Reactive & Functional Polymers* 53:205-215.
- Donatti, D.A., A.I. Ruiz, D.R. Vollet, H. Maceti. 2006. Structural evolution up to 1100 °C of xerogels prepared from TEOS sonohydrolysis and liquid phase exchanged by acetone. *Journal of Non-Crystalline Solids* 352:167-173.
- Ebdon, Les, Les Pitts, Rita Cornelis, Helen. Crews, O.F.X. Donard, and Philippe Quevauviller, eds. 2001. *Trace element speciation for environment, food and health*. Cambridge: The Royal Society of Chemistry.
- Environmental Protection Agency. Targeting and Analysis Branch Standards and Risk Management Division Office of Ground Water and Drinking Water United States Environmental Protection Agency Washington, D.C. 1999. *Technologies and Cost for Removal of Arsenic from Drinking Water*.
- El-Nahhal, I.M., N.M. El-Ashgar. 2007. A review on polysiloxane-immobilized ligand systems: Synthesis, characterization and applications. *Journal of Organometallic Chemistry* 692:2861-2886.
- Erdem, A. and A.E. Eroğlu. 2005. Speciation and preconcentration of inorganic antimony in waters by Duolite GT-73 microcolumn and determination by segmented flow injection-hydride generation atomic absorption spectrometry (SF-HGAAS). *Talanta* 68:86-92.
- Faria, S., R.E. Rodriguez, A. Ledesma, D.A. Batistoni. 2002. Assessment of acid media effects on the determination of tin by hydride generation inductively coupled plasma atomic emission spectrometry. *Microchemical Journal* 73:79-88.
- Gregor, J. 2001. Arsenic removal during conventional aluminium-based drinking-water treatment. *Water Research* 35:1659-1664.
- Gueu, S., B. Yao, K. Adouby, G. Ado. 2007. Kinetics and thermodynamics study of lead adsorption on to activated carbons from coconut and seed hull of the palm tree. *International Journal of Environmental Science and Technology* 4:11-17.
- Guibal, E., S. Milot, J.M. Tobin. 1998. Metal-Anion Sorption by chitosan beads: Equilibrium and kinetic studies. *Ind. Eng. Chem. Res.* 37:1453-1463.
- Gundiah, G. 2001. Macroporous silica-alumina composites with mesoporous walls. *Bulletin of Material Science* 24:211-214.

- Hench, L.L. and W. Vasconcelos. 1990. Gel-Silica Science. *Annual Review of Material Science* 20:269-98.
- Holland, B.T., C.F. Banford, T. Do, A. Stein. 1999. Synthesis of highly ordered, three-dimensional, macroporous structures of amorphous or crystalline inorganic oxides, phosphates, and hybrid composites. *Chemistry of Materials* 11:795-805.
- Huacai, G., P. Wan, L. Dengke. 2006. Graft copolymerization of chitosan with acrylic acid under microwave irradiation and its water absorbency. *Carbohydrate Polymers* 66:372-378.
- Hwang, K.T., S.T. Jung, G.D. Lee, M.S. Chinnan, Y.S. Park, H.J. Park. 2002. Controlling molecular weight and degree of deacetylation of chitosan by response surface methodology. *Journal of Agricultural and Food Chemistry* 50:1876-1882.
- Jaworska, M., K. Kula, P. Chassary, E. Guibal. 2003. Influence of chitosan characteristics on polymer properties:II. Platinum sorption properties. *Polymer International* 52:206-212.
- Jaworska, M., K. Sakurai, P. Gaudon, E. Guibal. 2003. Influence of chitosan characteristics on polymer properties. I:Crystallographic properties. *Polymer International* 52:198-205.
- Jiang, X., L. Chen, W. Zhong. 2003. A new linear potentiometric titration method for the determination of deacetylation degree of chitosan. *Carbohydrate Polymers* 54:457-463.
- Kartal, S.N. and Y. Imamura. 2005. Removal of copper, chromium, and arsenic from CCA- treated wood onto chitin and chitosan. *Bioresource Technology* 96:389-392.
- Karunasagar, D., M.V.B. Krishna, S.V. Rao, J. Arunachalam. 2005. Removal and preconcentration of inorganic and methyl mercury from aqueous media using a sorbent prepared from the plant *Coriandrum sativum*. *Journal of Hazardous Materials B* 118:133-139.
- Kasaai, M.R. 2007. Calculation of Mark–Houwink–Sakurada (MHS) equation viscometric constants for chitosan in any solvent–temperature system using experimental reported viscometric constants data. *Carbohydrate Polymers* 68:477-488.
- Kasaai, M.R., J. Arul, G. Charlet. 2000. Intrinsic viscosity-molecular weight relationship for chitosan. *Journal of Polymer Science: Part B: Polymer Physics* 38: 2591- 2598.
- Kavitha, D. and C. Namasivayam. 2007. Recycling coir pith, an agricultural solid waste, for the removal of procion orange from wastewater. *Dyes and Pigments* 74:237-248.
- Khan, T.A., K.K. Peh, H.S. Ch'ng. 2002. Reporting degree of deacetylation values of chitosan:the influence of analytical methods. *Journal of Pharmacy & Pharmaceutical Sciences* 5(3):205-212.

- Krajewska, B. 2004. Application of chitin- and chitosan-based materials for enzyme immobilizations: a review. *Enzyme and Microbial Technology* 35:126-139.
- Kumar, M.N.V. 2000. A review of chitin and chitosan applications. *Reactive & Functional Polymers* 46:1-27.
- Kurita, K. 2006. Chitin and chitosan: Functional biopolymers from marine crustaceans. *Marine Biotechnology* 8:203-226.
- Landfester, K. 2001. Polyreactions in miniemulsions. *Macromolecular Rapid Communications* 22:896-936.
- Le, X.C., W.R. Cullen, K.J. Reimer. 1994. Effect of cysteine on the speciation of arsenic by using hydride generation atomic absorption spectrometry. *Analytica Chimica Acta* 285:277- 285.
- Lev, O., M. Tsionsky, L. Rabinovich, V. Glezer, S. Sampath, I. Pankratov, J. Gun. 1995. Organically modified sol-gel sensors. *Analytical Chemistry* 67:22A-30A.
- Limousin, G., J.P. Gaudet, L. Charlet, S. Szenknect, V. Barthes, M. Krimissa. 2007. Sorption isotherms: A review on physical bases, modeling and measurement. *Applied Geochemistry* 22:249-275.
- Liu, X.D., S. Tokura, M. Haruki, N. Nishi, N. Sakairi. 2002. Surface modification of nonporous glass beads with chitosan and their adsorption property for transition metal ions. *Carbohydrate polymer* 49:103-108.
- Liu, X.D., S. Tokura, N. Nishi, N. Sakairi. 2003. A novel method for immobilization of chitosan onto nonporous glass beads through a 1,3-thiazolidine linker. *Polymer* 44:1021-1026.
- Mandal, B.K. and K.T. Suzuki. 2002. Arsenic round the world: a review. *Talanta* 58: 201-235.
- Menegario, A.A. and M.F. Gine. 2000. Rapid sequential determination of arsenic and selenium in waters and plant digests by hydride generation inductively coupled plasma-mass spectrometry. *Spectrochimica Acta Part B* 55:355-362.
- Miao, T. and S.N. Tan. 2001. Amperometric hydrogen peroxide biosensor with silica sol-gel/chitosan film as immobilization matrix. *Analytica chimica Acta* 437:87-93.
- Mohan, D. and C.U. Pittman. 2007. Arsenic removal from water/wastewater using sorbents-A critical review. *Journal of Hazardous Materials* 142:1-53.
- Munoz-Espi, R. 2006. Surface-functionalized latex particles as additives in the mineralization of zinc oxide: influence on crystal growth and properties. *Johannes Gutenberg University Thesis of Ph.D.*
- Muzzarelli, Riccardo A.A. 1973. *Natural Chelating Polymers*. Hungary: Pergamon Press.

- Nakamura, H., M. Ishii, A. Tsukigase, M. Harada, H. Nakano. 2005. Close-packed colloidal crystalline arrays composed of polystyrene latex coated with titania nanosheets. *Langmuir* 21:8918-8922.
- Niedzielski, P., M. Siepak, J. Siepak, J. Przybyłek. 2002. Determination of different forms of arsenic, antimony and selenium in water samples using hydride generation. *Polish Journal of Environmental Studies* 11:219-224.
- Odian, George 2004. *Principles of Polymerization*. New Jersey:John Willey & Sons.
- Oehmen, A., R. Vegas, S. Velizarov, M.A.M. Reis, J.G. Crespo. 2006. Removal of heavy metals from drinking water supplies through the ion exchange membrane bioreactor. *Desalination* 199:405-407.
- Ogawa, Kozo. 1991. Effect of heating an aqueous suspension of chitosan on the crystallinity and polymorphs. *Agricultural and Biological Chemistry* 55:2375-2379.
- Pajonk, G.M. 2003. Some applications of silica aerogels. *Colloid Polymer Science* 281:637-651.
- Pedroni, V.I., M.E. Gschaider, P.C. Schulz. 2003. UV Spectrophotometry: Improvements in the study of the degree of acetylation of chitosan. *Macromolecular Bioscience* 3:531-534.
- Planas, M.R. 2002. Development of techniques based on natural polymers for the recovery of precious metals. *Universitat Polytechnica de Catalunya Thesis of Ph.D.*
- Qi, L. and Z. Xu. 2004. Lead sorption from aqueous solutions on chitosan nanoparticles. *Colloid and Surfaces A: Physicochemical Engineering Aspects* 251:183-190.
- Qian, S., H. Wang, G. Huang, S. Mo, W. Wei. 2004. Studies of adsorption properties of crosslinked chitosan for vanadium(V), tungsten(VI). *Journal of Applied Polymer Science* 92:1584- 1588.
- Rhazi, M., J. Desbrieres, A. Tolaimate, M. Rinaudo, P. Vottero, A. Alagui, M. El Meray. 2002. Influence of the nature of the metal ions on the complexation with chitosan. Application to the treatment of liquid waste. *European Polymer Journal* 38:1523-1530.
- Sabarudin, K.O., M. Oshima, S. Motomizu. 2005. Synthesis of chitosan resin possessing 3,4-diamino benzoic acid moiety for the collection/ concentration of arsenic and selenium in water samples and their measurement by inductively coupled plasma-mass spectrometry. *Analytica Chimica Acta* 542:207-215.
- Sen, T., G.J.T. Tiddy, J.L. Casci, M.W. Anderson. 2004. Synthesis and characterization of hierarchically ordered porous silica materials. *Chemistry of Materials* 16:2044-2054.
- Sheng, I., J. Zhao, B. Zhou, X. Ding, Y. Deng, Z. Wang. 2006. In situ preparation of CaCO₃/polystyrene composite nanoparticles. *Materials Letters* 60:3248-3250.

- Smedley, P.L. and D.G. Kinniburgh. 2001. A review of the source, behaviour and distribution of arsenic in natural waters. *Applied Geochemistry* 17:517-568.
- Solomons, Graham and Graig Fryhle. 2000. *Organic Chemistry*. Danvers: John Willey & Sons.
- Şeker, A., T. Shahwan, A.E. Eroğlu, S. Yılmaz, Z. Demirel, M.C. Dalay. 2008. Equilibrium, thermodynamic and kinetic studies for the biosorption of aqueous lead(II) and nickel(II) ions on *Spirulina platensis*. *Journal of Hazardous Materials* 154:973-980.
- Taghizadeh, S.M. and G. Davari. 2006. Preparation, characterization, and swelling behaviour of N-acetylated and deacetylated chitosans. *Carbohydrate Polymers* 64:9-15.
- Tan, X., M. Li, P. Cai, L. Luo, X. Zou. 2005. An amperometric cholesterol biosensor based on multiwalled carbon nanotubes and organically modified sol-gel/chitosan hybrid composite film. *Analytical Biochemistry* 337:111-120.
- Tirkistani, F.A.A. 1998. Thermal analysis of some chitosan Schiff bases. *Polymer Degradation and Stability* 60:67-70.
- Tissot, I., J.P. Reymond, F. Lefebvre, E.B. Lami. 2002. SiOH- functionalized polystyrene latexes. A step toward the synthesis of hollow silica nanoparticles. *Chemistry of Materials* 14:1325-1331.
- Tolaimate, A., J. Desbrieres, M. Rhazi, A. Alagui, M. Vincendon, P. Vottero. 2000. On the influence of deacetylation process on the physicochemical characteristics of chitosan from squid chitin. *Polymer* 41:2463-2469.
- Tsaih, M.L. and R.H. Chen. 1999. Molecular weight determination of 83% degree of decetylation chitosan with non-Gaussian and wide range distribution by high-performance size exclusion chromatography and capillary viscometry. *Journal of Applied Polymer Science* 71:1905-1913.
- Umplebay II, R.J., S.C. Baxter, M. Bode, J.K. Berch Jr., R.N. Shaha, K.D. Shimizu. 2001. Application of the freundlich adsorption isotherm in the characterization of molecularly imprinted polymers. *Analytica Chimica Acta* 435:35-42.
- Ülkü, S., D. Balköse, H. Baltacboğlu 1993. Effect of preparation pH on pore structure of silica gels. *Colloid & Polymer Science* 271:709-713.
- Vasireddy, D. 2005. *Arsenic Adsorption onto Iron-Chitosan Composite from Drinking Water*. M.Sc. Thesis, University of Missouri, Columbia.
- Wang, G., J.J. Xu, H.Y. Chen, Z.H. Lu. 2003. Amperometric hydrogen peroxide biosensor with sol-gel/chitosan network-like film as immobilization matrix. *Biosensor&Bioelectronics* 18:335-343.

- Weska, R.F., J.M. Moura, L.M. Batista, J. Rizzi, L.A.A. Pinto. 2007. Optimization of deacetylation in the production of chitosan from shrimp wastes: Use of response surface methodology. *Journal of Food Engineering* 80:749-753.
- Whyha, J.J., M. Elimelech, J.G. Hering. 1997. Arsenic removal by RO and NF membranes. *J. AWWA* 89:102-114.
- Wu, W., D. Caruntu, A. Martin, M.H. Yu, C.J. O'Connor, W.L. Zhou, J.F. Chen. 2007. Synthesis of magnetic hollow silica using polystyrene bead as a template. *Journal of Magnetism and Magnetic Materials* 311:578-582.
- Xu, Q., C. Mao, N.N. Liu, J.J. Zhu, J. Shen. 2006. Immobilization of horseradish peroxidase on O-carboxymethylated chitosan/sol-gel matrix. *Reactive & Functional Polymers*.
- Yang, Y.M., J.W. Wang, R.X. Tan. 2004. Immobilization of glucose oxidase on chitosan-SiO₂ gel. *Enzyme and Microbial Technology* 34:126-131.
- Yersel, M., A. Erdem, A.E. Eroğlu, T. Shahwan. 2005. Separation of trace antimony and arsenic prior to hydride generation atomic absorption spectrometric determination. *Analytica Chimica Acta* 534:293-300.
- Yi, G.R., J.H.H. Moon, S.M. Yang. 2001. Ordered macroporous particles by colloidal templating. *Chemistry of Materials* 13:2613-2618.
- Zhang, W., J. Gao, C. Wu. 1997. Microwave preparation of narrowly distributed surfactant-free stable polystyrene nanospheres. *Macromolecules* 30:6388-6390.